AD_____

Award Number: DAMD17-03-01-0087

TITLE: Erbium:YAG Laser Incision of Urethral Strictures for Treatment of Urinary Incontinence after Prostate Cancer Surgery

PRINCIPAL INVESTIGATOR: Nathaniel Fried, Ph.D.

CONTRACTING ORGANIZATION: Johns Hopkins University School of Medicine
                           Baltimore, Maryland 21205

REPORT DATE: February 2006

TYPE OF REPORT: Final

PREPARED FOR: U.S. Army Medical Research and Materiel Command
               Fort Detrick, Maryland 21702-5012

DISTRIBUTION STATEMENT: Approved for Public Release;
                        Distribution Unlimited

The views, opinions and/or findings contained in this report are those of the author(s) and should not be construed as an official Department of the Army position, policy or decision unless so designated by other documentation.

REPORT DOCUMENTATION PAGE

Form Approved
OMB No. 0704-0188

Public reporting burden for this collection of information is estimated to average 1 hour per response, including the time for reviewing instructions, searching existing data sources, gathering and maintaining the data needed, and completing and reviewing this collection of information. Send comments regarding this burden estimate or any other aspect of this collection of information, including suggestions for reducing this burden to Department of Defense, Washington Headquarters Services, Directorate for Information Operations and Reports (0704-0188), 1215 Jefferson Davis Highway, Suite 1204, Arlington, VA 22202-4302. Respondents should be aware that notwithstanding any other provision of law, no person shall be subject to any penalty for failing to comply with a collection of information if it does not display a currently valid OMB control number. **PLEASE DO NOT RETURN YOUR FORM TO THE ABOVE ADDRESS.**

1. REPORT DATE 01-02-2006	2. REPORT TYPE Final	3. DATES COVERED 1 Feb 2003 – 31 Jan 2006

4. TITLE AND SUBTITLE Erbium:YAG Laser Incision of Urethral Strictures for Treatment of Urinary Incontinence after Prostate Cancer Surgery	5a. CONTRACT NUMBER
	5b. GRANT NUMBER DAMD17-03-1-0087
	5c. PROGRAM ELEMENT NUMBER
6. AUTHOR(S) Nathaniel Fried, Ph.D.	5d. PROJECT NUMBER
	5e. TASK NUMBER
	5f. WORK UNIT NUMBER

7. PERFORMING ORGANIZATION NAME(S) AND ADDRESS(ES) Johns Hopkins University School of Medicine Baltimore, Maryland 21205	8. PERFORMING ORGANIZATION REPORT NUMBER

9. SPONSORING / MONITORING AGENCY NAME(S) AND ADDRESS(ES) U.S. Army Medical Research and Materiel Command Fort Detrick, Maryland 21702-5012	10. SPONSOR/MONITOR'S ACRONYM(S)
	11. SPONSOR/MONITOR'S REPORT NUMBER(S)

12. DISTRIBUTION / AVAILABILITY STATEMENT
Approved for Public Release; Distribution Unlimited

13. SUPPLEMENTARY NOTES Original contains colored plates: ALL DTIC reproductions will be in black and white

14. **ABSTRACT**   Urethral strictures and bladder neck contractures occur in 5-20% of prostate cancer surgeries, causingincontinence. Conventional stricture treatments have widely variable success rates with sub-optimal results.Treatment failure is presumably due to mechanical and/or thermal damage to the urethra during the procedure.The objective of this research project was to test a novel Erbium:YAG laser for precise incision of the urethralstricture with minimal damage to adjacent healthy tissue. We hypothesized that minimal side-effects causedduring Erbium laser incision should translate into limited scarring and improved procedural success rates. Year#1 of this project was devoted to optimization of the laser and optical fiber delivery system for rapid and precisecutting of urethral tissue, ex vivo. We accomplished these tasks, and published our findings in the form of fourmanuscripts and two abstracts. Year #2 was devoted to in vivo animal studies comparing the wound healingafter Erbium and Holmium laser incision of the urethra and bladder neck. Further improvement of the opticalfiber delivery system was also accomplished. We published our findings in the form of five manuscripts and twoabstracts. Year #3 was devoted to preparing for clinical studies and obtaining further funding forcommercialization of the fiber optic delivery system. One manuscript was published and one is in review.

15. SUBJECT TERMS
erbium, fiber, laser, incision, urethral, stricture, prostate

16. SECURITY CLASSIFICATION OF:			17. LIMITATION OF ABSTRACT	18. NUMBER OF PAGES	19a. NAME OF RESPONSIBLE PERSON USAMRMC
a. REPORT U	b. ABSTRACT U	c. THIS PAGE U	UU	57	19b. TELEPHONE NUMBER *(include area code)*

Standard Form 298 (Rev. 8-98)
Prescribed by ANSI Std. Z39.18

TABLE OF CONTENTS

INTRODUCTION

Urethral and bladder neck strictures occur in 5-20 % of all prostate cancer surgeries, resulting in urinary incontinence. Conventional treatments for stricture (including balloon dilation, cold knife incision, electrocautery, and Holmium laser incision) have widely variable success rates with sub-optimal long-term results. The failure of these conventional stricture treatments is presumably due to mechanical and/or thermal damage to the urethral wall during the procedure. The purpose of this research project was to test a new laser, the Erbium:YAG laser, which is capable of precisely incising the urethral stricture with minimal peripheral damage to adjacent healthy tissue. We hypothesized that the minimal side-effects caused during Erbium laser incision should translate into limited scarring and improved procedural success rates. Year #1 of this project was devoted to optimization of the laser and optical fiber delivery system for rapid and precise cutting of urethral tissue, *ex vivo*. We accomplished these tasks, and published our findings in the form of four manuscripts and two abstracts. Year #2 of this project was devoted to *in vivo* animal studies comparing the wound healing after Erbium:YAG laser and Holmium:YAG laser incision of the urethra and bladder neck. Further improvement of the optical fiber delivery system was also accomplished as a continuation of previous work. We have completed these tasks, and published our findings in the form of five manuscripts and two abstracts. One of the tasks in Year #2 was not completed because the grant reviewers stated that the task was flawed and should not be addressed. Year #3 of this project was devoted to further development of the optical fiber delivery system, preparation for initial clinical studies, and writing of grant proposals to continue this work. One manuscript is in press and one manuscript has been submitted for review. The Erbium laser and fiber optic delivery system have been FDA approved for human use (510K clearance), and an IRB approval for treatment of patients beginning in January 2006. We have also recently received extramural funding from the National Insitutes of Health Phase II SBIR Program for further development and commercialization of the germanium oxide optical fiber delivery system for use with the Erbium:YAG laser. Overall, the pre-clinical work on this project has been a success, and the next step is to plan for clinical trials.

BODY

Statement of Work

TASK #1: Modification of Erbium:YAG laser system (Months 1-6).
a. Modify electronics in laser power supply to produce shorter laser pulses, more uniform temporal beam profile, and higher pulse repetition rates.

Status - COMPLETED
The Er:YAG laser pulse duration was shortened from 220 μs to 70 μs, using a variable pulse laser power supply. The laser pulse repetition rate was also increased from 5 Hz to 30 Hz (Page 7).

b. Optimize laser ablation parameters (laser energy, pulse duration, repetition rate, and irradiation time) using in vitro tissue samples.

Status - COMPLETED
Shortening the laser pulse duration resulted in a two-fold increase in tissue ablation rates and a corresponding two-fold decrease in peripheral thermal damage to adjacent healthy tissue during ex vivo tissue studies. Experiments were also performed studying the effect of laser pulse duration on peripheral thermal damage at 10, 20, and 30 Hz (Pages 7-9).

TASK #2: Determination of optimal optical fiber delivery system (Months 7-12).
a. Test fiber optic damage thresholds with chemical and microscopic analysis of fiber tips after laser ablation with fiber in contact with tissue.

Status – COMPLETED
Germanium oxide trunk fibers were tested in contact with ex vivo tissue, and the damage threshold was found to be 9 $\pm$ 1 mJ per pulse. Melting of the fiber tip during the high-temperature tissue vaporization process resulted in different phases of fiber tip damage, beginning with particulate formation, cracking, charring, and finally crystallization of the fiber surface, resulting in a sharp decrease in fiber transmission, as observed using light microscopy (Pages 9-11).

b. Design side-firing laser fibers with varying delivery angles for incision of urethral wall.

Status - COMPLETED
This task was delayed until Year 3, but has recently been completed. 450-μm side-firing germanium oxide fibers were designed, assembled, and successfully tested. The fiber tip was polished at a 45 degree angle, resulting in a 90 degree delivery angle. A protective quartz cap was placed over the fiber tip for use in contact with tissue, and the fiber was successfully tested for precise incision of tissue, ex vivo. Smaller, more flexible, 350-μm and 250-μm side-firing fiber have also recently been designed for potential use in flexible scopes in the urinary tract (Pages 11-12).

c. Build hybrid fibers combining flexible germanium oxide trunk fiber with durable sapphire probe tip to prevent fiber damage.

Status - COMPLETED
Hybrid fibers have been designed, assembled, and successfully tested using germanium oxide trunk fibers connected to a short, silica tip using PTFE heat-shrink tubing. Fibers with sizes of 450/550, 350/400, and 250/365 micron diameters have been assembled. Maximum transmission through the fiber is 180 $\pm$ 30 mJ / pulse, a 20-fold improvement over the 9 mJ transmitted through just the germanium trunk fibers. This improvement in damage thresholds for the fibers has allowed contact tissue ablation for potential use in treating urethral strictures (Pages 12-18).

TASK #3: Study wound healing after Er:YAG laser incision of normal urethra (Months 13-18).
a. Perform acute studies for comparison with ex vivo results from Task #1 to determine effect of hydration and perfusion on ablation parameters.

Status – COMPLETED
Acute, *in vivo*, Er:YAG laser incisions produced 20 ± 5 μm of thermal damage, comparable to the 10-20 μm measured during previous *ex vivo* results, and much smaller than the 660 ± 110 μm, measured for the conventional Holmium:YAG laser (Pages 18-21).

b. Conduct short-term chronic wound healing study to confirm minimum urethral scarring after Er:YAG laser incision.

Status - COMPLETED
Short-term chronic wound healing studies were conducted in a pig animal model with healing for up to 14 days. Erbium:YAG laser incisions produced 430 ± 100 μm of thermal damage, 4 times less thermal damage than the conventional Holmium:YAG laser, which produced a thermal damage zone of 1580 ± 250 μm (Pages 18-21).

TASK #4: Develop improved animal model for creating strictures (Months 19-26).
a. Create strictures in a porcine model using both electrocautery and Nd:YAG laser instruments.
b. Quantify degree of thermal damage and lumenal narrowing and which instrument provides most consistent stricture creation.

Status – NOT COMPLETED*
* Note that Task #4 was not completed. During the review of this grant proposal, the reviewers stated that Task #4 was flawed and should not be addressed - "Specific Aim 4, which deals with the animal model, has serious weaknesses and should be eliminated. The panel recommends that the investigators concentrate on the other four specific aims." In agreement with the reviewers' comments, we concentrated on completing Tasks #1-3.

TASK #5: Perform comparative study of cold knife, Ho:YAG, and Er:YAG laser for treating urethral strictures (Months 27-36).
a. Induce strictures using either electrocautery or laser as determined by Task #4.
b. Treat strictures using cold knife, Ho:YAG laser, or Er:YAG laser.
c. Quantify degree of strictures using radiography, cystography, and ultrasound.
d. Perform pathologic analysis of residual scar tissue at stricture site.

Status – NOT COMPLETED*
* Note that Task #5 was not completed in this project. Without a reliable animal model for studying strictures, we could not perform these tasks. Instead, we focused on further development of the optical fiber delivery system for use with the Er:YAG laser, planning for initial clinical studies, and writing grant proposals to continue this project. For Year #3, the following has been accomplished.
1. Task #2b was completed – side-firing optical fiber delivery system developed.
2. In collaboration with Infrared Fiber Systems, inc. (Silver Spring, MD), we applied for and received funding from the National Institutes of Health Phase II SBIR program (2R44EY013889-02, 2 years, $750,000) for commercialization of the hybrid germanium oxide / silica optical fiber delivery system for use with the Er:YAG laser, developed in part from this DOD grant.
3. We initiated collaboration with the Davison Medical Laser Center at Elliot Hospital, Manchester, NH, to begin clinical studies with the Er:YAG laser for treating urethral strictures. We requested and received from the FDA, 510K clearance for use of the Sciton Erbium:YAG laser and optical fiber delivery system for treating strictures. A research protocol has been submitted and IRB approval granted. Initial clinical studies began Jan. 16, 2006.

TASK 1.a. Modification of Erbium Laser

Problem: Our original Er:YAG laser was limited by a fixed laser pulse length of ~ 250 μs and low repetition rate of < 5 Hz. These laser parameters are sub-optimal for rapid and precise cutting of urethral tissue. The long laser pulse results in more peripheral thermal damage to adjacent tissue than necessary and the low repetition rate prevents rapid tissue removal, required for clinical use.
Solution: We replaced our original high-voltage laser power supply with a variable pulse power supply (Model 8800V, Analog Modules, Orlando, FL). This power supply allowed us to operate the Erbium:YAG laser system with pulse lengths ranging from 1-500 μs and with pulse repetition rates of 1-50 Hz. Figure 1abc shows the shorter pulse lengths achieved with the variable power supply, while Figure 1d shows the long-pulse profile of our original laser system.
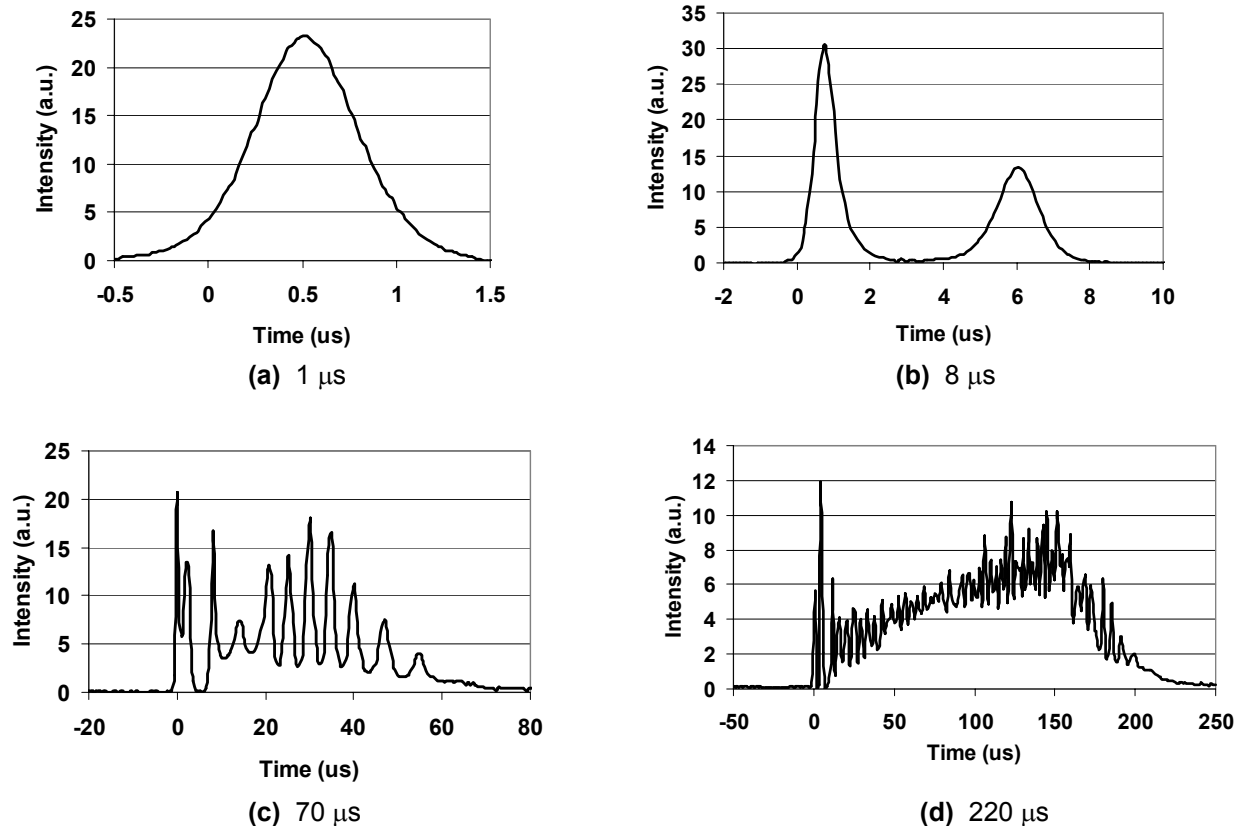

(a) 1 μs

(b) 8 μs

(c) 70 μs

(d) 220 μs

Figure 1. Temporal pulse profiles for Er:YAG laser operated with pulse lengths of 1, 8, 70, and 220 μs.

Task 1.b. Optimize Laser Ablation Parameters with In Vitro Tissue Samples

Problem: The optimal laser parameters (laser energy, pulse length, repetition rate, and irradiation time) for precision cutting of urethral tissue have never been studied.
Solution: Studies were conducted to determine the laser parameters that provided most rapid and efficient tissue cutting, while minimizing peripheral thermal damage to adjacent healthy tissue.

Tissue Studies

Fresh prostatic urethral tissue samples were obtained from male dogs after sacrifice for unrelated experiments at Johns Hopkins Medical School. The urethra was dissected from the prostate, spatulated, sectioned into 1 x 1 cm samples, stored in saline, and refrigerated. For the ablation measurements, tissue samples were sandwiched between microscope and plexiglass slides to a fixed thickness (350 $\pm$ 50 μm), and the optical fiber tip positioned in contact with the sample through 2-mm-diameter holes drilled in the front plexiglass holder. The tissue samples were

kept hydrated with saline during the experiments. The samples were placed in front of a pyroelectric detector, and the number of pulses required to perforate each sample was measured.

Ablation Results

The Er:YAG ablation rates are shown in Figure 2 for ex vivo tissue experiments. Perforation of the tissue occurred at laser fluences of 3-5 J/cm^2 and pulse energies of 1.5-2.5 mJ. There was a two-fold increase in the ablation rate when reducing the laser pulse duration from 220 μs to 70 μs. The 220-μs line shows an ablation rate of 4 μm per J/cm^2, while the 70-μs line shows an ablation rate of 7 μm per J/cm^2. Reducing the pulse to 8 μs produced a minor increase in the ablation rate, but at the expense of much lower laser energy output and peripheral mechanical tissue damage.
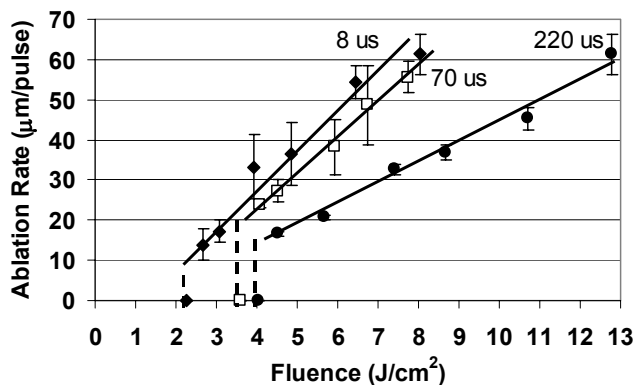

Figure 2. Er:YAG ablation rates using laser pulse lengths of 8, 70, 220 μs, and plotted as a function of laser fluence. Bars signify mean values $\pm$ S.D. (n=6). Note that the perforation threshold decreases as the laser pulse is decreased, and ablation is also more efficient.

Figure 2 demonstrates that we can predict exactly how much tissue is removed per laser pulse as a function of the laser energy and pulse length, and therefore we can precisely control the incision depth during Erbium laser treatment of strictures. Figure 2 also demonstrates that by shortening the laser pulse length from 220 μs to 70 μs, we can almost double the rate at which tissue is removed, making the Erbium laser more efficient.

Thermal Damage Measurements

Histological measurements of thermal damage were conducted as a function of laser pulse duration. The results for ex vivo tissue studies are shown in Figure 3. When the Er:YAG laser was operated in its normal long pulse mode (220 μs pulse length), a thermal damage zone of 30-60 μm was observed. Shortening the laser pulse to 70 μs resulted in a reduction of the thermal damage to 15-30 μm. The shortest laser pulse, measuring 8 μs, further reduced the thermal damage zone to 10-20 μm, but also resulted in a rougher cut, due to mechanical tissue-tearing effects.
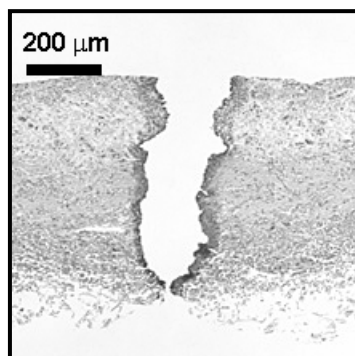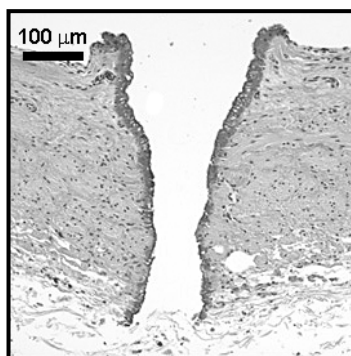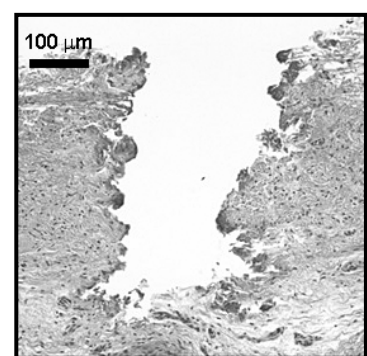
(a) 220 μs; Damage: 30-60 μm **(b)** 70 μs; Damage: 15-30 μm **(c)** 8 μs; Damage: 10-20 μm

Figure 3. Photomicrographs showing H&E stained histologic cross-sections of ureteral tissues ablated with the Er:YAG laser, ex vivo. The thermal damage zone decreases as the laser pulse duration is decreased. Rough, jagged borders of the ablation crater produced by 8 μs laser pulses may be due to mechanical tissue-tearing caused during ablation.

Figure 3 shows that by shortening the laser pulse length from 220 μs to 70 μs, we also decrease the amount of undesirable peripheral thermal damage by a factor of 2.

An ex vivo study was also performed to determine whether the thermal damage zone would increase with laser operation at higher pulse repetition rates, due to residual heat accumulation in the tissue with deposition of successive laser pulses. The pulse duration, energy per pulse, and total number of pulses were all kept constant at 70 μs, 10 mJ, and 20 pulses (total energy = 200 mJ), respectively, while the pulse repetition rate was varied from 10-30 Hz. The thermal damage zone increased as the laser pulse repetition rate increased, and a large increase in thermal damage was observed when the pulse repetition rate was increased from 20 to 30 Hz (Figure 4).
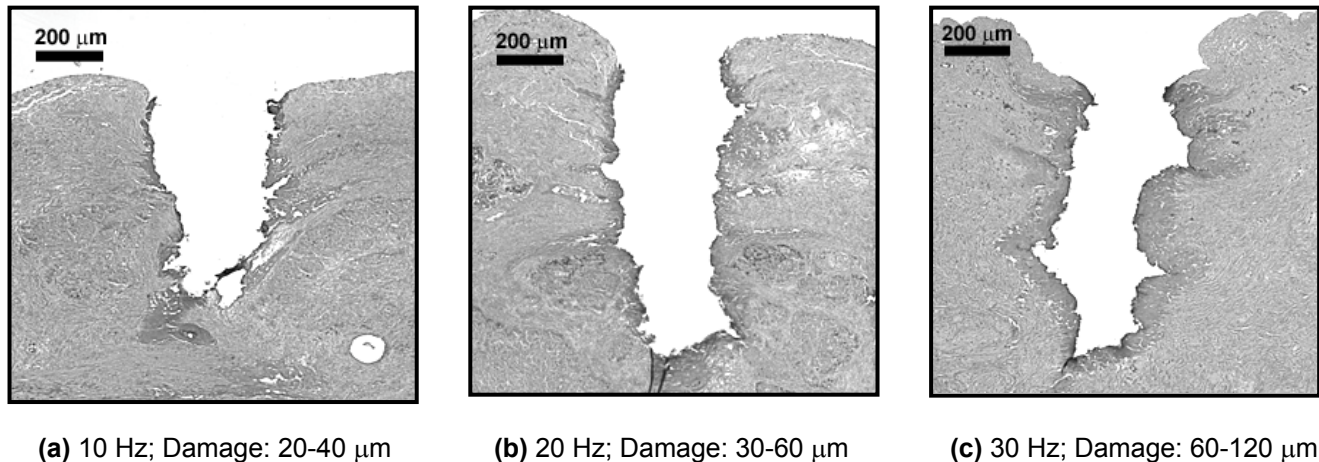

(a) 10 Hz; Damage: 20-40 μm   **(b)** 20 Hz; Damage: 30-60 μm   **(c)** 30 Hz; Damage: 60-120 μm

Figure 4. Photomicrographs showing H&E stained histologic cross-sections of urethral tissues ablated with the Er:YAG laser, ex vivo, with varying laser pulse repetition rates of 10–30 Hz. Energy was kept fixed at 10 mJ per pulse with a total of 20 pulses (200 mJ) delivered to the tissue. Note that there is a large increase in the thermal damage zone from 20 – 30 Hz, due to residual heat accumulation in the tissue during ablation.

Figure 4 shows that if the Erbium:YAG laser is operated at a pulse repetition rate higher than ~ 20 pulses per second, then the peripheral thermal damage to adjacent healthy tissue will increase and reach unacceptable levels, capable of causing increased scarring and increased probability of stricture recurrence.

The Er:YAG laser, operating at a pulse duration of ~ 70 μs, a fluence of 4 J/cm^2, and a repetition rate of 20 Hz, is capable of rapidly incising urethral tissues with minimal thermal and mechanical side-effects. The Er:YAG laser is more efficient than the Ho:YAG laser for cutting ureteral and urethral tissues, with perforation thresholds measuring 2 J/cm^2 vs. 34 J/cm^2, respectively. The Er:YAG laser is also more precise than the Ho:YAG laser, with peripheral thermal damage zones measuring 10-20 μm versus 300 μm, respectively.

Task 2.a. Test Damage Thresholds of Optical Fibers

Problem: Erbium:YAG laser energy (λ=2.94 μm) cannot be delivered through conventional silica optical fibers because glass does not transmit light at wavelengths beyond approximately 2.5 μm. Specialty mid-infrared optical fibers are needed to transmit the Er:YAG laser energy. Although there are several fibers available for delivery of mid-IR laser radiation, including chalcogenide, zirconium fluoride, sapphire, germanium oxide, and hollow silica waveguides, all of these delivery systems have major limitations. The ideal mid-IR optical fiber that combines high-power delivery, flexibility, chemical and mechanical durability, and biocompatibility, has yet to be developed.

Solution: The germanium oxide optical fiber is the most promising type of mid-infrared fiber for use in treating strictures because it is capable of delivering high laser power and it is the most flexible of the mid-IR fibers, making it suitable for use with flexible endoscopes in urology. The goal of this study was to determine the limitations of the germanium fiber, and identify how it can be improved for use as an optical fiber delivery system for the treatment of urethral and bladder neck strictures.

Methods

Laser ablation tests were conducted with 250- and 450-μm-core germanium fibers in contact with urological soft tissue samples. A total of 500 pulses was delivered to the tissue. Pre- and post-ablation fiber output energies were measured to determine whether any damage occurred to the fiber tip. An optical microscope was used to analyze the output ends of the germanium fibers for evidence of fiber tip degradation after contact tissue ablation.

Fiber Damage Thresholds

The fiber damage thresholds for the soft tissue studies were 4 mJ (7 J/cm^2) and 9 mJ (6 J/cm^2) for the 250 μm and 450 μm fibers, respectively (Figure 5). These values are above the threshold for perforating samples of ureteral tissue, 2 mJ (4.1 J/cm^2) and 5.1 mJ (3.7 J/cm^2), respectively. ***These results demonstrate that the germanium fiber can ablate soft tissues without fiber tip damage. However, the fiber is limited to operation at low energies during contact tissue ablation, which is not practical for clinical applications requiring rapid tissue ablation.***
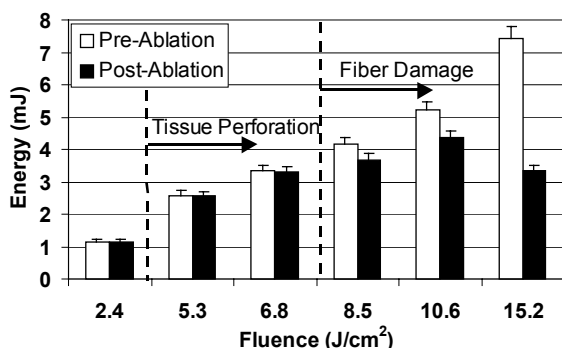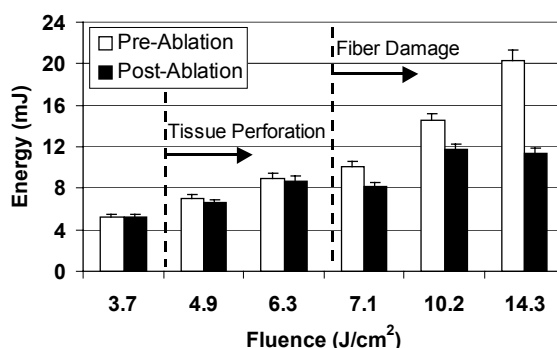
**(a)** 250 μm fiber **(b)** 450 μm fiber

Figure 5. Germanium fiber damage thresholds for (a) 250-μm-core fibers, and (b) 450-μm-core fibers, placed in direct contact with soft tissue. A total of 500 pulses were delivered with a pulse length of 70 μs and repetition rate of 10 Hz. Error bars signify a $\pm$ 5% variation in pulse to pulse energy stability.

Microscopic Analysis of Fiber Tips

The primary mechanism of germanium fiber damage during contact tissue ablation is melting of the fiber tip due to the high ablative temperatures. Figure 6 shows the fiber tips at different stages of meltdown, beginning with a normal tip surface, then particle formation, cracking and charring, and finally crystalline formation. During these phases, the fiber output energy also steadily dropped.
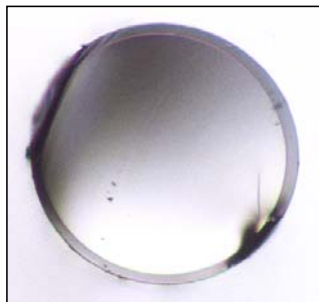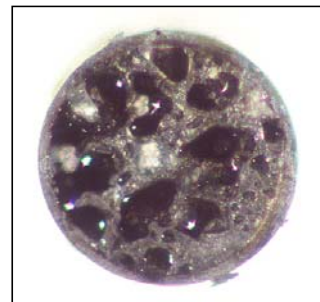

(a) **(b)** **(c)** **(d)**

Figure 6. Mechanism of germanium oxide fiber tip damage when tested in contact with tissue. (a) normal fiber tip, (b) particulate formation on the fiber tip, (c) cracking and charring, and (d) crystalline formation. The progressive deterioration is due to melting of the fiber tip when in contact with the tissue during high-temperature tissue ablation. Fiber tip damage was not observed during non-contact ablation studies. The parameters were: 450-μm-core fiber, 10 mJ/pulse, 70-μs-pulse duration, 10 Hz pulse repetition rate, and a total of 500 pulses.

Task 2.b. Design Side-Firing Laser Fibers for Incision of Urethral Wall.

Problem: In confined areas during endoscopic urology procedures, it may be difficult to bend the optical fiber to deliver the laser radiation to the tissue wall. In these cases, a side-firing fiber could be dragged across the tissue surface, delivering the laser radiation at a 90 degree angle for incision of the tissue. Unfortunately, side-firing fibers for use with the Er:YAG laser do not currently exist.
Solution: The goal of this study was to design a side-firing germanium oxide fiber for use with the Er:YAG laser. The germanium oxide trunk fiber tip was polished at a 45 degree angle, and a protective quartz cap was placed over the tip for use in contact tissue ablation.

Side-Firing Fiber Assembly

The side-firing germanium fiber was assembled by polishing the distal tip at a 45 degree angle using a fiber optic polisher (Fibrmet, Buehler, Lake Bluff, IL), and then placing a 1-cm-long quartz cap (CV7087Q, Vitrocom, Mountain Lakes, NJ) over the tip and fiber jacket (Figure 7). The quartz cap had an inner diameter, outer diameter, and wall thickness of 700 μm, 870 μm, and 85 μm, respectively. The entire fiber assembly had an outer diameter of less than 1 mm, for potential insertion through the working port of an endoscope.

Fiber damage tests were performed to determine the maximum output pulse energies that the side-firing germanium fibers could transmit. Preliminary tissue ablation studies were also performed using the 450-μm side-firing fiber for Er:YAG laser incision of tissue, ex vivo. The side-firing fiber was moved across the tissue surface in contact mode, creating 1-cm-long full-thickness incisions.
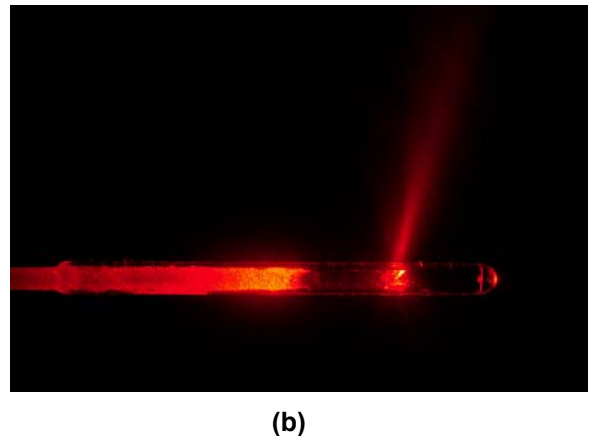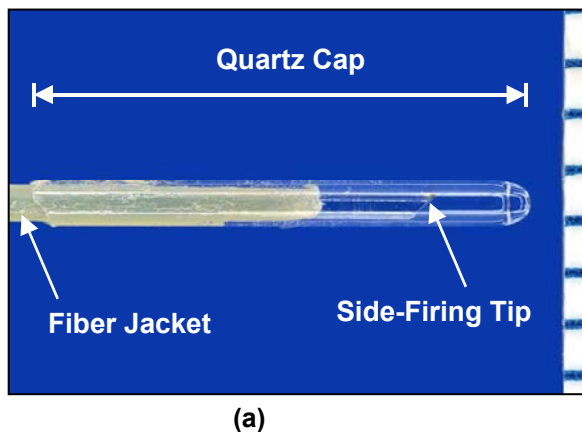

(a)   (b)

Figure 7. (a) Image of side-firing germanium oxide fiber tip with quartz cap. Scale bars on the right = 1 mm; (b) Image of red HeNe aiming beam delivered through side-firing fiber.
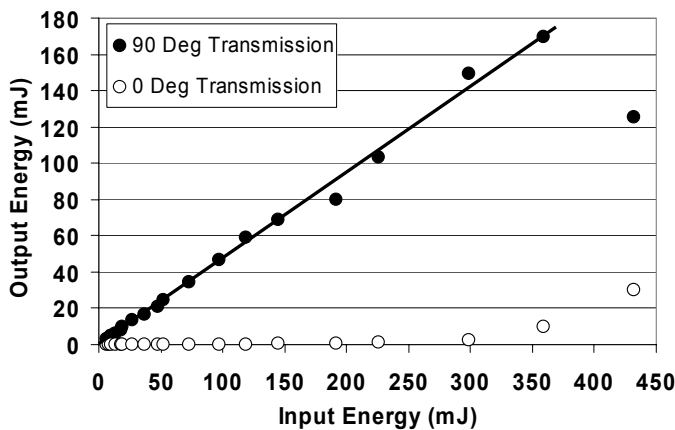
RESULTS

Fiber transmission and damage threshold studies were conducted with the side-firing germanium oxide fibers. Fiber transmission averaged 48 $\pm$ 4 % for the 1.45-m-long fibers, and the damage threshold was 149 $\pm$ 37 mJ at 3 Hz (n = 6 fibers). The maximum damage threshold measured for an individual fiber was 210 mJ.   These measurements are lower than the normal germanium oxide and hybrid germanium / silica fibers previously tested but still sufficient for contact tissue ablation (Table 1). For comparison, the transmission rate of the normal germanium trunk

fibers measured 66 $\pm$ 3 %. Figure 8a shows a plot of the transmission for a typical side-firing fiber. At the damage threshold, the transmission drops sharply, and the forward transmission increases sharply, as the angle-polished tip experiences damage. ***Figure 8b shows an H&E-stained histologic cross-section of urological tissue precisely incised using the Er:YAG laser and a side-firing germanium fiber with an output pulse energy of 80 mJ. Note that the thermal damage zone at edges of the incision measures only approximately 30 μm, as compared to a 300-μm thermal damage zone typically produced using the conventional Holmium:YAG laser.***
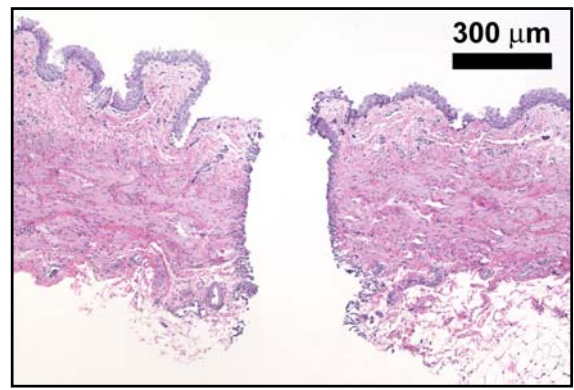
Table 1. Comparison of germanium fiber delivery systems for delivery of Er:YAG laser radiation at λ= 2.94 μm.

Fiber Type	Assembly Method	Damage Threshold (mJ)	Transmission (%)	N
Normal Germanium fiber	None	2000*	66 $\pm$ 3	5
Hybrid germanium/silica tip	Heat-shrink tubing / silica tip	180 $\pm$ 30	56 $\pm$ 3	7
Side-firing germanium	45° angle polish / quartz cap	149 $\pm$ 37	48 $\pm$ 4	6

* Commercial germanium oxide fibers are rated for use at up to 2 J / pulse at 10 Hz or 20 W by Infrared Fiber Systems.

(a) (b)

Figure 8. (a) Plot of transmission rate through side-firing fiber in both the 90 degree side and 0 degree forward directions. Damage to the fiber tip is clearly observed by a sharp drop in the side transmission and a corresponding sharp increase in the forward transmission, occurring at an output pulse energy of greater than 170 mJ for this fiber; (b) H&E-stained histologic cross-section of porcine ureteral tissue incised with the Er:YAG laser and a 450-μm side-firing germanium fiber at a pulse energy of 80 mJ. Note that the thermal damage zone at the edges of the incision measures only approximately 30 μm, as compared to a minimum thermal damage zone of 300 μm typically produced with the conventional Holmium:YAG laser in urology.

Task 2.c. Build Hybrid Optical Fibers that are both Flexible and Robust

Problem: Studies performed in Task 2.a. showed that the germanium fiber is limited to operation at very low Erbium:YAG laser energies when the fiber tip is in contact with tissue. This is a problem for laser treatment of strictures, which may require application of higher pulse energies for rapid and efficient incision of the urethra and bladder neck.

Solution: The goal of this study is to test a hybrid optical fiber with the Er:YAG laser, which combines the high-power transmission and flexibility of the germanium fiber with the robust and biocompatible low-OH silica fiber tips currently in clinical use with the Holmium:YAG laser. This study demonstrates that long hybrid fibers are capable of being assembled with a simple process that reduces many of the limitations associated with current mid-IR optical fibers, and that sufficient Er:YAG laser energy can be transmitted through these fibers during insertion into a flexible endoscope for use in applications requiring soft tissue ablation.

Hybrid Germanium / Silica Fiber Assembly

The hybrid fiber consisted of a 1-cm-long, 550-μm-core, low-OH silica fiber tip attached to either a 350-μm- or 450-μm germanium trunk fiber. For the initial fiber preparation, the germanium fiber jacket was softened using chemical treatment (1-methyl-2-pyrrolidinone at 150 $^{\circ}$C for 2 min. then isopropanol for 3 min.) and then stripped with a razor blade. The germanium and silica fibers were polished with rough 600-grit and then fine 5-micron sandpaper. The fibers were then aligned under a microscope using a laboratory-constructed mechanical setup.

Several different methods of attachment were explored (Figure 9). First, index-matching UV-cured optical epoxy (Norland, New Brunswick, NJ) was applied with a syringe needle either around the fibers or at the fiber interface (n = 10 fibers). Second, 30-gauge PTFE heat shrink tubing (normal ID=850 μm, shrunk ID=375 μm, wall thickness = 150 μm, length = 5 mm) was shrunk around the germanium/silica fiber interface using a heat gun (n = 10 fibers). The PTFE tubing (Small Parts, Miami Lakes, FL) also served the purpose of acting as a biocompatible jacket surrounding any exposed germanium fiber. Third, stainless steel hypodermic tubing (Small Parts, ID=0.675 mm, OD=1.05 mm) was used to align the fibers (n = 5 fibers). Fourth, glass capillary tubing (VitroCom, Mountain Lakes, NJ, ID=0.7 mm, OD=0.87 mm) was used for fiber attachment. Two attachment methods were explored: the fibers in contact at the interface (n = 10 fibers) or with an air gap (~200 μm) at the interface (n = 10 fibers).
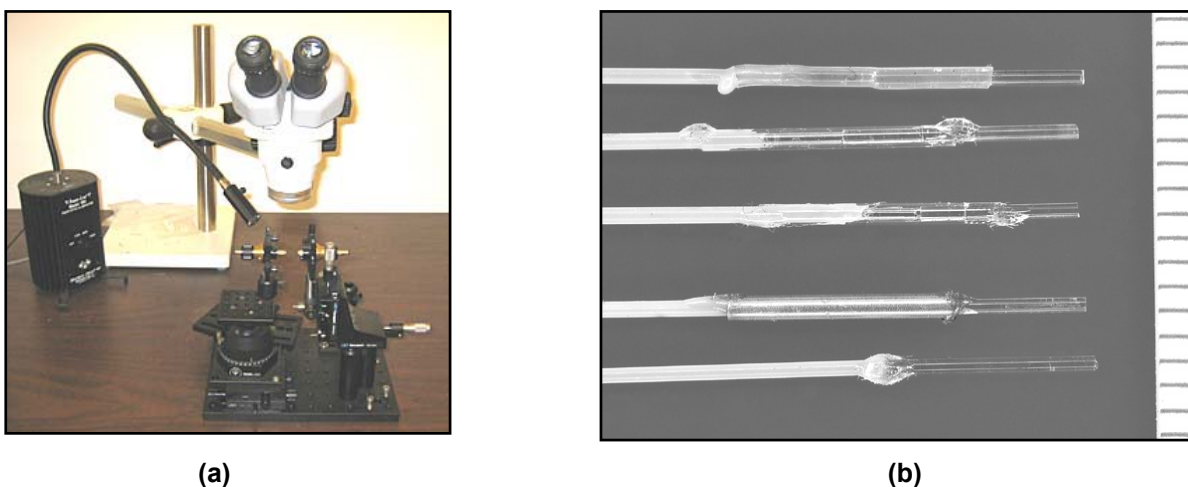

(a) **(b)**

Figure 9. (a) Experimental setup used to assemble the hybrid fibers. (b) Image of the germanium / silica hybrid fibers assembled using 5 different methods: (1) heat-shrink tubing, (2) glass capillary tubing, (3) glass tubing with an air gap at the fiber interface, (4) stainless steel hypodermic tubing, and (5) UV-cured optical epoxy. For all of the methods, an approximately 1 cm-long, 550-μm-core, low-OH silica tip was attached to a 450-μm-core germanium trunk fiber. Ball-shaped glue drops are present in Figures b-e at the interface between the yellow germanium jacket and the conduit material and at the interface between the silica tip and the conduit. The ruler lines = 1 mm.

To overcome the limitations of the germanium fiber for contact tissue ablation, a hybrid fiber consisting of a short low-OH silica fiber tip was attached to the germanium trunk fiber using several different methods. Table 2 shows the average output energy transmitted through the fiber for each of these methods before a drop in output energy was observed due to damage at the germanium / silica interface. The damage threshold for the germanium fiber without silica tip during contact soft tissue ablation is also included for comparison. ***Using the heat-shrink tubing method, hybrid fiber output energies measured 180 ± 30 mJ before fiber damage was observed (n=10), a 20-fold increase over the bare germanium fibers which damaged at only 9 mJ in contact with tissue (n=3).***

Table 2. Comparison of results for different methods used to construct germanium / silica hybrid fibers.

Assembly Method[a]	Maximum Pulse Energy (mJ)	N
Germanium tip only[b]	9 ± 1	3
Silica tip attached with:		
UV-cured epoxy	10 ± 5	10
Steel hypodermic tubing	109 ± 47	10
Glass capillary tubing:		
with air gap at interface	104 ± 38	10
without air gap at interface	139 ± 49	10
Heat-shrink tubing	180 ± 30	10

[a] All fibers were constructed using a 450-μm-core germanium trunk fiber and a 1-cm-long, 550-μm-core silica fiber tip. The fibers were tested using an Er:YAG laser with a 220 μs laser pulse length at 3 Hz.

[b] Values for the germanium fibers without silica tip represent maximum pulse energies achieved during contact soft tissue ablation. No problems were encountered during non-contact ablation.

Fiber Bending Tests

Preliminary fiber bending tests were conducted with germanium and sapphire optical fibers, ranging in core diameter from 150 – 500 μm. The fibers were inserted into a 15 Fr flexible cysto-urethroscope with a 7 Fr working channel. Basic fiber testing was performed to determine whether the fiber could withstand high mechanical stress under tight bending conditions and whether the fiber presence hindered maximum deflection of the scope. Peak Er:YAG energy transmission through the hybrid fibers was then measured for both straight and bent configurations.

Earlier tests showed that the sapphire optical fibers were more robust than the germanium fibers, as evidenced by the difference in their melting temperatures (2030 $^{\circ}$C versus 680 $^{\circ}$C) and the absence of fiber tip damage during contact soft tissue ablation. However, the sapphire fiber was not pursued further because both 250-μm- and 450-μm-core sapphire fibers suffered multiple fractures upon insertion into the flexible cysto-urethroscope under tight bending conditions (Table 3). While the 450-μm-core germanium fibers also fractured upon repeated bending, the 150-μm-, 250-μm-, and 350-μm-core germanium fibers suffered no mechanical damage under similar test conditions. Figure 10 shows a 350-μm-core germanium oxide fiber inserted through the 7 Fr working channel of a 15 Fr flexible cysto-urethroscope. The scope was deflected at a maximum angle corresponding to a bend radius of approximately 15 mm with and without the fiber inserted.

Table 3. Bending tests using 15 Fr flexible cysto-urethroscope with 7 Fr working channel and 15 mm bend radius.

Fiber Type / Core Size	Minimum Bend Radius[a]	Flexible Scope Breaking Test
Sapphire		
150 μm	20 mm	Passed
250 μm	30 mm	Failed
325 μm	60 mm	Not tested
425 μm	80 mm	Failed
Germanium Oxide		
150 μm	5 mm	Passed
250 μm	10 mm	Passed
350 μm	15 mm	Passed
450 μm	25 mm	Failed
500 μm	40 mm	Failed

[a] Minimum bend radius values taken from commercial literature (www.photran.com andwww.infraredfibersystems.com).
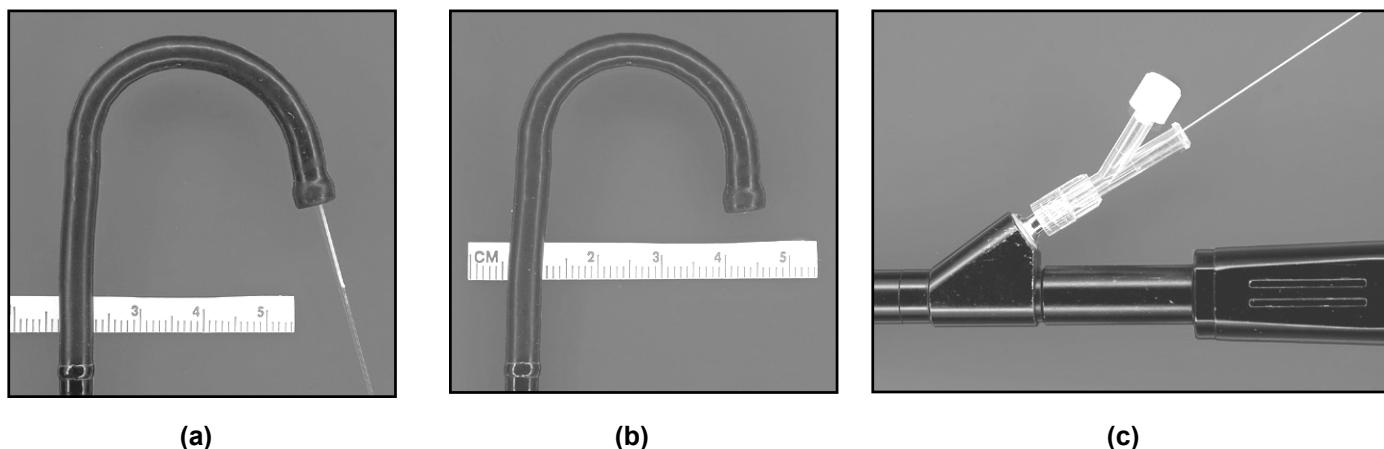
| **(a)** | **(b)** | **(c)** |

Figure 10. Images of 350-μm-core germanium/silica hybrid fiber inserted through 15 Fr flexible cysto-urethroscope with 7 Fr working channel. (a) The fiber is bent to 15-mm bend radius without breaking under maximum scope deflection. (b) Maximum deflection of the scope without fiber present corresponds to 15-mm bend radius, demonstrating that the fiber does not hinder scope deflection. (c) The fiber is successfully inserted at a 30-degree angle into the working channel.

Both the 350/550 and 450/550 germanium/silica hybrid fibers showed a significant decrease in energy output when bent to just above their minimum bending radius, 15 mm for the 350 μm trunk fiber and 25 mm for the 450 μm trunk fiber (Table 4). The damage mechanism was usually observed as sparking at the germanium/silica fiber interface, resulting in a melting of the germanium surface at the fiber interface, and noted as an immediate loss in energy greater than 5%. The difference in results between the 250-, 350- and 450-μm trunk fibers can be explained in part by the difference in the cross-sectional area at the germanium fiber tip. Assuming the melting temperature of the germanium fiber tip at the interface is the limiting factor, the maximum fluence that the interface can handle before melting is a function of both energy and fiber diameter. Thus, a larger trunk fiber diameter transmits greater energy, as observed in Table 4.

Table 4. Damage thresholds during germanium / silica fiber bending tests.

Fiber Core (μm) (Trunk / Tip)	Maximum Energy (mJ)		Bend Radius (mm)	N
	Straight	Bent		
450 / 550	180 $\pm$ 30	82 $\pm$ 20	30	10
350 / 550	93 $\pm$ 13	65 $\pm$ 20	20	10
250 / 365	27 $\pm$ 8	28 $\pm$ 9	20	8

Overall, our results show that by adding a robust silica fiber tip to the germanium fiber, fiber output energies may be increased to 180 $\pm$ 30 mJ (76 $\pm$ 13 J/cm^2) and 82 $\pm$ 20 mJ (35 $\pm$ 9 J/cm^2), in straight and tight bending configurations, respectively, without fiber damage. This represents a 20-fold increase over the 9 mJ (6 J/cm^2) peak energy achieved during testing of the bare germanium fiber in contact with soft tissue during Task 2.a (Figure 5b). These results demonstrate that the hybrid germanium / silica fiber transmits sufficient energy for contact soft tissue ablation through a flexible endoscope.

TASK #2.c (cont.): Build Hybrid Fibers

Problem: We previously designed hybrid germanium/silica fibers for use in endoscopic urology. However, it was necessary to further develop and optimize these fibers before routine use.

Solution: We explored different heat-shrink materials for attaching fiber tip to germanium trunk fiber, optimized power transmission through these fibers, and measured transmission rates and attenuation losses through fibers. The results demonstrated that there is sufficient transmission of Erbium laser energy for use in endoscopic applications including laser incision of the urethra.

METHODS

An SEO 1-2-3 laser, operated with either an Er:YSGG (λ = 2.79 μm) or an Er:YAG (λ = 2.94 μm) laser rod, was used for the experiments. The laser was operated in free-running mode with a 300 μs pulse length and in short-pulse mode with a 500 ns pulse length produced by a rotating mirror Q-switch. The Q-switched Er:YAG and Er:YSGG laser pulse energy measured 25 mJ at 3 Hz. The laser radiation was focused with a 20-mm-FL CaFl lens into hybrid germanium/silica optical fibers consisting of a 1-m-length germanium trunk fiber (IFS, Silver Spring, MD) with a 1-cm-length low-OH silica fiber tip. The trunk/tip fiber-core diameters measured 250/365, 350/365, and 450/550 μm and were attached with three different types of heat-shrink tubing: (a) PTFE, (b) PET, and (c) PTFE / FEP combination (Table 5, Figure 11). A linear fit to the data points provided the ave. % transmission of the fibers, which was then corrected by subtracting the Fresnel losses, and the attenuation calculated in dB/m. The data points represent the ave. of 7 independent measurements from 7 different fibers, and the error bars represent the minimum and maximum values recorded.

Table 5. Heat-shrink tubing materials used to connect hybrid fibers.

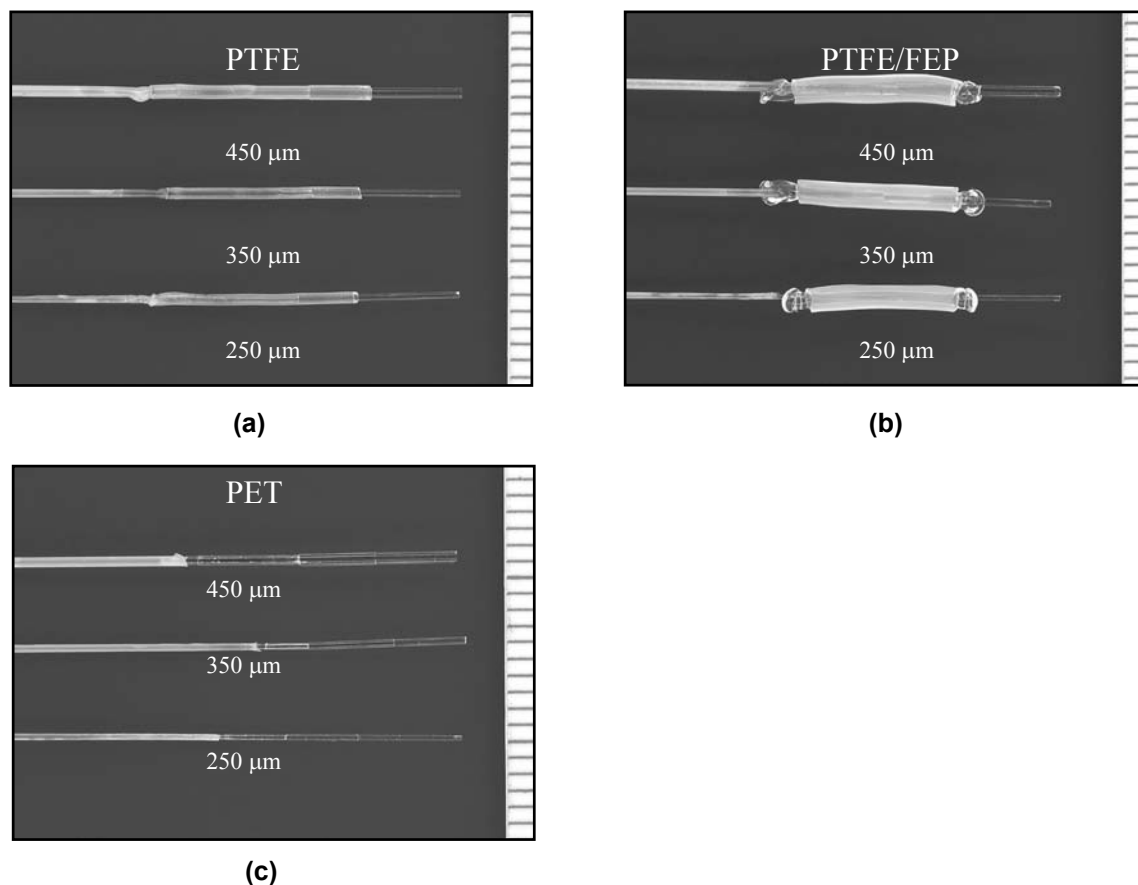| Material	Pre-/Post-Shrink ID (μm)	Wall Thickness (μm)	Shrink Temp. (^{o}C)
PTFE	850 / 375	150	343
PTFE / FEP	900 / 0	575	343 / 17
PET	350 / 280	12.5	85-190
	450 / 360	12.5	
	725 / 580	25	

(a)

(b)

(c)

Figure 11. Hybrid germanium/silica fibers assembled using: (a) PTFE; (b) PTFE / FEP; (c) PET. A 1-cm-long, silica tip was attached to a 1-m-long germanium fiber. Germanium fiber diameters are 450, 350, and 250 μm. Ruler bar = 1 mm increments.

RESULTS

Hybrid Fiber Assembly

PTFE was the most reliable material producing the highest Er:YAG pulse energy transmission, although the high shrink temperature resulted in melting of Hytrel coating on the germanium fiber (Figure 11a). The PTFE / FEP shrink-melt combination produced the worst results. The shrink pressure and melted FEP pushed the silica tip away from the germanium trunk fiber, causing poor alignment at the fiber interface and resulting in poor laser transmission and low damage thresholds (Figure 11b). The major limitation of the PET tubing was its wall thickness (12.5 – 25 μm), which results in weak bending strength (Figure 11c). PET is also limited to ~ 20% shrinkage, so the trunk and tip fiber outer diameters need to match more precisely than with PTFE. However, PET has some advantages: its low shrink temperature eliminates melting of germanium Hytrel jacket, its transparency provides better alignment of fiber interface, and it shrinks more uniformly than PTFE.

Peak Output Energies

Maximum hybrid fiber transmission of free-running Er:YAG laser radiation was measured (Table 6). The peak fiber transmission was ~ 100 J/cm^2 for all of the fiber diameters (250/365, 350/365, 450/550) tested, with pulse energies reaching as high as 233 mJ at 10 Hz. Average fiber transmission measured ~ 70 J/cm^2 for these fiber diameters. Transmission of Q-switched Er:YAG laser energy was also measured through 450/550 hybrid fibers, with peak pulse energies of 13 mJ.

Table 6. Peak and average Er:YAG pulse energies transmitted through hybrid germanium / silica fibers.

Fiber Core (μm) (Trunk / Tip)	Maximum		Average	
	Energy (mJ)	Fluence (J/cm^2)	Energy (mJ)	Fluence (J/cm^2)
250 / 365	103	98	74 $\pm$ 29	71
350 / 365	112	107	79 $\pm$ 24	75
450 / 550	233	98	157 $\pm$ 46	66

Transmission and Attenuation Measurements

The % transmission of free-running and Q-switched Er:YAG and Er:YSGG laser radiation through 1-m-long germanium fibers with a 1-cm-length silica tip was measured (Figure 12). Transmission rates for the free-running Er:YAG and Er:YSGG lasers measured 56% and 65%, respectively (n = 7 fibers). After correction for Fresnel reflection losses at the fiber interfaces, the attenuation was 1.1 $\pm$ 0.1 dB/m and 0.6 $\pm$ 0.1 dB/m, respectively. The transmission rate for the Q-switched Er:YAG and Er:YSGG lasers was 55% and 65%, with an attenuation of 1.1 $\pm$ 0.2 dB/m and 0.9 $\pm$ 0.3 dB/m, respectively. Both Q-switched lasers transmitted a maximum pulse energy of 13 mJ (n = 7 fibers).
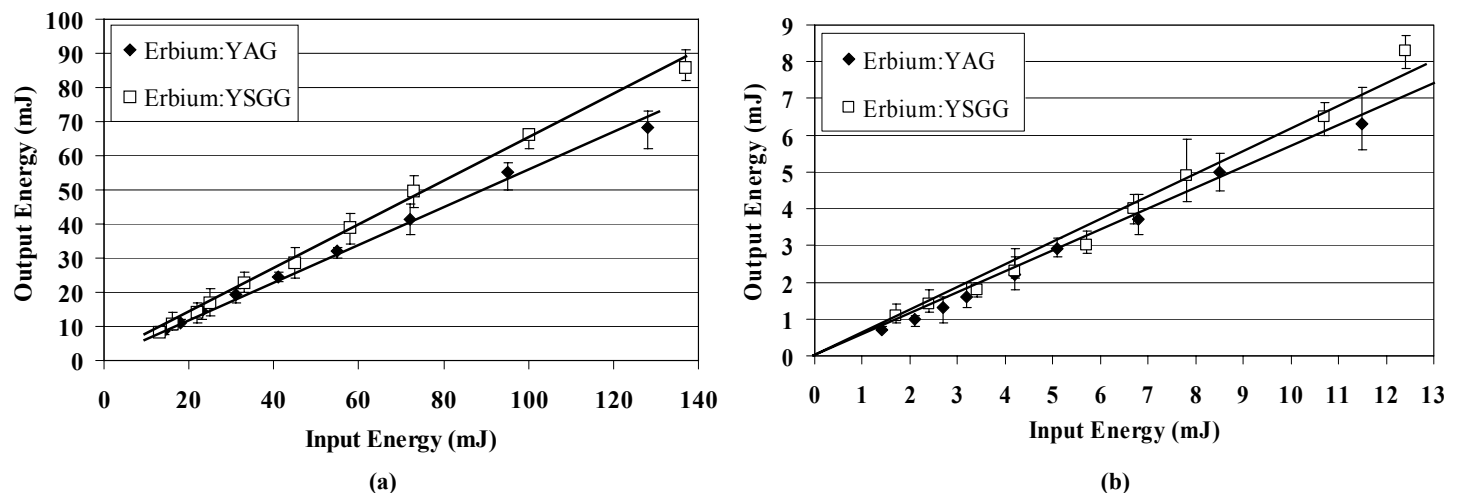

Figure 12. Hybrid fiber transmission rates for Er:YAG and Er:YSGG laser radiation during (a) free-running (300 μs) and (b) Q-switched (500 ns) operation. All fibers tested were 450 / 550 μm hybrid fibers.

In this study, we demonstrated a simple, biocompatible, and inexpensive method of assembling hybrid germanium/silica fibers using PTFE heat-shrink tubing. Peak hybrid fiber energies of up to 233 mJ at 10 Hz were transmitted through the fibers with the fluence reaching approximately 100 J/cm^2 for all the fiber diameters (250/365, 350/365, 450/550) tested. Although average pulse energies were lower and bending losses have previously been recorded, transmitted energies are still well above what is necessary for Er:YAG laser ablation of most soft tissues, which typically only require a fluence of 1-5 J/cm^2.

Tables 7 and 8 provide a comparison of free-running and Q-switched Er:YAG and Er:YSGG laser fiber transmission and attenuation between the hybrid fibers and previous studies characterizing the bare germanium and sapphire fibers. The attenuation through the hybrid fiber is significantly higher than that through the germanium and sapphire fibers. This is most likely due to coupling losses at the germanium / silica interface as well as the high attenuation through the silica tip. However, considering the relatively low pulse energies necessary to ablate tissue (a few mJ), the availability of high-power Erbium lasers (Joules/pulse), and the need for only a few meters of fiber length for most medical applications, a fiber attenuation of 0.6 – 1.1 dB/m is more than adequate.

Table 7. Percent transmission of Er:YAG and Er:YSGG laser radiation through mid-IR fibers.

Fiber Type/Size	Er:YSGG (λ = 2.79 μm)		Er:YAG (λ = 2.94 μm)	
	Free-running	Q-switched	Free-running	Q-switched
Sapphire (425)	88 $\pm$ 6	65 $\pm$ 3	77 $\pm$ 5	74 $\pm$ 4
Germanium (450)	76 $\pm$ 2	57 $\pm$ 1	68 $\pm$ 2	64 $\pm$ 6
Hybrid (450/550)	65 $\pm$ 2	62 $\pm$ 5	56 $\pm$ 3	55 $\pm$ 4

Table 8. Attenuation (dB/m) of Er:YAG and Er:YSGG laser radiation through mid-IR fibers.

Fiber Type/Size	Er:YSGG (λ = 2.79 μm)		Er:YAG (λ = 2.94 μm)	
	Free-running	Q-switched	Free-running	Q-switched
Sapphire (425)	0.2 $\pm$ 0.1	1.0 $\pm$ 0.2	0.4 $\pm$ 0.2	0.6 $\pm$ 0.2
Germanium (450)	0.3 $\pm$ 0.1	1.3 $\pm$ 0.1	0.7 $\pm$ 0.1	0.9 $\pm$ 0.3
Hybrid (450/550)	0.6 $\pm$ 0.1	0.9 $\pm$ 0.3	1.1 $\pm$ 0.1	1.1 $\pm$ 0.2

A novel, hybrid germanium oxide/silica optical fiber was optimized for delivery of free-running and Q-switched Er:YAG and Er:YSGG laser radiation. Peak fiber transmission and attenuation was measured. Sufficient Erbium laser energy was transmitted for use in soft tissue ablation. This optical fiber is useful in endoscopic applications requiring a flexible fiber for contact tissue ablation, such as incision of urethral and bladder neck strictures.

TASK #3.a. Acute In Vivo Studies for Comparison with Ex Vivo Results

Problem: Previous ex vivo tissue studies demonstrated that the Erbium laser was capable of precise incision of urethral tissue with a thermal damage zone of only 10-20 μm. This thermal damage zone was much less than that of the Holmium laser which produced 300 μm of thermal damage. However, it is necessary to perform more realistic in vivo animal studies to determine whether differences in tissue hydration and perfusion will effect our results.

Solution: We performed in vivo animal studies in a pig animal model using both the Erbium and Holmium lasers. H&E stained histologic cross-sections of the tissue were examined using optical microscopy and the thermal damage zone measured quantitatively. Collateral thermal damage at Day 0 measured 20 $\pm$ 5 μm for the Erbium laser and 660 $\pm$ 110 μm for the Holmium laser, thus verifying that the Erbium laser results are comparable to previous ex vivo results, and also much better than the conventional Holmium laser.

TASK #3.b. Short-term Chronic Wound Healing Study

Problem: Although Er:YAG laser produced minimal thermal damage during incision of urethra and bladder neck, it is unclear how this damage will translate into scar formation during wound healing.
Solution: Short-term, chronic wound healing studies were performed in pigs to 14 days, to quantify scar formation after Holmium:YAG and Er:YAG laser incision. We observed 4 times less scarring after Er:YAG laser incision of healthy urethra and bladder neck as compared with the Ho:YAG laser, after 14 days of wound healing. The Er:YAG laser incisions also healed twice as rapidly as Ho:YAG laser incisions. For any given day of wound healing, there was also less granulation tissue and smaller incision depth for Er:YAG laser than Ho:YAG laser.

METHODS:
Laser Parameters
An Er:YAG laser (λ = 2.94 μm) with a pulse duration of 70 μs, fiber output pulse energy of 20 mJ, and repetition rate of 10 Hz was used. The laser radiation was focused into a 250-μm-core sapphire optical fiber (Photran, Amherst, NH).   A Ho:YAG laser (SEO 1-2-3) operating at a wavelength of 2.12 μm, pulse duration of 300 μs, fiber output energy of 500 mJ, and repetition rate of 3 Hz, was also used. The laser radiation was focused into a 300-μm silica optical fiber (Table 9).

Table 9. Summary of laser parameters used in this study.

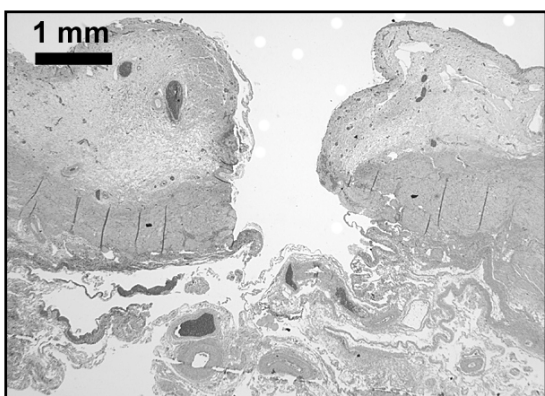| Laser Parameters	Holmium	Erbium
Wavelength (μm):	2.12	2.94
Energy / pulse (mJ):	500	20
Pulse Length (μs):	300	70
Pulse Repetition Rate (Hz):	3	10
Fiber Core Diameter (μm):	300	250
Fiber Type:	silica	sapphire

Animal Studies
All procedures were approved by the JHU Animal Review Committee (ACR# SW01M293). A total of 18 female pigs (30-45 kg) were divided into two arms, with 9 pigs in each laser arm. Three animals in each arm were sacrificed on postop days 0, 6, and 14. Access to the urethra and bladder neck was obtained using a 17F rigid cystoscope with 30-degree lens. Three 1-cm-long incisions were made in each pig, two at the bladder neck and one in the mid-urethra. After the procedure a 14F urethral catheter was left in bladder then removed after 3-4 hours. The pigs were euthanized, and the bladder and urethra samples were removed for histopathological processing. Measurements of collateral injury and incision depth were made. Collateral damage on day 0 was recorded as coagulative necrosis from the incision outward, while on days 6 and 14 as the extent of granulation width at wound base. These parameters were analyzed using a Student's t-test.
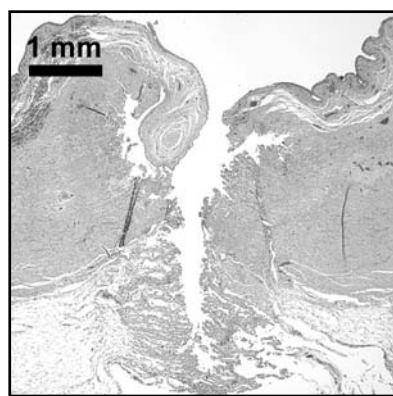
RESULTS
On day 0, Er:YAG and Ho:YAG laser incisions in mid-urethra and bladder neck were of comparable depth, 2540 $\pm$ 390 μm and 2530 $\pm$ 780 μm (p = 0.49) (Table 10). The coagulative necrosis zone (Figure 13a-b) was higher for Ho:YAG than for Er:YAG (660 $\pm$ 110 μm vs 20 $\pm$ 5 μm, p = 0.01). On day 6 (Figure 13c-d), granulation tissue width at incision base was 900 $\pm$ 100 μm and 2280 $\pm$ 700 μm, for Er:YAG and Ho:YAG lasers (p = 0.04). After 14 days granulation tissue created by Er:YAG was less than Ho:YAG laser (430 $\pm$ 100 μm vs 1580 $\pm$ 250 μm, p = 0.03) (Figure 13e-f). As wound healing progressed, granulation tissue filled the wound bed and decreased incision depth. At day 6, Er:YAG and Ho:YAG laser incisions were 45% and 60% of initial depth (1100 $\pm$ 200 μm vs 1500 $\pm$ 300 μm, p = 0.04). On day 14, Er:YAG and Ho:YAG incisions were 25% and 50% of initial depth (670 $\pm$ 140 μm vs 1240 $\pm$ 140 μm) (p = 0.02). Images of tissue surface at 14 days demonstrate accelerated wound healing after Er:YAG incision compared with Ho:YAG incision (Figure 14a-b).

Table 10. Injury parameters after incisions made with Ho:YAG and Er:YAG lasers at day 0, 6, and 14.
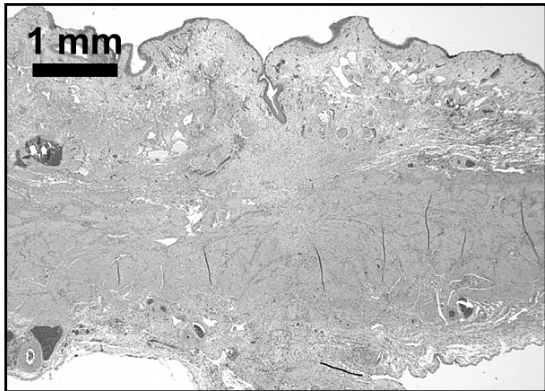
Laser	n	Day 0		n	Day 6		n	Day 14	
		Incision Depth (μm)	Thermal Damage (μm)		Incision Depth (μm)	Granulation Width (μm)		Incision Depth (μm)	Granulation Width (μm)
Holmium	3	2530 ± 780	660 ± 110	3	1500 ± 300	2280 ± 700	3	1240 ± 140	1580 ± 250
Erbium	3	2540 ± 390	20 ± 5	3	1100 ± 200	900 ± 100	3	670 ± 140	430 ± 100
P value		0.49	0.01		0.04	0.04		0.02	0.03

(a) Er:YAG, Day 0

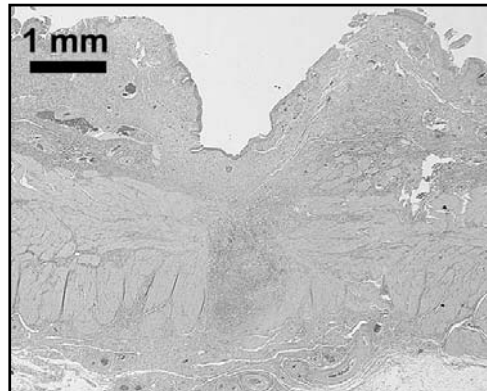**(b)** Ho:YAG, Day 0

(c) Er:YAG, Day 6
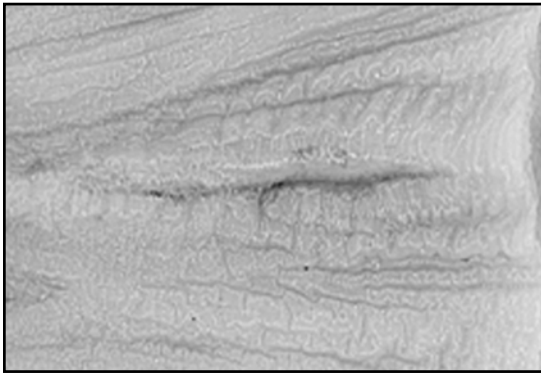

(d) Ho:YAG, Day 6
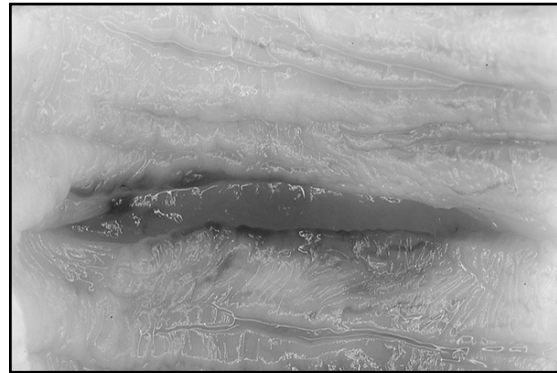

(e) Er:YAG, Day 14

(f) Ho:YAG, Day 14

Figure 13. H&E stained histologic cross-sections of incisions made with the Er:YAG and Ho:YAG laser on post-operative days 0, 6, and 14. Arrows demarcate the border between native tissue and thermally coagulated tissue.

(a) Er:YAG, Day 14   **(b)** Ho:YAG, Day 14

Figure 14. Images of incisions made with Er:YAG and Ho:YAG lasers at day 14. (a) Er:YAG; (b) Ho:YAG.

This study confirms the minimal collateral thermal damage caused acutely by the Er:YAG laser by gross and histologic examination. Histologic examination demonstrated that the Er:YAG laser produced approximately four times less scar tissue than the Ho:YAG laser. The granulation zone and incision depth were also less in the Er:YAG laser arm than in the Ho:YAG laser for a given POD. Incisions made with the Er:YAG laser healed twice as rapidly as those with the Ho:YAG laser. This difference was also observed with tissue examination prior to formalin fixation. Er:YAG laser incisions at day 14 were difficult to identify because of almost complete healing.

KEY RESEARCH ACCOMPLISHMENTS

- Determined the energy threshold for Erbium:YAG laser ablation of urethral tissues.

- Constructed a chart measuring tissue removed per a laser pulse as a function of laser energy and pulse duration. This chart is important because during clinical studies it will provide the urologist with a method for choosing and predicting how deep to make the laser incision, based on the laser energy level and number of laser pulses delivered to the tissue. Thus, a laser incision in the scar tissue can be made without cutting too deep into healthy tissue.

- Decreased the peripheral thermal damage zone in urethral tissue caused by the Erbium laser by a factor of 2, from 30-60 μm to 15-30 μm. For comparison, the Holmium laser currently used in urology for incision of urethral and bladder neck strictures causes a minimum of 300-400 μm of thermal damage. Thus, our Erbium laser is 10-20 times more precise than the Holmium laser.

- Increased the rate of Erbium laser tissue cutting rate by a factor of 2, by reducing the laser pulse length from 220 to 70 μs. This will result in more rapid and efficient tissue cutting for clinical use.

- Determined the damage threshold and damage mechanism for the germanium optical fibers when used in contact mode for tissue ablation. This will allow the urologist to operate the laser at laser parameters that provide rapid and precise incision of tissue, without concern about permanently damaging the optical fiber delivery system.

- Constucted side-firing germanium oxide fibers with a quartz cap for 90 degree delivery of the laser radiation to the tissue in contact mode.

- Constructed hybrid germanium / silica optical fiber delivery system capable of being used with flexible endoscopes for laser incision of strictures. Damage threshold of the hybrid fibers was measured to be 20 times greater than that of conventional germanium oxide fibers alone, making contact fiber optic tissue cutting feasible.

- Determined the transmission losses of the hybrid germanium / silica fibers when used in a bent configuration. These studies define the limits of the fiber when used in extreme bending configurations in flexible scopes, thus avoiding fibers from breaking and permanently damaging the endoscope.

- Characterized the hybrid fiber transmission rate, attenuation rate, and maximum pulse energy that the fiber can deliver for endoscopic applications in urology. The hybrid fiber was improved to deliver a maximum of 233 mJ of Erbium:YAG laser energy per pulse at a repetition rate of 10 Hz, and with fiber attenuation of only ~ 1 dB/m, more than sufficient for our medical application.

- Acute, *in vivo*, thermal damage zones measured 20 $\pm$ 5 μm for the Erbium:YAG laser (comparable to previous *ex vivo* results of 10-20 μm), much smaller than 660 $\pm$ 110 μm for Holmium:YAG laser. This result confirms our previous, *ex vivo*, studies reporting that the Erbium:YAG laser is 20-30 times more precise than the Holmium:YAG laser for incision of the urethra and bladder neck.

- Demonstrated that there is 4 times less scarring after Erbium:YAG laser incision of healthy urethra and bladder neck as compared with the Holmium:YAG laser, after 14 days of wound healing in a pig model. The Erbium:YAG laser incisions also healed twice as rapidly as Holmium:YAG laser incisions. For any given day of wound healing, there was less granulation tissue and smaller incision depth for Erbium:YAG laser than Holmium:YAG laser.

REPORTABLE OUTCOMES

<u>**MANUSCRIPTS**</u>

1. **Fried NM**, Tesfaye Z, Ong AM, Rha KH, Hejazi P. Optimization of the erbium:YAG laser for precise incision of ureteral and urethral tissues: in vitro and in vivo results. <u>Lasers in Surgery and Medicine</u> 33:108-114, 2003. (cover article)

2. Chaney CA, Yang Y, **Fried NM**. Hybrid germanium / silica optical fibers for endoscopic delivery of Erbium:YAG laser radiation. <u>Lasers in Surgery and Medicine</u> 34(1):5-11, 2004.

3. **Fried NM**, Tesfaye Z, Ong AM, Rha KH, Hejazi P. Variable pulsewidth Erbium:YAG laser ablation of the ureter and urethra in vitro and in vivo: optimization of the laser fluence, pulse duration, and pulse repetition rate. <u>Proc. SPIE: Lasers in Surgery 14</u> 5312:105-111, 2004.

4. Chaney CA, Yang Y, **Fried NM.** Assembly and testing of germanium / silica optical fibers for flexible endoscopic delivery of Erbium:YAG laser radiation. <u>Proc. SPIE: Optical Fibers and Sensors for Medical Applications 4</u> 5317:1-8, 2004.

5. Levin K, Tran D, Tchapijnikov A, **Fried NM**. Specialty fiber expands infrared laser applications. <u>Biophotonics International</u> 11(4):41-43, 2004. (cover article)

6. **Fried NM**, Yang Y, Chaney CA, Fried D. Transmission of Q-switched Erbium:YSGG and Erbium:YAG laser radiation through germanium oxide and sapphire optical fibers at high pulse energies. <u>Lasers in Medical Science</u> 19(3):155-160, 2004.

7. Varkarakis IM, Inagaki T, Allaf ME, Chan TY, Rogers CG, Wright EJ, **Fried NM**. Comparison of Erbium:YAG and Holmium:YAG lasers for incision of the urethra and bladder neck in a chronic porcine model. <u>Urology</u> 65(1):191-195, 2005.

8. **Fried NM**, Yang Y, Lee K, Tafti HA. Transmission of free-running and Q-switched Er:YAG laser energy through germanium / silica fibers. <u>Proc. SPIE: Optical Fibers and Sensors for Medical Applications 5</u> 5691:155-119, 2005.

9. Varkarakis IM, Inagaki T, Allaf ME, Chan TY, Rogers CG, Wright EJ, **Fried NM**. Erbium vs. Holmium laser incision of urethra and bladder neck. <u>Proc. SPIE: Photonic Therapeutics and Diagnostics</u> 5686:171-175, 2005.

10. Ngo AK, **Fried NM**. Delivery of Erbium:YAG laser radiation through side-firing germanium oxide fibers. <u>Proc. SPIE</u>. In press.

11. Ngo AK, **Fried NM**. Side-firing germanium oxide optical fibers for use with the Erbium:YAG laser. <u>Journal of Endourology</u>. In review.

<u>**ABSTRACTS**</u>

1. **Fried NM**, Ong AM, Rha KH, Tesfaye Z, Hejazi P. Erbium:YAG laser incision of the ureter and urethra: optimization of the laser parameters. <u>Journal of Endourology</u> 17(9):832, 2003.

2. **Fried NM**, Chaney CA. Hybrid germanium / silica optical fibers for flexible endoscopic delivery of high-power Erbium:YAG laser radiation. <u>Journal of Endourology</u> 17 (Suppl. 1):A40, 2003.

3. **Fried NM**, Yang Y, Chaney CA. Comparison of sapphire & germanium fibers for transmission of Q-switched & long-pulse Er:YSGG & Er:YAG laser radiation. <u>J Endourology</u>18(7):696-697, 2004.

4. Varkarakis IM, Inagaki T, Allaf ME, Rogers CG, **Fried NM**. Comparison of Erbium:YAG and Holmium:YAG lasers for incision of the urethra and bladder neck: an in vivo chronic study in pigs. <u>Journal of Endourology</u> 18(7):698-699, 2004. [2nd place, best poster competition in basic science, Engineering and Urology Society Meeting, San Francisco, CA, May 2004.]

<u>CONCLUSIONS</u>

In the first year of this research project, we accomplished several objectives. First, we demonstrated that the Erbium:YAG laser is more precise than the Holmium:YAG laser (currently the laser of choice in urology) for incision of urethral tissue. The Erbium laser produced a factor of 20 times less peripheral thermal damage to adjacent healthy tissue than does the Holmium laser (15-30 μm for the Erbium versus 300-400 μm for the Holmium laser). This result is important because the amount of thermal damage is believed to be a major factor in causing tissue scarring during wound healing and stricture recurrence. Second, we constructed a novel optical fiber delivery system for delivering the Erbium laser radiation through either a rigid or flexible endoscope for use in minimally invasive laser treatment of strictures. This hybrid optical fiber combines the high laser power transmission of the germanium oxide fiber optic material used as a "trunk" fiber with a robust fiber tip made of silica, and able to withstand high laser powers without damaging.

In the second year of this research project, we accomplished several aims. First, we demonstrated in an acute, *in vivo* pig model that the thermal damage zones measured only 20 $\pm$ 5 μm for the Erbium:YAG laser, comparable to previous *ex vivo* results of 10-20 μm, and much smaller than 660 $\pm$ 110 μm for Holmium:YAG laser. This result confirms our previous, *ex vivo*, studies reporting that the Erbium:YAG laser is 20-30 times more precise than the Holmium:YAG laser for incision of the urethra and bladder neck. We also performed short-term, chronic wound healing studies and discovered that there was 4 times less scarring after Erbium:YAG laser incision of healthy urethra and bladder neck as compared with the Holmium:YAG laser after 14 days. The Erbium:YAG laser incisions also healed twice as rapidly as Holmium:YAG laser incisions. For any given day of wound healing, there was less granulation tissue and smaller incision depth for Erbium:YAG laser than Holmium:YAG laser. We then worked on further improving the optical fiber delivery system for the Erbium laser. We characterized the hybrid fiber transmission rate, attenuation rate, and maximum pulse energy that the fiber can deliver for endoscopic applications in urology. The hybrid fiber was improved to deliver a maximum of 233 mJ of Erbium:YAG laser energy per pulse at a repetition rate of 10 Hz, and with fiber attenuation of only ~ 1 dB/m, more than sufficient for our medical application.

In the third year of this research project, we continued the development of the optical fiber delivery system, with the assembly of side-firing germanium fibers for use with the Er:YAG laser in the urological tract. In collaboration with Infrared Fiber Systems, inc. (Silver Spring, MD) we have applied for and received funding from the National Institutes of Health Phase II SBIR program (2R44EY013889-02) for commercialization of the hybrid germanium oxide / silica optical fiber delivery system developed in part from this DOD grant. The NIH award is a 2-year, $750,000 grant. We have also initiated collaboration with the Davison Medical Laser Center at Elliot Hospital in Manchester, NH, to begin clinical studies with the Er:YAG laser for treating urethral strictures. We have requested and received from the FDA, 510K clearance for use of a commercially available Erbium:YAG laser (Sciton, Palo Alto, CA) and optical fiber delivery system for treating strictures. A research protocol has been submitted and IRB approval granted. Initial clinical studies began Jan. 16, 2006.

REFERENCES

1. R. A. Santucci, J. W. McAninch, "Urethral reconstruction of strictures resulting from treatment of benign prostatic hypertrophy and prostate cancer," Urol. Clin. North Am., vol. 29, pp. 417-427, 2002.
2. C. F. Heyns, J. W. Steenkamp, M. L. De Kock, P. Whitaker, "Treatment of male urethral strictures: is repeated dilation or internal urethrotomy useful?," J. Urol., vol. 160, pp. 356-358, 1998.
3. P. Albers, J. Fichtner, P. Bruhl, S. C. Muller, "Long-term results of internal urethrotomy," J. Urol., vol. 156, pp. 1611-1614, 1996.
4. G. H. Jordan, S. M. Schlossberg, C. J. Devine, "Surgery of the penis and urethra," In P. C. Walsh, A. B. Retik, E. D. Vaughan, A. J. Wein (Eds): Campbell's Urology. 7th ed, Philadelphia, W. B. Saunders, vol 3, pp 3341-3347, 1998.
5. T. A. McNicholas, J. Colles, S. G. Bown, J. E. A. Wickham et al, "Treatment of urethral strictures with a prototype CO_2 laser endoscope," Lasers Med. Sci., vol. 3, p. 427, 1988.
6. H. C. Becker, J. Miller, H. D. Noske, J. P. Klask, W. Weidner, "Transurethral laser urethrotomy with argon laser: experience with 900 urethrotomies in 450 patients," Urol. Int., vol. 55, pp. 150-153, 1995.
7. J. A. Smith Jr., "Treatment of benign urethral strictures using a sapphire tipped neodymium:YAG laser," J. Urol., vol. 142, pp. 1221-1222, 1989.
8. P. N. Dogra, G. Nabi, "Core-through urethrotomy using neodymium: YAG laser for obliterative urethral strictures after traumatic urethral disruption and/or distraction defects:long-term outcome," J. Urol., vol.167, pp.543-546, 2002.
9. P. J. Turek, T. R. Malloy, M. Cendron, V. L. Carpiniello, A. J. Wein AJ, "KTP-532 laser ablation of urethral strictures," Urology, vol. 40, pp. 330-334, 1992.
10. A. R. Kural, E. R. Coskuner, I. Cevik, "Holmium laser ablation of recurrent strictures of urethra and bladder neck: preliminary results," J. Endourol., vol. 14, pp. 301-304, 2000.
11. B. A. Laven, R. C. O'Connor, G. D. Steinberg, G. S. Gerber, "Long-term results of antegrade endoureterotomy using holmium laser in patients with ureterointestinal strictures," Urology, vol. 58, pp. 924-929, 2001.
12. K. Matsuoka, M. Inoue, S. Lida, K. Tomiyasu, S. Noda, "Endoscopic antegrade laser incision in the treatment of urethral stricture," Urology, vol. 60, pp. 968-972, 2002.
13. T. Niesel, R. G. Moore, H. J. Alfert, L. R. Kavoussi, "Alternative endoscopic management in the treatment of urethral strictures," J. Endourol., vol. 9, pp. 31-39, 1995.
14. **N. M. Fried**, "Potential applications of Er:YAG laser in endourology," J. Endourol.,vol. 15, pp.889, 2001.
15. **N. M. Fried**, Z. Tesfaye, A. Ong, Koon H. Rha, Pooya Hejazi, "Optimization of Er:YAG laser for incision of ureteral & urethral tissues: in vitro & in vivo results," Lasers Surg Med, vol. 33, pp.108-114, 2003.
16. **N. M. Fried**, "Potential applications of Er:YAG laser in endourology," J. Endourol., vol. 15, 889, 2001.
17. **N. M. Fried**, Z. Tesfaye, A.M. Ong, K.H. Rha, P. Hejazi, "Optimization of the Erbium:YAG laser for precise incision of ureteral and urethral tissues," Lasers Surg. Med., vol. 33, 108-114, 2003.
18. J. A. Harrington. Infrared fibers and their applications. SPIE Press: Bellingham, WA, 2004.
19. C. A. Chaney, Y. Yang, **N. M. Fried**, "Hybrid germanium / silica optical fibers for endoscopic delivery of Erbium:YAG laser radiation," Lasers Surg. Med., vol. 34, pp. 5-11, 2004.
20. K. Levin, D. Tran, A. Tchapijnikov, **N. M. Fried**, "Specialty fiber expands infrared laser applications," Biophoton. Internat., vol. 11, 41-43, 2004.
21. J. T. Walsh Jr, T. J. Flotte, T. F. Deutsch, "Er:YAG laser ablation of tissue: effect of pulse duration and tissue type on thermal damage," Lasers Surg. Med., vol. 9, pp. 314-326, 1989.
22. E. Papagiakoumou, D. N. Papadopoulos, N. Anastasopoulou, A. A. Serafetinides, "Comparative evaluation of HP oxide glass fibers for Q-switched and free-running Er:YAG laser beam propagation," Opt. Commun., vol. 220, pp. 151-160, 2003.
23. **N. M. Fried**, Y. Yang, C. A. Chaney, D. Fried, "Transmission of q-switched Erbium:YSGG (λ = 2.79 μm) and Erbium:YAG (λ = 2.94 μm) laser radiation through germanium oxide and sapphire fibers at high pulse energies," Lasers Med. Sci. vol. 19(3), 155-160, 2004.
24. I. M. Varkarakis, T. Inagaki, M. E. Allaf, T. Y. Chan, C. G. Rogers, E. J. Wright, **N. M. Fried**. "Comparison of Erbium:YAG and Holmium:YAG lasers for incision of the urethra and bladder neck in a chronic porcine model." Urology vol. 65(1), 191-195, 2005.

APPENDIX

PERSONNEL

<u>Urology Faculty</u>
Nathaniel M. Fried, Ph.D.   Principal Investigator
E. James Wright, M.D.   Co-Investigator

<u>Pathology Faculty</u>
Theresa Chan, M.D.

<u>Clinical Urology Fellows</u>
Ioannis Varkarakis, M.D., Ph.D.
Takaheshi Inagaki, M.D., Ph.D.

<u>Clinical Urology Residents</u>
Mohamad Allaf, M.D.
Craig Rogers, M.D.

<u>Laboratory Technicians</u>
Zelalem Tesfaye, M.S.
Charles Chaney, M.S.
Yubing Yang, Ph.D.
Hussain Tafti, Ph.D.
Travis Polletto, B.S.

<u>Engineering Students</u>
Anthony Ngo
Kyunhee Lee, B.S.

<u>Industrial Collaborators</u>   Infrared Fiber Systems, inc. (Silver Spring, MD)
Danh Tran, Ph.D.
Ken Levin, Ph.D.
Alexei Tchapnijnikov, M.S.

<u>Clinical Collaborators</u>
John Munoz, M.D.   Davison Medical Laser Center, Elliot Hospital (Manchester, NH)

ATTACHED MANUSCRIPTS

1. **Fried NM**, Tesfaye Z, Ong AM, Rha KH, Hejazi P. Variable pulsewidth Erbium:YAG laser ablation of the ureter and urethra in vitro and in vivo: optimization of the laser fluence, pulse duration, and pulse repetition rate. <u>Proc. SPIE</u>, vol. 5312:105-111, 2004.
2. Chaney CA, Yang Y, **Fried NM.** Assembly and testing of germanium / silica optical fibers for flexible endoscopic delivery of Erbium:YAG laser radiation. <u>Proc. SPIE:</u>, vol. 5317:1-8, 2004.
3. Levin K, Tran D, Tchapijnikov A, **Fried NM**. Specialty fiber expands infrared laser applications. <u>Biophotonics International</u> 11(4):41-43, 2004. (cover article)
4. **Fried NM**, Yang Y, Lee K, Tafti HA. Transmission of free-running and Q-switched Er:YAG laser energy through germanium / silica fibers. <u>Proc. SPIE:</u>, vol. 5691:155-119, 2005.
5. Varkarakis IM, Inagaki T, Allaf ME, Chan TY, Rogers CG, Wright EJ, **Fried NM**. Erbium vs. Holmium laser incision of urethra and bladder neck. <u>Proc. SPIE:</u>, vol. 5686:171-175, 2005.
6. Ngo AK, **Fried NM**. Delivery of Erbium:YAG laser radiation through side-firing germanium oxide fibers. Proc. SPIE. In press.

Variable Pulsewidth Erbium:YAG Laser Ablation of the Ureter and Urethra In Vitro and In Vivo: Optimization of the Laser Fluence, Pulse Duration, and Pulse Repetition Rate

Nathaniel M. Fried[a*], Zelalem Tesfaye[a], Albert M. Ong[a], Koon H. Rha[a], Pooya Hejazi[b]
[a]Dept. of Urology, Johns Hopkins Medical Institutions, Baltimore, MD 21224
[b]Dept. Electrical Engineering & Computer Science, Johns Hopkins Univ., Baltimore, MD 21218

ABSTRACT

Stricture recurrence frequently occurs due to mechanical or thermal insult during endourologic treatment of ureteral and urethral strictures. Optimization of the Er:YAG laser for precise incision of strictures was conducted using ureteral and urethral tissue samples, ex vivo, and a laparoscopic porcine ureteral model with exposed ureter, in vivo. Erbium:YAG laser radiation with a wavelength of 2.94 microns, pulse lengths of 8, 70, and 220 microseconds, output energies of 2-35 mJ, fluences of 1-25 J/cm^2, and pulse repetition rates of 5-30 Hz, was delivered through germanium oxide optical fibers in contact with the tissue. Incision of the ureteral wall was achieved in vivo with less than 20 pulses at a laser fluence of 4 J/cm^2. Thermal damage was reduced from 30-60 microns to 10-20 microns by shortening the laser pulse duration from 220 to 70 microseconds. Pulse repetition rates above 20 Hz resulted in larger thermal damage zones ranging from 60-120 microns. The Er:YAG laser, operating at a pulse duration of approximately 70 microseconds, a fluence of 4 J/cm^2 or greater, and a repetition rate less than 20 Hz, is capable of rapidly incising urethral and ureteral tissues, in vivo, with minimal thermal and mechanical side-effects.

Keywords: erbium, laser, stricture, urethra, ureter

1. INTRODUCTION

Urethral and ureteral strictures occur as a result of trauma caused during surgery (e.g. transurethral resection of the prostate, radical retropubic prostatectomy, minimally invasive prostate thermal therapies, and upper urinary tract endosurgery) [1,2]. Lumenal scarring and narrowing may then lead to incontinence and urinary tract infection.

Several minimally invasive techniques are available for treatment of urological strictures [1,2]. Balloon dilation and cold knife incision are the preferred methods of treatment, but they have widely variable success rates ranging from 20-80 % [3-6]. Balloon dilation is ineffective when there is scar tissue present, and may cause further stress-induced damage. Cold knife incision may also cause mechanical damage, resulting in stricture recurrence. Electrocautery and Ho:YAG laser produce significant thermal damage, which may induce further scar formation and re-stricture. None of these methods work well, and it is often necessary to repeatedly dilate or incise the stricture. However, multiple dilations or incisions of complicated strictures do not provide increased benefit, leaving patients without an effective method for treating recalcitrant scarring, voiding disfunction and urinary incontinence [2].

Several different lasers have been used for treating strictures [7], including CO_2 [8], argon [9,10], KTP [11,12], Nd:YAG [13-16], Ho:YAG [17-24], and excimer [25] lasers. Laser therapy has been sub-optimal due to stricture recurrence, caused by excessive thermal damage to adjacent tissue and subsequent scar formation. Recently, the Ho:YAG laser has been used for incision of strictures. However, the Ho:YAG laser produces 300-400 μm of peripheral thermal damage during soft tissue ablation, and therefore, may not be optimal for incision of strictures. Excessive thermal damage during stricture treatment may increase recurrence, as shown by animal models [26,27].

Previous studies have shown that the Er:YAG laser efficiently ablates soft tissues with minimal peripheral thermal damage. The Er:YAG laser is being used in several medical fields (e.g. dermatology, dentistry, and ophthalmology) which require precise tissue ablation. Recent applications of the Er:YAG laser in urology have also been reported, including lithotripsy [28,29], and incision of soft tissues for potential treatment of strictures [30,31]. The goal of this study is to optimize the Er:YAG laser parameters for rapid and precise incision of urethral and ureteral tissues.

2. MATERIALS AND METHODS

2.1 Laser Parameters

An Erbium:YAG laser (SEO 1-2-3, Schwartz Electro-optics, Orlando, FL) operating at a wavelength of 2.94 μm was connected to a variable pulsewidth laser power supply (Model 8800V, Analog Modules, Longwood, FL), producing laser pulse lengths from 1-220 μs. The laser radiation was focused with a 50-mm-FL calcium fluoride lens into either 250-μm or 425-μm germanium oxide optical fibers (Infrared Fiber Systems, Silver Spring, MD). The laser was operated at pulse repetition rates of 5-30 Hz, pulse energies of 2-35 mJ, and fluences of 1-25 J/cm^2. The laser energy was measured using a pyroelectric detector (Gentec ED-200, Ste.-Foy, Quebec), and the pulse duration was measured using a photovoltaic infrared detector (PD-10.6, Boston Electronics, Brookline, MA). Figure 1 shows the temporal beam profiles from 1-220 μs. Ablation rate studies were performed at only the 8, 70, and 220 μs pulse lengths, because there was insufficient output energy for tissue ablation at the 1 μs pulse duration.
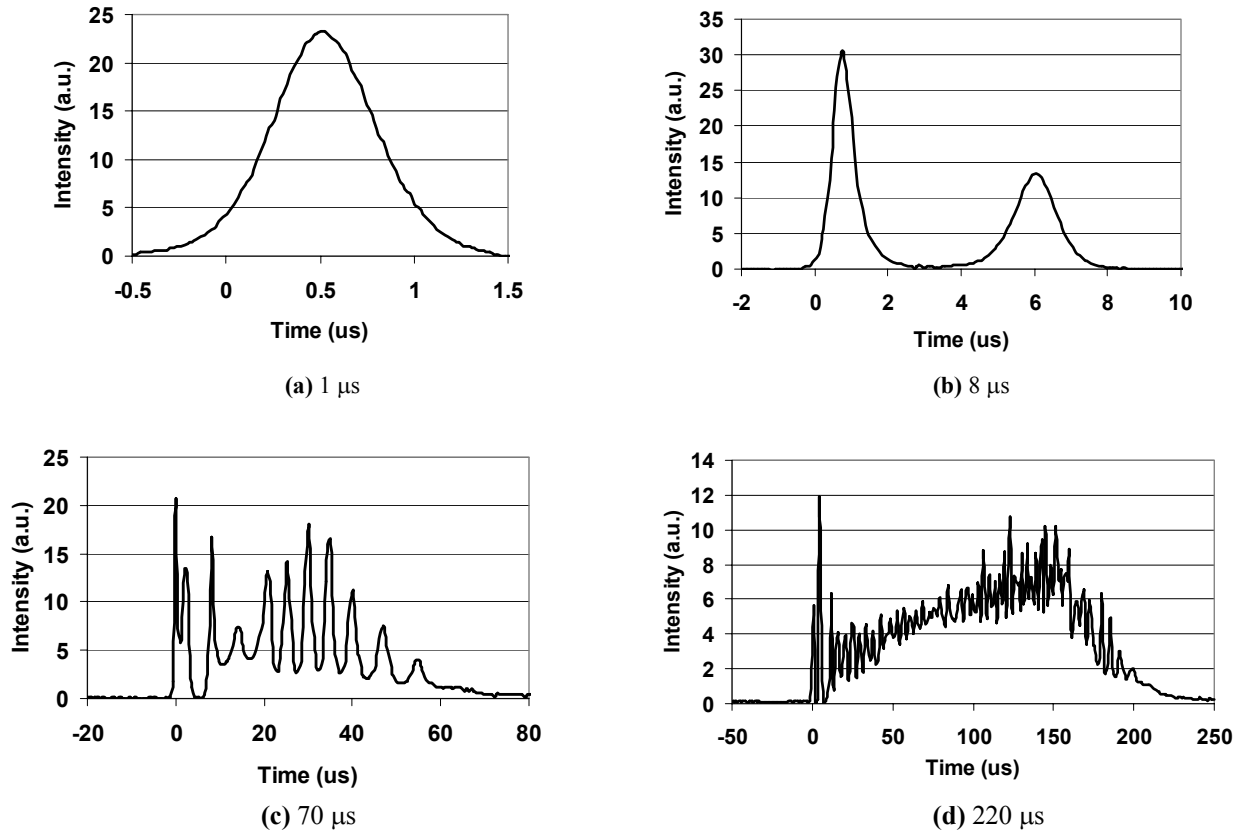
(a) 1 μs

(b) 8 μs

(c) 70 μs

(d) 220 μs

Figure 1. Temporal pulse profiles for the Er:YAG laser operated with laser pulse lengths of 1, 8, 70, and 220 μs.

2.2 In Vitro Tissue Preparation

Fresh ureteral tissue samples were removed from adult female pigs (100 kg) directly after sacrifice at the local slaughterhouse (Mt. Airy Locker Company, Mt. Airy, MD). Fatty tissue was shaved from the ureter with a scalpel blade, the tissue was spatulated, cut into 1 x 1 cm samples, stored in normal saline, and refrigerated for use within 24 hours. Fresh prostatic urethral tissue samples were obtained from male dogs (25-30 kg) after sacrifice for unrelated experiments at the Johns Hopkins Medical School. The posterior urethra was dissected from the prostate, spatulated, sectioned into 1 x 1 cm samples, stored in saline, and refrigerated.

For the ablation measurements, tissue samples were sandwiched between microscope and plexiglass slides to a fixed thickness (350 $\pm$ 50 μm), and the optical fiber tip positioned in contact with the sample through 2-mm-diameter holes drilled in the front plexiglass holder. The tissue samples were kept hydrated with saline using a syringe during the ablation experiments. The samples were placed in front of a pyroelectric detector, and the number of pulses required to perforate each sample was measured.

2.3 In Vivo Animal Experiments

All animal protocols were reviewed and approved by the Animal Care and Use Committee at the Johns Hopkins School of Medicine. A total of 4 female pigs (30-45 kg, Archer Farms, Belcamp, MD) were pretreated with acepromazine 0.39 mg/kg IM and ketamine 2 mg/kg IM. After the animals were sedated, intravenous access was obtained and normal saline administered as a 5 ml/cc bolus followed by a maintenance rate of 1.5 ml/kg/h. Intravenous propofol was administered for anesthesia. After adequate depth of anesthesia, the animal was positioned and laparoscopic ports were placed in the standard 3-port configuration, using a Visiport (US Surgical Corp., Norwalk, CT) for initial access. Using laparoscopic instrumentation, the ipsilateral ureter was identified and isolated, taking care to avoid excessive dissection and skeletonization. The distal ureter was ligated and transected close to the bladder. A small incision was made in the body wall and the ureter brought external to the body. The ureter was then spatulated and marked with 6-0 prolene sutures. The laser fiber was placed on the ureteral lumen, and the number of laser pulses required to perforate the ureter was recorded. An average of 12 perforations were made in each ureter, spaced approximately 5 mm apart, and marked by sutures on each side. Perforation was confirmed by the green aiming beam, an audible change in the acoustic ablation signal, and by histologic analysis.

2.4 Data Analysis

A minimum of six perforations was made for each set of laser parameters. For the ex vivo tissue studies, ablation rates (μm/pulse) were defined as the sample thickness divided by the average number of pulses required to perforate the sample and recorded as the mean ± standard deviation (SD). The optical fiber tip was kept fixed in contact with the tissue during the ex vivo tissue experiments. For the in vivo studies, the optical fiber was advanced during ablation. The in vivo ablation results were recorded in terms of the number of pulses required to perforate the ureteral wall because it was not possible to control for the tissue wall thickness across different ureters and animals.

3. RESULTS

3.1 Ablation Rates

The Er:YAG ablation rates are shown in Figure 2 for the ex vivo tissue experiments. Perforation of the ureteral tissue samples was achieved at laser fluences of 3-5 J/cm^2 and pulse energies of 1.5 - 2.5 mJ, without advancing the fiber into the tissue. There was an almost two-fold increase in the ablation rate for a given fluence when reducing the laser pulse duration from 220 μs to 70 μs. The 220-μs line shows an ablation rate of 4 μm per J/cm^2, while the 70-μs line shows an ablation rate of 7 μm per J/cm^2. Reducing the pulse length to 8 μs produced a minor increase in the ablation rate, but at the expense of much lower laser energy output and peripheral mechanical tissue damage.

The in vivo ablation results are shown in Figure 3, plotted as the number of laser pulses to perforate the ureter, with the fiber advanced into the tissue during ablation. The ureteral wall was perforated with less than 20 pulses at a fluence of 3.6 J/cm^2 for all of the laser pulse lengths tested. At the lowest fluence of 1.8 J/cm^2, near the perforation threshold, the shorter laser pulse lengths were observed to be more efficient. This perforation threshold was lower than that observed for the ex vivo tissue experiments using thick or thin tissue samples.
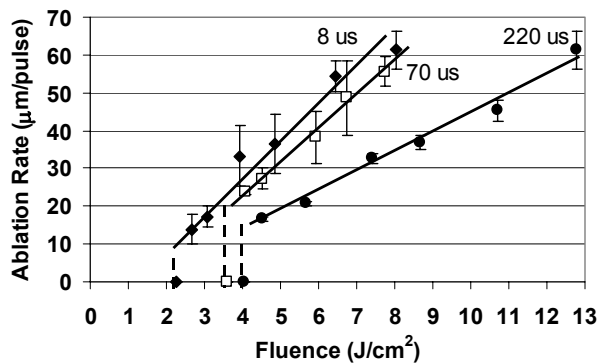

Figure 2. Er:YAG ablation rates for ex vivo ureter tissue using laser pulse lengths of 8, 70, 220 μs, and plotted as a function of laser fluence. Bars signify mean values ± S.D. (n=6). Note that the perforation threshold decreases as the laser pulse is decreased, and ablation is also more efficient.
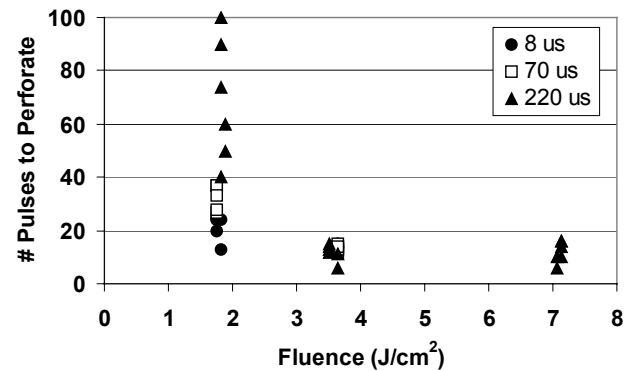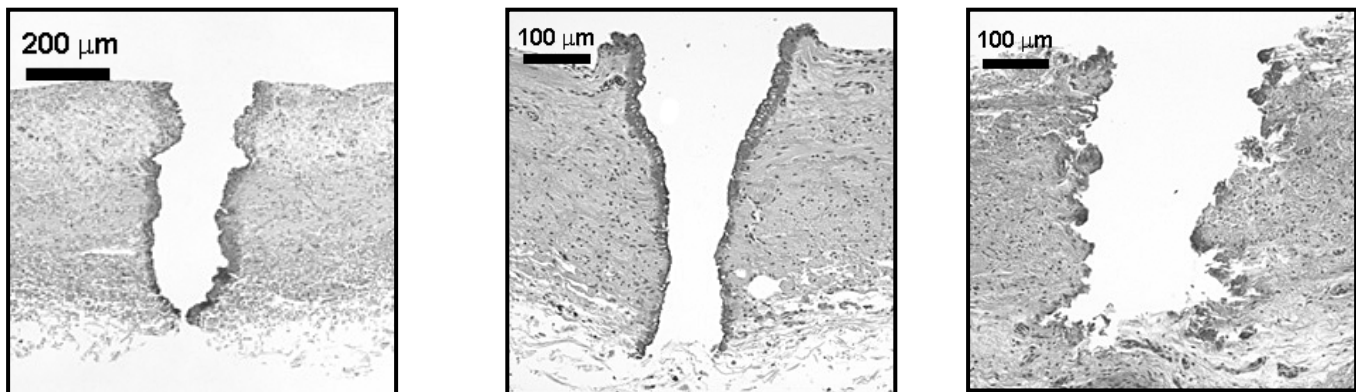
Figure 3. Er:YAG results for in vivo ureter ablation as a function of laser pulse length and fluence. The perforation threshold is approximately 1.8 J/cm^2, based on the increase in the number of pulses for perforation, and the large spread in the data points.

3.2 Thermal Damage Measurements

Histological measurements of thermal damage were conducted as a function of laser pulse duration. The results for the ex vivo tissue studies are shown in Figure 4. When the Er:YAG laser was operated in its normal long pulse mode (220 μs pulse length), a thermal damage zone of 30-60 μm was observed. Shortening the laser pulse to 70 μs resulted in a reduction of the thermal damage to 15-30 μm. The shortest laser pulse, measuring 8 μs, further reduced the thermal damage zone to 10-20 μm, but also resulted in a rougher cut, due to mechanical tissue-tearing effects.

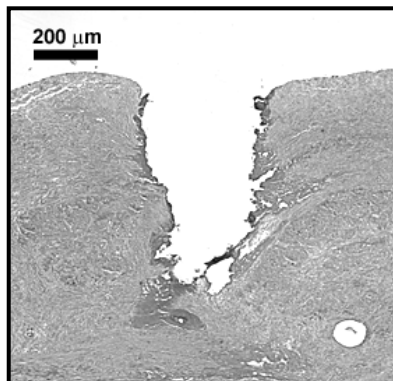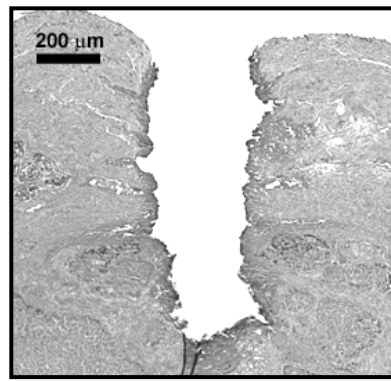**(a)** 220 µs; Damage = 30-60 µm   **(b)** 70 µs; Damage = 15-30 µm   **(c)** 8 µs; Damage = 10-20 µm

Figure 4. Photomicrographs showing H&E stained histologic cross-sections of ureteral tissues ablated with the Er:YAG laser, ex vivo. The thermal damage zone decreases as the laser pulse duration is decreased. Rough, jagged borders of the ablation crater produced by 8 µs laser pulses may be due to mechanical tissue-tearing caused during ablation.

An ex vivo study was also performed to determine whether the thermal damage zone would increase with laser operation at higher pulse repetition rates, due to residual heat accumulation in the tissue with deposition of successive laser pulses. The pulse duration, energy per pulse, and total number of pulses were all kept constant at 70 µs, 10 mJ, and 20 pulses (total energy = 200 mJ), respectively, while the pulse repetition rate was varied from 10-30 Hz. The thermal damage zone increased as the laser pulse repetition rate increased, and a large increase in thermal damage was observed when the pulse repetition rate was increased from 20 to 30 Hz (Figure 5).
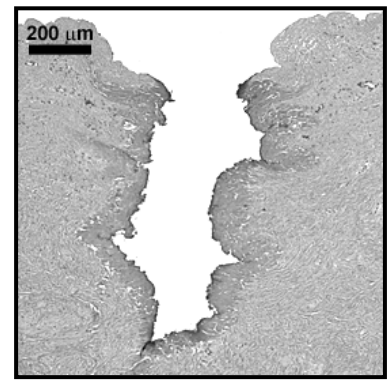
(a) 10 Hz; Damage = 20-40 µm   **(b)** 20 Hz; Damage = 30-60 µm   **(c)** 30 Hz; Damage = 60-120 µm

Figure 5. Photomicrographs showing H&E stained histologic cross-sections of urethral tissues ablated with the Er:YAG laser, ex vivo, with varying laser pulse repetition rates of 10–30 Hz. Energy was kept fixed at 10 mJ per pulse with a total of 20 pulses (200 mJ) delivered to the tissue. Note that there is a large increase in the thermal damage zone from 20 – 30 Hz, due to residual heat accumulation in the tissue during ablation. The dotted lines demarcate the border of the thermal damage zone.

The in vivo histological results are shown in Figure 6, for the 70 µs pulse duration. The thermal damage zone of 10-20 µm is slightly less than the 15-30 µm of thermal damage observed in the ex vivo tissue studies for 70 µs pulse lengths and considerably less than the 30-60 µm of thermal damage observed for the long pulse mode of 220 µs.
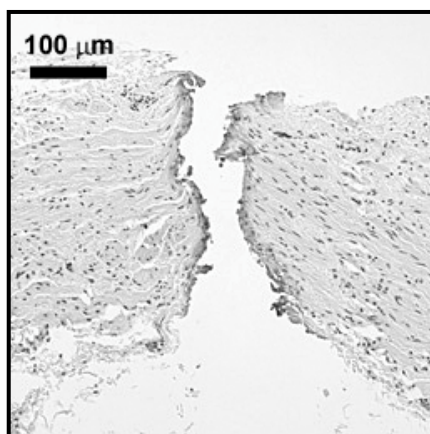

Figure 6. Photomicrographs showing H&E stained histologic cross-sections of ureteral tissue ablated with the Er:YAG laser, in vivo. The thermal damage zone measures 10-20 µm. The dotted lines demarcate the border of the thermal damage zone.

4. DISCUSSION

Success rates in treating strictures vary widely from 20-80 %, dependent on a variety of factors, including surgical technique and skill, type of stricture, scar tissue caused by previous treatment failures, patient follow-up and evaluation, and definition of stricture. While the use of the Ho:YAG laser has resulted in improved treatment of strictures, we hypothesize that the further reduction of peripheral thermal damage to the urethral or ureteral wall with Er:YAG laser incision may further improve these success rates. By operating at the 2.94 μm wavelength of the Er:YAG laser, and shortening the laser pulse length to approximately 70 μs, the thermal damage zone has been reduced to 10-20 μm, in vivo. This represents a 15-30 fold decrease in damage in comparison to the 300 μm of damage typically produced by the Ho:YAG laser, which is currently the laser of choice in urology.

This study has focused on the optimization of the Er:YAG laser for rapid and precise incision of urological tissues. Our results are similar to those of previous studies using the Er:YAG laser for ablation of other soft tissues. For example, reported threshold fluences of ablation for the long-pulse Er:YAG laser are 0.6-1.5 J/cm^2 for skin [32], ~ 2 J/cm^2 for aorta [33], ~ 1 J/cm^2 for retina [34], and ~ 1.8 J/cm^2 for the ureter reported here. Note that these low ablation thresholds also demonstrate that the Er:YAG laser is more efficient than the Ho:YAG laser, which has an ablation threshold of ~ 34 J/cm^2.

Thermal damage zones in other soft tissues for the long-pulse Er:YAG laser operated at low fluences (< 25 J/cm^2) have been reported to be 10-40 μm for skin [35], 10-20 μm for aorta [35], 20-40 μm for cornea [35], < 50 μm for trabecular tissue [36], 20-30 μm for retina [34], and 30-60 μm for ureter reported here. Mechanical tissue-tearing effects have also been observed in other tissues, e.g. aorta and cornea [35], and at pulse lengths of 50 μs and shorter [36]. Although we did not observe any mechanical tissue damage at the 70 μs pulse length, the 8-μs-pulse-length showed evidence of tissue shredding consistent with that observed in these previous studies.

Problems with the fiber tip "sticking" to the tissue during contact tissue ablation with the Er:YAG laser have also been previously reported [37,38]. This phenomenon was explained by the presence of overheated tissue debris at the fiber tip. During our preliminary in vivo experiments, however, we did not observe any "sticking" effects during advancement of the fiber into the ureter. This may be due to the use of different laser parameters, optical fibers, and/or tissues, and needs to be further studied.

In general, lower perforation thresholds, higher ablation rates, and less thermal damage were observed when progressing from ex vivo to in vivo experiments. Several factors may have contributed to these differences. First, the ability to advance the optical fiber into the tissue during in vivo ablation studies resulted in lower perforation thresholds and higher ablation rates for a given fluence. This occurred because the fluence at the tissue surface was not diminished due to divergence of the laser radiation at the output end of the fiber tip. Second, the decreased thermal damage seen in vivo may also be due to the level of hydration maintained in the tissue and absence of tissue desication which can occur during ex vivo tissue experiments.

5. CONCLUSIONS

The Er:YAG laser, operating at a pulse duration of ~ 70 μs, a fluence of 4 J/cm^2, and a repetition rate of 20 Hz, is capable of rapidly incising urethral and ureteral tissues, in vivo, with minimal thermal and mechanical side-effects. The Er:YAG laser is more efficient than the Ho:YAG laser for cutting ureteral and urethral tissues, with perforation thresholds measuring 2 J/cm^2 versus 34 J/cm^2, respectively. The Er:YAG laser is also more precise than the Ho:YAG laser, with peripheral thermal damage zones measuring 10-20 μm versus 300 μm, respectively. Chronic animal wound healing studies are planned to quantify scarring induced during Er:YAG laser incision, and optimization of mid-infrared fiber optic delivery systems for endoscopic laser delivery has begun.

ACKNOWLEDGMENTS

REFERENCES

1. R. V. Clayman, E. M. McDougall, S. Y. Nakada SY, "Endourology of the upper urinary tract: percutaneous renal and ureteral procedures," In: P. C. Walsh, A. B. Retik, E. D. Vaughan, A. J. Wein, eds. Campbell's Urology, 7th ed., Vol. 3, Philadelphia: WB Saunders. Pp. 2853-2863, 1998.

2. G. H. Jordan, S. M. Schlossberg, C. J. Devine, "Surgery of the penis and urethra," P. C. Walsh, A. B. Retik, E. D. Vaughan, A. J. Wein, eds. Campbell's Urology, 7th ed., Vol. 3, Philadelphia: WB Saunders, pp. 3341-3347, 1998.

3. M. A. Rosen, P. A. Nash, J. E. Bruce, J. W. McAninch, "The actuarial success rate of surgical treatment of urethral strictures," *J. Urol.*, vol. 151, p. 360A, 1994 (Abstract).

4. P. Albers, J. Fichtner, P. Bruhl, S. C. Muller, "Long-term results of internal urethrotomy," *J. Urol.*, vol. 156, pp. 1611-1614, 1996.

5. A. Benchekroun, A. Lachkar, A. Soumana, M. H. Farih, Z. Belahnech, M. Marzouk, M. Faik, "Internal urethrotomy in treatment of urethral stenoses (longterm results)," *Ann. Urol. (Paris)*, vol. 32, pp. 99-102, 1998.

6. C. F. Heyns, J. W. Steenkamp, M. L. De Kock, P. Whitaker, "Treatment of male urethral strictures: is repeated dilation or internal urethrotomy useful?" *J. Urol.*, vol. 160, pp. 356-358, 1998.

7. R. Klammert, P. Schneede, M. Kriegmair, "Die laserbehandlung von Harnrohrenstrikturen," *Urologie A*, vol. 33, pp. 295-298, 1994.

8. T. A. McNicholas, J. Colles, S. G. Bown, J. E. A. Wickham, "Treatment of urethral strictures with a prototype CO_2 laser endoscope," *Lasers Med. Sci.*, vol. 3, pp. 427, 1988.

9. W. C. Adkins, "Argon laser treatment of urethral stricture and vesical neck contracture," *Lasers Surg. Med.*, vol. 8, pp. 600-603, 1988.

10. H. Becker, J. Miller, H. D. Noske, J. P. Klask, W. Weidner, "Transurethral laser urethrotomy with argon laser: experience with 900 urethrotomies in 450 patients from 1978-1993," *Urol. Int.*, vol. 55, pp. 150-153, 1995.

11. A. Shanberg, R. Baghdassarian, L. Tansey, D. Sawyer, "K.T.P. 532 laser in treatment of urethral strictures," *Urology*, vol. 32, pp. 517-520, 1988.

12. P. J. Turek, T. R. Malloy, M. Cendron, V. L. Carpiniello, A. J. Wein, "KTP-532 laser ablation of urethral strictures," *Urology*, vol. 40, pp. 330-334, 1992.

13. J. A. Smith JA, Dixon JA, "Neodymium:YAG laser treatment of benign urethral strictures," *J. Urol.*, vol. 131, pp. 1080-1081, 1984.

14. J. A. Smith, "Treatment of benign urethral strictures using a sapphire tipped neodymium:YAG laser," *J. Urol.*, vol. 142, pp. 1221-1222, 1989.

15. P. N. Dogra, G. Nabi, "Core-through urethrotomy using the neodymium:YAG laser for obliterative urethral strictures after traumatic urethral disruption and/or distraction defects: long-term outcome," *J. Urol.*, vol. 167, pp. 543-546, 2002.

16. G. Nabi, P. N. Dogra, "Endoscopic management of post-traumatic prostatic and supraprostatic strictures using Neodymium-YAG laser," *Int. J. Urol.*, vol. 9(12), pp. 710-714, 2002.

17. R. K. Singal, J. D. Denstedt, H. A. Razvi, S. S. Chun, "Holmium:YAG laser endoureterotomy for treatment of ureteral stricture," *Urology*, vol. 50, pp. 875-880, 1997.

18. G. S. Gerber, D. Kuznetzov, J. A. Leef, J. Rosenblum, G. D. Steinberg, "Ho:YAG laser endoureterotomy in the treatment of ureteroenteric strictures following orthotopic urinary diversion," *Tech. Urol.*, vol. 5, pp. 45-48, 1999.

19. H. Hibi, K. Mitsui, T. Taki, H. Mizumoto, Y. Yamamda, N. Honda, H. Fukatsu, "Holmium laser incision technique for ureteral stricture using a small-calibre ureteroscope," *J.S.L.S.*, vol. 4, pp. 214-220, 2000.

20. A. R. Kural, E. R. Coskuner, I. Cevik, "Holmium laser ablation of recurrent strictures of urethra and bladder neck: preliminary results, *J. Endourol.*, vol. 14, pp. 301-304, 2000.

21. B. A. Laven, R. C. O'Connor, G. D. Steinberg, G. S. Gerber, "Long-term results of antegrade endoureterotomy using the holmium laser in patients with ureterointestinal strictures," *Urology*, vol. 58, pp. 924-929, 2001.

22. J. Kourambas, F. C. Delvecchio, G. M. Preminger, "Low-power holmium laser for the management of urinary tract calculi, strictures, and tumors," *J. Endourol.*, vol. 15(5), pp. 529-32, 2001.

23. K. Matsuoka, M. Inoue, S. Iida, K. Tomiyasu, S. Noda, "Endoscopic antegrade laser incision in the treatment of urethral stricture," *Urology*, vol. 60(6), pp. 968-972, 2002.

24. J. D. Watterson, M. Sofer, T. A. Wollin, L. Nott, J. D. Denstedt, "Holmium:YAG laser endoureterotomy for ureterointestinal strictures," *J. Urol.*, vol. 167(4), pp. 1692-1695, 2002.

25. H. Baur, W. Schneider, J. E. Altwein, "Treatment of recurrent urethral strictures by photoablation with the EXCIMER laser," *B.A.U.S.*, vol. 118, 1992 (Abstract).

26. M. Anidjar, P. Mongiat-Artus, J. P. Broulard, P. Meria, P. Teillac, A. Le Duc, P. Berthon, O. Cussenot, "Thermal radiofrequency induced porcine ureteral stricture: a convenient endourologic model," *J. Urol.*, vol. 161, pp. 298-303, 1999.

27. P. Meria, M. Anidjar, J. P. Brouland, P. Teillac, A. Le Duc, P. Berthon, O. Cussenot, "An experimental model of bulbar urethral stricture in rabbits using endoscopic radiofrequency coagulation," *Urology*, vol. 53, pp. 1054-1057, 1999.

28. J. M. H. Teichman, K. F. Chan, P. P. Cecconi, N. S. Corbin, A. D. Kamerer, R. D. Glickman, A. J. Welch, "Er:YAG versus Ho:YAG lithotripsy," *J. Urol.*, vol. 165, pp. 876-879, 2001.

29. K. F. Chan, H. Lee, J. H. M. Teichman, A. D. Kamerer, H. S. McGuff, G. Vargas, A. J. Welch, "Erbium:YAG laser lithotripsy mechanism," *J. Urol.*, vol. 168(2), pp. 436-441, 2002.

30. N. M. Fried, "Potential applications of the Erbium:YAG laser in endourology," *J. Endurol.*, vol. 15(9), pp. 889-894, 2001.

31. N. M. Fried, G. M. Long, "Erbium:YAG laser ablation of urethral and ureteral tissues," *Proc. S.P.I.E.: Lasers in Urology*, vol. 4609, pp. 122-127, 2002.

32. J. T. Walsh, T. F. Deutsch, "Er:YAG laser ablation of tissue: measurement of ablation rates," *Lasers Surg. Med.*, vol. 9, pp. 327-337, 1989.
33. J. T. Walsh, "Pulsed ablation of tissue: analysis of the removal process and tissue healing," Ph.D. Thesis. Northwestern University, Evanston, IL. 1988.
34. T. Wesendahl, P. Janknecht, B. Ott, M. Frenz, "Erbium:YAG laser ablation of retinal tissue under perfluorodecaline: determination of laser-tissue interaction in pig eyes," *Invest. Ophthalmol. Vis. Sci.*, vol. 41, pp. 505-512, 2000.
35. J. T. Walsh, T. J. Flotte, T. F. Deutsch, "Er:YAG laser ablation of tissue: effect of pulse duration and tissue type on thermal damage," *Lasers Surg. Med.*, vol. 9, pp. 314-326, 1989.
36. R. A. Hill, D. Stern, M. L. Lesiecki, J. Hsia, M. W. Berns, "Effects of pulse width on erbium:YAG laser photothermal trabecular ablation (LTA)," *Lasers Surg. Med.*, vol. 13, pp. 440-446, 1993.
37. S. Sporri, M. Frenz, H. J. Altermatt, H. U. Bratschi, V. Romano, M. Forrer, E. Dreher, H. P. Weber, "Effects of various laser types and beam transmission methods on female organ tissue in the pig: an in vitro study," *Lasers Surg. Med.*, vol. 14, pp. 269-277, 1994.
38. P. D. Brazitkos, D. J. D'Amico, T. W. Bochow, M. Hmelar, G. R. Marcellino, N. T. Stangos, "Experimental ocular surgery with a high-repetition-rate erbium:YAG laser," *Invest. Ophthalmol. Vis. Sci.*, vol. 39, pp. 1667-1675, 1998.

Assembly and Testing of Germanium / Silica Optical Fibers for Flexible Endoscopic Delivery of Erbium:YAG Laser Radiation

Charles A. Chaney, Yubing Yang, Nathaniel M. Fried*

Dept. of Urology, Johns Hopkins Medical Institutions, Baltimore, MD 21224

ABSTRACT

Endoscopic applications of the Erbium:YAG laser have been limited due to the lack of an optical fiber delivery system that is robust, flexible, and biocompatible. This study reports the assembly and testing of hybrid optical fibers consisting of 1-cm-length, 550-micron-core, silica fiber tips attached to either 350-micron or 425-micron germanium oxide "trunk" fibers. Er:YAG laser radiation with a wavelength of 2.94 microns, pulse lengths of 70 and 220 microseconds, repetition rates of 3-10 Hz, and laser output energies of up to 300 mJ was delivered through the fibers for testing. Maximum fiber output energies measured 180 + 30 mJ and 82 + 20 mJ (n=10) under straight and tight bending configurations, respectively, before fiber interface damage occurred. By comparison, the damage threshold for the germanium fibers without silica tips during contact soft tissue ablation was only 9 mJ (n=3). Studies using the hybrid fibers for lithotripsy also resulted in fiber damage thresholds (55-114 mJ) above the stone ablation threshold (15-23 mJ). Hybrid germanium / silica fibers represent a robust, flexible, and biocompatible method of delivering Er:YAG laser radiation during contact soft tissue ablation. Significant improvement in the hybrid fibers will be necessary before their use in Er:YAG laser lithotripsy.

Key Words: ablation, erbium, holmium, laser, lithotripsy, stricture, ureter, urethra

1. INTRODUCTION

The Erbium:YAG laser has been used extensively for precise tissue ablation in medical fields which do not require a flexible optical fiber delivery system, such as dermatology [1,2], dentistry [3,4], and ophthalmology [5-11]. In these fields, the use of an articulated arm delivery system or semi-rigid optical fibers is adequate for performing surgery. However, for medical applications requiring delivery of laser radiation through a flexible endoscope, such as the upper urinary tract, current optical fibers and waveguides for the Er:YAG laser remain inadequate.

Although there are several types of optical fibers and waveguides available for delivery of mid-infrared laser radiation, including chalcogenide, zirconium fluoride, sapphire, germanium oxide, and hollow silica waveguides, all of these delivery systems have major limitations [12-14]. The chalcogenide fibers cannot handle high power, they are toxic, and they break easily. The zirconium fluoride fibers are also brittle, hygroscopic, and toxic in tissue. The sapphire fibers suffer from mechanical stress and breakage during tight bending conditions. The germanium oxide fibers have a low melting temperature preventing their use in contact mode at high powers. The hollow silica waveguides are not biocompatible and have limited bending ability with high transmission losses during tight bending. Thus, the ideal mid-infrared optical fiber that combines high-power delivery, flexibility, chemical and mechanical durability, and biocompatibility, has yet to be developed.

The goal of this study is to test a hybrid optical fiber with the Erbium:YAG laser, which combines the high-power transmission and flexibility of the germanium oxide fiber with the robust and biocompatible low-OH silica fiber tips currently in clinical use with the Holmium:YAG laser. Although increased absorption limits the use of long low-OH silica fibers beyond wavelengths of approximately 2.5 μm, previous studies have demonstrated that short low-OH silica fiber lengths, on the order of a few centimeters, are capable of transmitting sufficient Er:YAG laser energy for soft tissue ablation [5,6,8,15]. This study demonstrates that long hybrid fibers are capable of being assembled with a simple process that reduces many of the limitations associated with current mid-IR optical fibers, and that sufficient Er:YAG laser energy can be transmitted through these fibers during insertion into a flexible endoscope for use in applications requiring soft and hard tissue ablation.

2. MATERIALS AND METHODS

2.1 Laser Parameters

An Erbium:YAG laser (SEO 1-2-3, Schwartz Electro-Optics, Orlando, FL) operating at a wavelength of 2.94 μm was connected to either a fixed long-pulse laser power supply (220-μs-pulse length, 400 mJ/pulse) or a variable pulse width laser power supply (Model 8800V, Analog Modules, Longwood, FL), producing up to 30 mJ per pulse at 70-μs-pulse-lengths. The laser radiation was externally focused with a 50-mm-focal-length calcium fluoride lens into either 250, 350, or 425-μm-core germanium oxide optical fibers (Infrared Fiber Systems, Silver Spring, MD), with and without low-OH silica fiber tips attached to the output end of the germanium "trunk" fiber. Fiber output energy was measured using a pyroelectric detector (Gentec ED-200, Ste.-Foy, Quebec), and the laser pulse duration was measured using a photovoltaic infrared detector (PD-10.6, Boston Electronics, Brookline, MA).

2.2 Germanium "Trunk" Fibers

Preliminary laser ablation tests were conducted with 250-μm-core and 425-μm-core germanium oxide fibers in direct contact with ex vivo hard and soft tissue samples, including porcine ureters, and uric acid and calcium oxalate monohydrate (COM) stones. A total of 500 pulses were delivered to the tissue. Pre- and post-ablation fiber output energies were measured to determine whether any damage occurred to the fiber tip. An optical microscope was used to analyze the output ends of the germanium fibers for evidence of fiber tip degradation after contact tissue ablation.

2.3 Hybrid Fiber Assembly

The hybrid fiber consisted of a 1-cm-long, 550-μm-core, low-OH silica fiber tip attached to either a 350-μm- or 425-μm germanium trunk fiber. For the initial fiber preparation, the germanium fiber jacket was softened using chemical treatment (1-methyl-2-pyrrolidinone at 150 °C for 2 min. then isopropanol for 3 min.) and then stripped with a razor blade. The germanium and silica fibers were polished with rough 600-grit and then fine 5-micron sandpaper. The fibers were then aligned under a microscope using a laboratory-constructed mechanical setup. Several different methods of attachment were explored (Figures 1 and 2). First, index-matching UV-cured optical epoxy (Norland, New Brunswick, NJ) was applied with a syringe needle either around the fibers or at the fiber interface (n = 10 fibers). Second, 30-gauge PTFE heat shrink tubing (normal ID=850 μm, shrunk ID=375 μm, wall thickness = 150 μm, length = 5 mm) was shrunk around the germanium/silica fiber interface using a heat gun (n = 10 fibers). The PTFE tubing (Small Parts, Miami Lakes, FL) also served the purpose of acting as a biocompatible jacket surrounding any exposed germanium fiber. Third, stainless steel hypodermic tubing (Small Parts, ID=0.675 mm, OD=1.05 mm) was used to align the fibers (n = 5 fibers). Fourth, glass capillary tubing (VitroCom, Mountain Lakes, NJ, ID=0.7 mm, OD=0.87 mm) was used for fiber attachment. Two attachment methods were explored: with the fibers in contact at the interface (n = 10 fibers) or with an air gap (~200 μm) at the interface (n = 10 fibers).
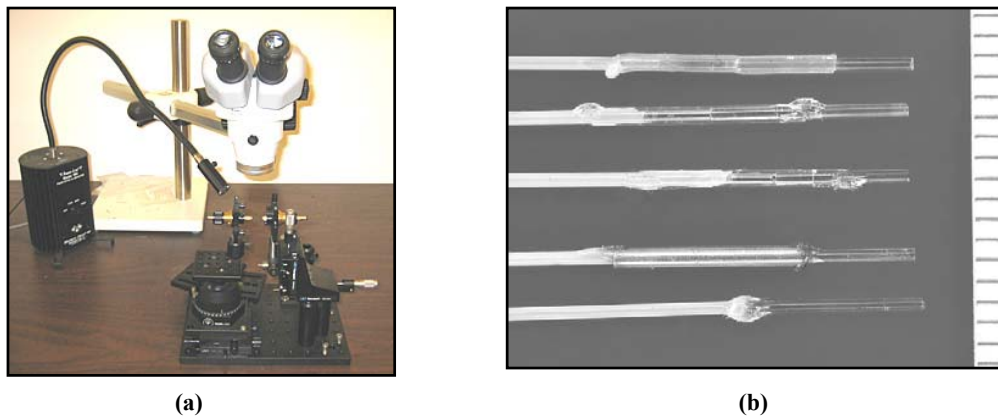

Figure 1. (a) Experimental setup used to assemble the hybrid fibers. (b) Image of the germanium / silica hybrid fibers assembled using 5 different methods: (1) heat-shrink tubing, (2) glass capillary tubing, (3) glass tubing with an air gap at the fiber interface, (4) stainless steel hypodermic tubing, and (5) UV-cured optical epoxy. For all of the methods, an approximately 1 cm-long, 550-mm-core, low-OH silica tip was attached to a 425-mm-core germanium trunk fiber. Ball-shaped glue drops are present in Figures b-e at the interface between the yellow germanium jacket and the conduit material and at the interface between the silica tip and the conduit. The ruler lines = 1 mm.
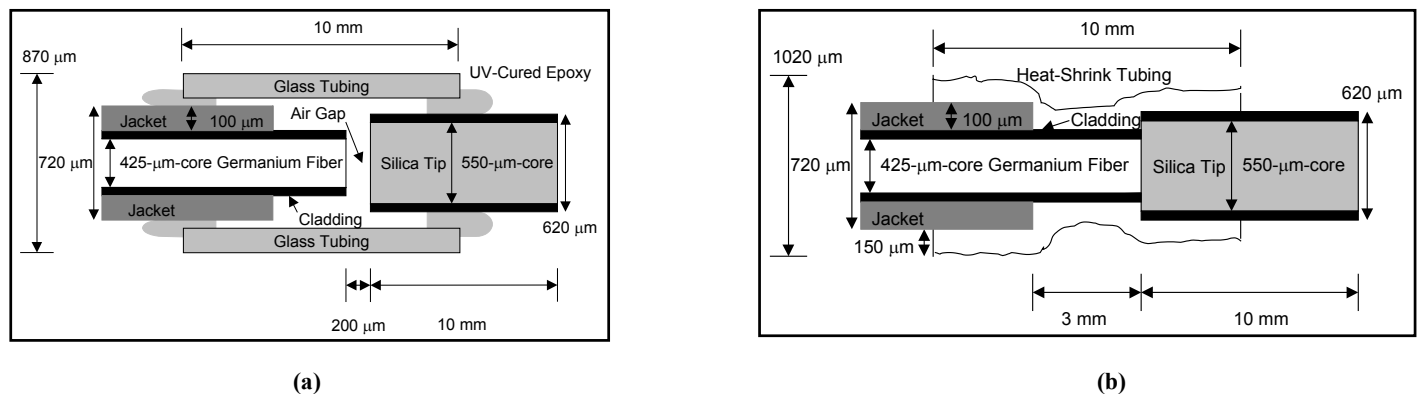

Figure 2. Diagrams of the dimensions of the 425/550 hybrid fiber assembled using (a) heat shrink tubing, and (b) glass capillary tubing with epoxy and an air gap at the germanium / silica interface.

2.4 Fiber Transmission and Bending Tests

Preliminary fiber bending tests were conducted with germanium and sapphire optical fibers, ranging in core diameter from 150 – 500 μm. The fibers were inserted into a 15 Fr flexible cysto-urethroscope with a 7 Fr working channel. Basic fiber testing was performed to determine whether the fiber could withstand high mechanical stress under tight bending conditions and whether the

fiber presence hindered maximum deflection of the scope. Peak Er:YAG energy transmission through the hybrid fibers was then measured for both straight and bent configurations.

2.5 Stone Ablation Studies

Limited studies were also performed with the Er:YAG laser and the hybrid (350/550 and 425/550) fibers for contact tissue ablation of urological stones. The goal of these studies was to demonstrate that sufficient energy could be delivered through the hybrid fibers in contact mode for endoscopic stone ablation. Human uric acid and calcium oxalate monohydrate stones were obtained from a stone analysis laboratory (UroCore LabCorp, Oklahoma City, OK), sectioned with a water-cooled band saw into cylindrical samples (~ 10-mm-diameter), and then weighed with an analytical balance (dry weight = 300-450 mg). The stone samples were then placed in a water bath, and the hybrid fiber tip placed in contact with the stone. Er:YAG laser radiation was delivered to the stone with pulse lengths of 220 μs, pulse repetition rates of 3 Hz, and fiber output energies of from 5-150 mJ.

2.6 Data Analysis

For the fiber damage studies, a total of 500 laser pulses was delivered through the fiber at each energy level between pre- and post-testing measurements. For the bare germanium fibers, the measurements were done during contact soft tissue ablation and represented the fiber tip damage threshold. For the hybrid fiber testing, measurements were initially made in air and then in contact with the stone samples. Maximum fiber output energy was recorded as the mean $\pm$ standard deviation (S.D.) for N samples tested. Statistical analysis was conducted between the data sets for maximum pulse energies achieved with each method of hybrid fiber assembly. ANalysis Of Variance (ANOVA) was used to determine statistical significance between data sets ($P < 0.05$ was considered statistically significant).

3. RESULTS

3.1 Germanium Trunk Fibers

Preliminary laser ablation tests were conducted with 250-μm-core and 425-μm-core germanium oxide fibers in direct contact with ex vivo samples of hard and soft urological tissues. The fiber damage thresholds for the soft tissue studies were 4 mJ (7 J/cm^2) and 9 mJ (6 J/cm^2) for the 250 μm and 425 μm fibers, respectively (Figure 3). These values are above the threshold for perforating samples of ureteral tissue, 2 mJ (4.1 J/cm^2) and 5.1 mJ (3.7 J/cm^2), respectively [16]. For the hard tissue studies, the fiber damage thresholds measured 12 mJ and 30 mJ (22 J/cm^2), for the uric acid and COM stones, respectively (Figure 4). These results demonstrate that the germanium oxide fiber is capable of ablating soft and hard tissues without fiber tip damage. However, the fiber is limited to operation at relatively low laser energies during contact tissue ablation, which may not be practical for clinical applications requiring rapid and efficient tissue ablation.
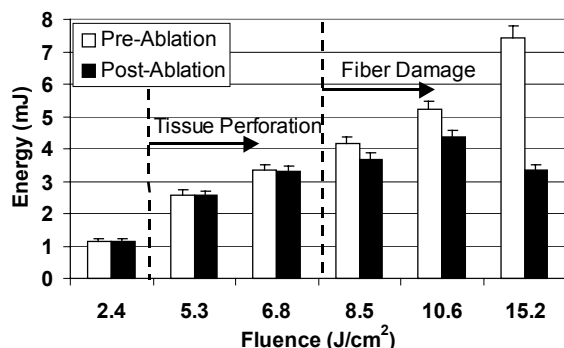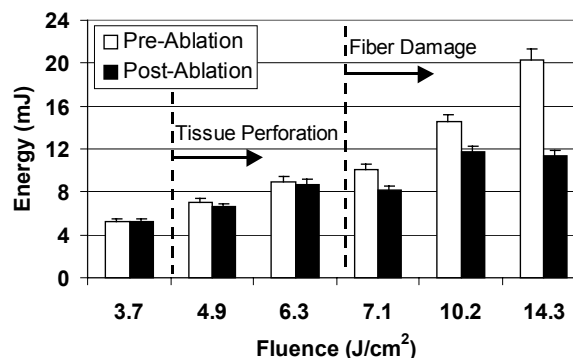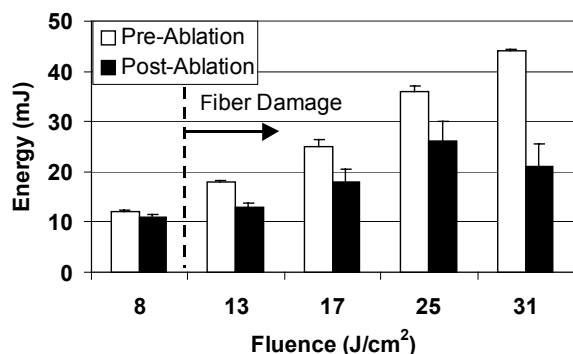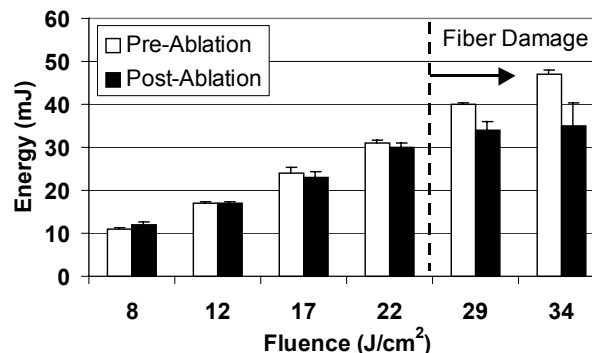

(a) Ureter, 250 μm fiber   **(b)** Ureter, 425 μm fiber

Figure 3. Germanium oxide fiber damage thresholds for (a) 250-μm-core fibers, and (b) 425-μm-core fibers, placed in direct contact with soft ureteral tissue. A total of 500 pulses were delivered with a pulse length of 70 μs and a pulse repetition rate of 10 Hz. Error bars signify a $\pm$ 5% variation in pulse to pulse energy stability.

(a) Uric Acid stone, 425 μm fiber   **(b)** COM stone, 425 μm fiber

Figure 4. Germanium oxide fiber damage thresholds for 425-μm-core fibers placed in contact with (a) uric acid stones, and (b) calcium oxalate monohydrate stones. A total of 500 pulses were delivered with a pulse length of 220 μs and pulse repetition rate of 3 Hz. Error bars represent mean $\pm$ standard deviation (n = 4).

The primary mechanism of germanium fiber damage during contact tissue ablation is melting of the fiber tip due to the high ablative temperatures. Figure 5 shows the fiber tips at different stages of meltdown, beginning with a normal tip surface, then particle formation, cracking and charring, and finally catastrophic meltdown with crystalline formation. During these progressive phases of fiber degradation, the fiber output energy also steadily dropped.
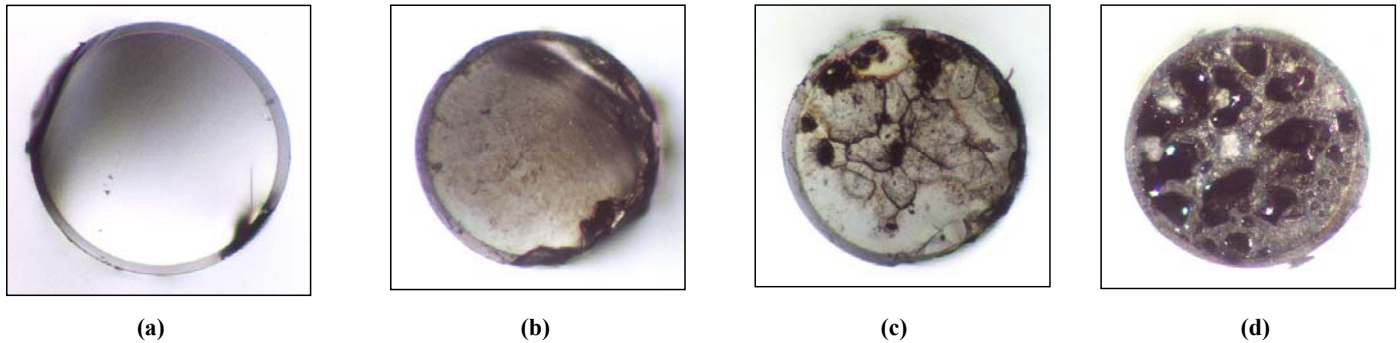

| (a) | (b) | (c) | (d) |

Figure 5. Mechanism of germanium oxide fiber tip damage when tested in contact with tissue. (a) normal fiber tip, (b) particulate formation on the fiber tip, (c) cracking and charring, and (d) crystalline formation. The progressive deterioration is due to melting of the fiber tip when in contact with the tissue during high-temperature tissue ablation. Fiber tip damage was not observed during non-contact ablation studies. The parameters were: 425-μm-core fiber, 10 mJ/pulse, 70-μs-pulse duration, 10 Hz pulse repetition rate, and a total of 500 pulses.
There was no evidence of fiber damage when the germanium fibers were used previously for tissue ablation in non-contact mode.

These trunk fibers have transmitted up to 20 Watts (2 Joules at 10 Hz) without problem [17].

3.2 Hybrid Germanium / Silica Fibers
To overcome the limitations of the germanium fiber for contact tissue ablation, a hybrid fiber consisting of a short low-OH silica fiber tip was attached to the germanium trunk fiber using several different methods. Table 1 shows the average output energy transmitted through the fiber for each of these methods before a drop in output energy was observed due to damage at the germanium / silica interface. The damage threshold for the germanium fiber without silica tip during contact soft tissue ablation is also included for comparison. Using the heat-shrink tubing method, hybrid fiber output energies measured 180 ± 30 mJ (76 ± 13 J/cm^2), before fiber damage was observed (n=10).

Table 1. Comparison of results for different materials and methods used to construct germanium / silica hybrid fibers.

Assembly Method[a]	Maximum Pulse Energy (mJ)	N
Germanium tip only[b]	9 ± 1	3
Silica tip attached with:		
UV-cured epoxy	10 ± 5	10
Steel hypodermic tubing	109 ± 47	10
Glass capillary tubing:		
with air gap at interface	104 ± 38	10
without air gap at interface	139 ± 49	10
Heat-shrink tubing	180 ± 30	10

[a] All fibers were constructed using a 425-μm-core germanium trunk fiber and a 1-cm-long, 550-μm-core silica fiber tip. The fibers were tested using an Er:YAG laser with a 220 μs laser pulse length at 3 Hz.

[b] Values for the germanium fibers without silica tip represent maximum pulse energies achieved during contact soft tissue ablation. No problems were encountered during non-contact ablation.

3.3 Fiber Bending and Transmission Tests
Earlier tests showed that the sapphire optical fibers were more robust than the germanium fibers, as evidenced by the difference in their melting temperatures (2030 °C versus 680 °C) and the absence of fiber tip damage during contact soft tissue ablation [12, 18]. However, the sapphire fiber was not pursued further because both 250-μm- and 425-μm-core sapphire fibers suffered multiple fractures upon insertion into the flexible cysto-urethroscope under tight bending conditions (Table 2). While the 425-μm-core

germanium fibers also fractured upon repeated bending, the 150-μm-, 250-μm-, and 350-μm-core germanium fibers suffered no mechanical damage under similar test conditions. Figure 6 shows a 350-μm-core germanium oxide fiber inserted through the 7 Fr working channel of a 15 Fr flexible cysto-urethroscope. The scope was deflected at a maximum angle corresponding to a bend radius of approximately 15 mm with and without the fiber inserted.

Table 2. Bending tests performed using a 15 Fr flexible cysto-urethroscope with 7 Fr working channel and ~ 15 mm bend radius.

Fiber Type / Core Size	Minimum Bend Radius[a]	Flexible Scop Breaking Test
Sapphire		
150 μm	20 mm	Passed
250 μm	30 mm	Failed
325 μm	60 mm	Not tested
425 μm	80 mm	Failed
Germanium Oxide		
150 μm	5 mm	Passed
250 μm	10 mm	Passed
350 μm	15 mm	Passed
425 μm	25 mm	Failed
500 μm	40 mm	Failed

[a] Minimum bend radius values are taken from commercial literature (www.photran.com and www.infraredfibersystems.com).
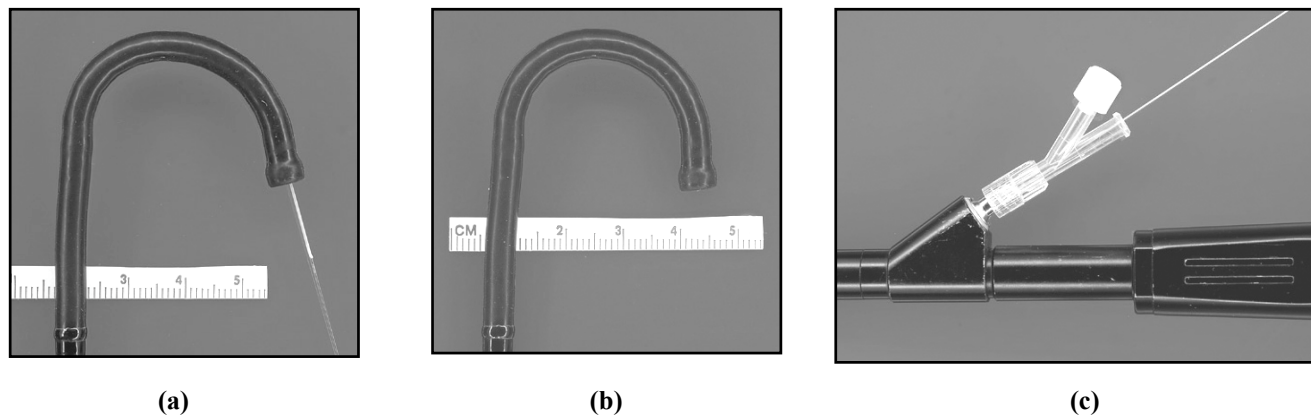

(a)   **(b)**   **(c)**

Figure 6. Images of a 350-μm-core germanium / silica hybrid fiber inserted through a 15 Fr flexible cysto-urethroscope with a 7 Fr working channel. (a) The fiber is bent to a ~ 15-mm bend radius without breaking under maximum scope deflection. (b) Maximum deflection of the scope without fiber present also corresponds to a ~ 15-mm bend radius, demonstrating that the fiber does not hinder scope deflection. (c) The fiber is successfully inserted at a 30-degree angle into the working channel.

Both the 350/550 and 425/550 germanium/silica hybrid fibers showed a significant decrease in energy output when bent to just above their minimum bending radius, 15 mm for the 350 μm trunk fiber and 25 mm for the 425 μm trunk fiber (Table 3). The damage mechanism was usually observed as sparking at the germanium/silica fiber interface, resulting in a melting of the germanium surface at the fiber interface, and noted as an immediate loss in energy greater than 5%. The difference in results between the 250-, 350-, and 425-μm trunk fibers can be explained in part by the difference in the cross-sectional area at the germanium fiber tip. Assuming the melting temperature of the germanium fiber tip at the interface is the limiting factor, the maximum fluence that the interface can handle before melting is a function of both energy and fiber diameter. Thus, a larger trunk fiber diameter transmits greater energy, as observed in Table 3.

Table 3. Damage thresholds during germanium / silica fiber bending tests.

Fiber Core (μm) (Trunk / Tip)	Maximum Energy (mJ) Straight	Bent	Bend Radius (mm)	N
425 / 550	180 ± 30	82 ± 20	30	10
350 / 550	93 ± 13	65 ± 20	20	10
250 / 365	27 ± 8	28 ± 9	20	8

3.4 Lithotripsy Studies

Both the 350/550 and 425/550 hybrid germanium/silica fibers were tested for Er:YAG laser ablation of uric acid and calcium oxalate monohydrate (COM) stones. The ablation threshold for the stones and the peak energies transmitted through the fibers before fiber interface damage occurred was measured (Table 4). Ablation craters were first observed in the stones at energy levels of 15-23 mJ. There was no statistically significant dependence on stone type or trunk fiber used. The peak energies, however, were again dependent on fiber trunk diameter (350 or 425 μm), similar to the previous results for the fiber bending studies.

Table 4. Results using hybrid germanium / silica fibers for Er:YAG lithotripsy.

Fiber Core (μm) (Trunk / Tip)	Stone Type	Stone Ablation Threshold (mJ)	Fiber Damage Threshold (mJ)	N
350/550	uric acid	15 ± 2	55 ± 8	3
	COM*	22 ± 5	63 ± 11	3
425/550	uric acid	19 ± 1	90 ± 32	4
	COM	23 ± 9	114 ± 8	4

*COM = calcium oxalate monohydrate

4. DISCUSSION

Several applications in urology may benefit from the availability of a suitable optical fiber for tissue ablation using the Erbium:YAG laser. Potential applications include more precise laser incision of ureteral and urethral strictures and more efficient laser lithotripsy. Previous studies by our research group suggest that Er:YAG laser incision of the ureter and urethra reduces peripheral thermal damage by a factor of 10 in comparison with the Ho:YAG laser (30 ± 10 μm vs. 290 ± 30 μm), which may translate into less scarring and improved success rates [14,16,18].

Teichmann, et al, have reported that Er:YAG laser lithotripsy is approximately 2.4 times more efficient than Ho:YAG laser lithotripsy, and that the lack of a reliable optical fiber delivery system is the major limitation to clinical application of Er:YAG laser lithotripsy [19]. They demonstrated that both the 425-μm-core sapphire and germanium fibers suffered significant degradation during Er:YAG laser lithotripsy studies, with fiber output energies declining to less than 70% of their initial 100 mJ and 200 mJ energies, respectively. Other experiments with the sapphire fiber were limited to energies of 50 mJ to minimize fiber damage [21].

Recently, Papagiakoumou, et al, have also reported the characterization of the germanium oxide fibers for flexible transmission of Er:YAG laser radiation [22]. They reported that the fibers exhibited no significant bending losses when bent to a radius of 40 mm and transmitting up to 20 mJ of energy. While these testing conditions were different than those of the current study (e.g. no silica tip, lower energy transmission, and higher bend radius), they nevertheless further demonstrate the potential of the germanium fiber as a flexible delivery system.

When comparing our methods used to assemble the hybrid fibers, it should be noted that there was a large difference in peak output energy between some of the methods. The bare germanium fibers and hybrid fibers attached with epoxy performed poorly in comparison with the hybrid fibers attached with metal, glass, and heat-shrink tubing. This can be explained again by considering the low melting temperature of the germanium fiber. The epoxy presumably acted as an absorbing material, resulting in thermal buildup at the interface, and eventual fiber decay and transmission loss. On the contrary, the heat-shrink and glass tubing were more efficient in transmitting coupling losses at the fiber interface through the wall, resulting in less thermal buildup. The alignment of the germanium / silica fiber interface inside the steel tubing was difficult because the material was not transparent.

The performance of the hybrid fibers was also limited when the fibers were placed either in tight bending configurations or in contact with hard tissue (e.g. stones). Some of the fiber damage and transmission losses may be due to limitations in the spatial and temporal beam quality of the input laser beam and the introduction of higher modes during bending. Future research will focus on delivering a single mode Gaussian or flat-top spatial beam profile and eliminating the micro-pulse spikes that compose the Er:YAG temporal beam profile [16].

Overall, our results show that by adding a robust silica fiber tip to the germanium fiber, fiber output energies may be increased to 180 ± 30 mJ (76 ± 13 J/cm^2) and 82 ± 20 mJ (35 ± 9 J/cm^2), in straight and tight bending configurations, respectively, without fiber damage. This represents a large improvement over the 9 mJ (6 J/cm^2) peak energy achieved during testing of the bare germanium fiber in contact with soft tissue (Figure 3b). While these results demonstrate that the hybrid germanium / silica fiber currently transmits sufficient energy for contact soft tissue ablation through a flexible endoscope, further improvements will be necessary before the hybrid fiber can be used effectively for Er:YAG laser lithotripsy. These fiber output energies are still too low to efficiently ablate stones at a rate suitable for clinical use. We are currently working to further refine our hybrid fiber assembly method to provide even higher and more consistent Er:YAG laser output energy and smaller, more flexible fibers for use in flexible endoscopes.

5. CONCLUSIONS

A robust, flexible, and biocompatible hybrid germanium / silica fiber was assembled capable of delivering Erbium:YAG laser radiation through a flexible endoscope. This fiber may serve as a reliable delivery system with the Er:YAG laser for applications in the urological tract which may benefit from more precise and efficient laser ablation. Such applications may include laser ablation of urethral and ureteral strictures and laser lithotripsy. Assembly of smaller diameter hybrid fibers, more rigorous endoscope bending tests, and achievement of higher fiber output energy thresholds will all be pursued in the further development and testing of these hybrid fibers.

ACKNOWLEDGMENTS

REFERENCES

1. R. Kaufmann, "Role of the Erbium:YAG laser in the treatment of aged skin," *Clin. Exp. Dermatol.*, vol. 26(7), pp. 631-636, 2001.
2. T. S. Alster, J. R. Lupton, "Er:YAG cutaneous laser resurfacing," *Dermatol. Clin.*, vol. 19, pp. 453-466, 2001.
3. P. Rechmann, D. S. Glodin, T. Hennig, "Er:YAG lasers in dentistry: an overview," *Proc. S.P.I.E.: Lasers Dent. IV*, vol. 3248, pp. 2-13, 1998.
4. D. M. Clarkson, "A review of technology and safety aspects of erbium lasers in dentistry," *Dent. Update*, vol. 28(6), pp. 298-302, 2001.
5. S. A. Ozler, R. A. Hill, J. J. Andrews, G. Baerveldt, M. W. Berns, "Infrared laser sclerostomies," *Invest. Ophthalmol. Vis. Sci.*, vol. 32(9), pp. 2498-2503, 1991.
6. R. A. Hill, G. Baerveldt, S. A. Ozler, M. Pickford, G. A. Profeta, M. W. Berns, "Laser trabecular ablation (LTA)," *Lasers Surg. Med.*, vol. 11(4), pp. 341-346, 1991.
7. M. L. McHam, D. L. Eisenberg, J. S. Schuman, N. Wang, "Erbium:Yag laser trabecular ablation with a sapphire optical fiber," *Exp. Eye Res.*, vol. 65, pp. 151-155, 1997.
8. G. Stevens Jr, B. Long, J. M. Hamann, R. C. Allen, "Erbium:YAG laser-assisted cataract surgery," *Ophthalmic Surg. Lasers*, vol. 29(3), pp. 185-189, 1998.
9. P. D. Brazitkos, D. J. D'Amico, T. W. Bochow, M. Hmelar, G. R. Marcellino, N. T. Stangos, "Experimental ocular surgery with a high-repetition-rate erbium:YAG laser," *Invest. Ophthalmol. Vis. Sci.*, vol. 39, pp. 1667-1675, 1998.
10. C. C. Neubaur, G. Stevens Jr, "Erbium:YAG laser cataract removal: role of fiber-optic delivery system," *J. Cataract Refract. Surg.*, vol. 25(4), pp. 514-520, 1999.
11. T. Wesendahl, P. Janknecht, B. Ott, M. Frenz, "Erbium:YAG laser ablation of retinal tissue under perfluorodecaline: determination of laser-tissue interaction in pig eyes," *Invest. Ophthalmol. Vis. Sci.*, vol. 41, pp. 505-512, 2000.
12. J. A. Harrington, "A review of infrared fibers," http://irfibers.rutgers.edu/ir-rev-index.html. Adapted from the OSA Handbook, Vol. III, McGraw-Hill. Editor, Michael Bass, 2000.
13. G. N. Merberg, "Current status of infrared fiber optics for medical laser power delivery," *Lasers Surg. Med.*, vol. 13, pp. 572-576, 1993.
14. N. M. Fried, "Potential applications of the Erbium:YAG laser in endourology," *J. Endurol.*, vol. 15(9), pp. 889-894, 2001.
15. M. Mrochen, P. Riedel, C. Donitsky, T. Seiler, "Erbium:yttrium-aluminum-garnet laser induced vapor bubbles as a function of the quartz fiber tip geometry," *J. Biomed. Opt.*, vol. 6(3), pp. 344-350, 2001.
16. N. M. Fried, Z. Tesfaye, A. M. Ong, K. H. Rha, P. Hejazi, "Optimization of the Erbium:YAG laser for precise incision of ureteral & urethral tissues: in vitro & in vivo results," *Lasers Surg. Med.*, vol. 33, pp. 108-144, 2003.
17. Personal communication with Alex Tchap, Infrared Fiber Systems, inc., Silver Spring, MD.
18. N. M. Fried, G. M. Long, "Erbium:YAG laser ablation of urethral and ureteral tissues," *Proc. S.P.I.E.: Lasers Urol.*, vol. 4609, pp. 122-127, 2002.
19. J. M. H. Teichman, K. F. Chan, P. P. Cecconi, N. S. Corbin, A. D. Kamerer, R. D. Glickman, A. J. Welch, "Er:YAG versus Ho:YAG lithotripsy," *J. Urol.*, vol. 165, pp. 876-879, 2001.
20. H. Lee, T. R. Ryan, A. Lee, J. H. Teichman, A. J. Welch, "Feasibility study of Er:YAG lithotripsy," *Lasers Surg. Med.*, Suppl 15:12, 2003.
21. K. F. Chan, H. Lee, J. M. H. Teichman, A. Kamerer, H. S. McGuff, G. Vargas, A. J. Welch, "Erbium:YAG laser lithotripsy mechanism," *J. Urol.*, vol. 168, pp. 436-441, 2002.
22. E. Papagiakoumou, D. N. Papadopoulos, N. Anastasopoulou, A. A. Serafetinides, "Comparative evaluation of HP oxide glass fibers for Q-switched and free-running Er:YAG laser beam propagation," *Opt. Comm.*, vol. 220, pp. 151-160, 2003.

Infrared Fibers for Laser Surgery

Ken Levin, PhD, Danh Tran, PhD and Alexei Tchapijnikov, Infrared Fiber Systems, Silver Spring, MD
Nathaniel Fried, PhD, Dept. of Urology, Johns Hopkins Medical School, Baltimore, MD

Lasers are currently being used extensively in medicine for therapeutic applications. Some examples of common therapeutic laser systems include the argon ion (green), excimer (ultraviolet), carbon dioxide (infrared), Neodymium:YAG (near-infrared), and Erbium:YAG (mid-infrared) lasers. The Er:YAG and Er:YSSG lasers are unique in that they operate close to the water absorption band at a wavelength of 2.9 microns, and are capable of precise tissue ablation at almost the cellular level with minimal thermal damage to adjacent healthy tissue. In addition, due to their high ablation efficiency, these laser systems can potentially be made compact at low cost. Erbium:YSGG and Erbium:YAG lasers are currently being used for a variety of medical applications in dermatology, dentistry, and ophthalmology. Their laser precision has proven beneficial for applications involving skin resurfacing, cavity preparation, and retinal surgery. Each of these medical applications has different requirements for the Erbium laser and optical fiber delivery system. Dental applications require high-power delivery to efficiently ablate hard tissues (e.g. dentin and enamel). Ophthalmic applications require precision laser surgery of delicate tissues with minimal thermal and mechanical damage to surrounding ocular structures. Cosmetic applications require both high-power and high-repetition-rate delivery of laser radiation for rapid skin resurfacing of large facial skin areas.

IR Fiber Delivery Systems

For lasers operating in the visible and near-infrared spectrum, conventional silica optical fibers can be used as a small, flexible, and inexpensive means of performing minimally invasive laser surgery via small openings in the body. However, for mid-infrared lasers such as the Er:YAG (2.94 µm) and Er:YSGG (2.79 µm), the laser radiation cannot be transmitted through conventional silica optical fibers due to the high absorption at these wavelengths. While for some Erbium medical applications, the use of a large, rigid articulated arm consisting of a series of rotating mirrors is sufficient, the use of a small, flexible optical fiber delivery system for delivery of mid-infrared laser radiation would be a significant improvement. There are a number of specialty IR fibers made from materials such as germanium oxide glass, fluoride glass, sapphire, as well as the hollow waveguide fiber.

Each of these fiber optic based delivery systems has its advantages and disadvantages. Fluoride glass fibers have the best transmission at 2.94 µm, but they are weak, moisture sensitive, can degrade with time, and generate toxic gases such as fluorine and hydrogen fluoride when damaged. Sapphire fiber is biocompatible and made of an extremely hard material which makes it perfect for reusable tips which come in direct contact with the tissue. However, sapphire is not the best choice for the long "trunk" fiber, because of its limited minimum bend radius and long-term mechanical degradation related to its crystalline structure. Sapphire fiber also has a relatively high absorption at 2.9 µm due to the lack of a core/clad structure. Hollow waveguides can handle power, but their transmission fluctuates greatly during actual use due to bending induced losses.

An infrared fiber based on germanium oxide glass has been optimized for use with mid-IR lasers such as Er:YSGG and Er:YAG. The germanium fiber has several advantages compared to other IR fibers. Germanium oxide is stronger, can handle more power, and is more chemically durable than fluoride fibers. Unlike the sapphire fiber and hollow waveguide, the germanium fiber has an optical cladding which minimizes bending losses. Fiber transmission losses are very low (less than 0.7 dB/meter at 2.94 microns and 0.25 dB/meter at 2.79 microns) with power handling over 20 watts for a 450-micron-core fiber (Figure 1).
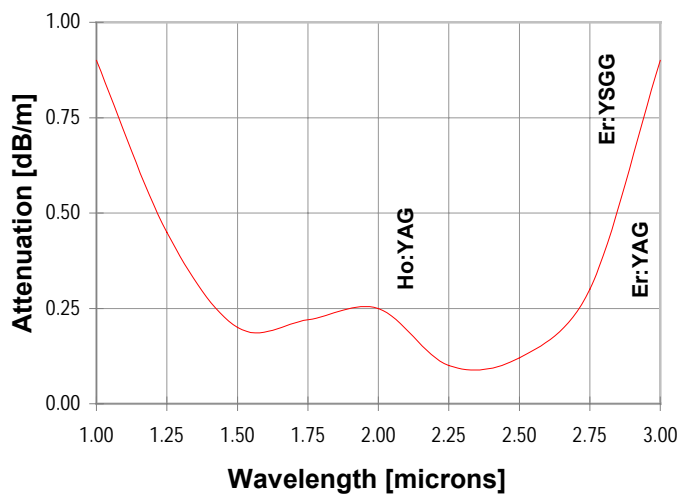
Figure 1. Transmission loss of germanium fibers (from IFS).   **Figure 2.** Dental cable with handpiece

A typical delivery system for the Er:YAG laser consists of an approximately 2 meter long "trunk" fiber to deliver laser power from the laser system to the patient. The distal end of the fiber is attached to a probe terminated with a reusable or disposable tip made from sapphire or low-OH silica, and customized for the specific medical procedure of interest. Figure 2 shows one such delivery system being developed at IFS in conjunction with W&H Dentalwerk (Austria). This cable is designed to couple with different brands of Er:YAG lasers and features ease of alignment and robustness, as well as high power handling for different applications.

Er:YAG Laser Systems and Applications

There are currently a number of Er:YAG and Er:YSGG laser systems on the market, including dental lasers from Biolase and KaVo, aesthetic lasers from Asclepion Laser, Fotona and Sciton, and ophthalmic lasers from Austrian Laser and InPro. In addition, there are other lasers in the final stages of development.
In dentistry, the Er:YAG and Er:YSGG lasers have proven unique in their ability to cut dentin and enamel in a precise and char-free manner for applications such as cavity preparation and caries removal, usually without the need for anesthetic. These lasers are also being used in endodontics (sterilization and drying of the root canal), periodontics (closed curettage with removal of subgigival concrement), dental surgery (incisions and excisions, impacted wisdom teeth, removal of herpes), and tooth etching and sealing of fissures. The Er:YAG is being used in dermatology for skin resurfacing, removal of warts and lesions, hair removal, and the smoothing of scars, blemishes and wrinkles. Several ophthalmic applications are being investigated such as cataract removal, capsulorrhexis, capsulotomy, sclerostomy, and photorefractive keratotomy (PRK).

Er:YAG and Er:YSGG lasers with a flexible fiber optic delivery system have high potential in medical fields such as dentistry, ophthalmology, ENT, orthopedics, urology, and general surgery. Some of these applications, as mentioned above, are already on the market while others are at the stage of intensive development in research centers all over the world. The realization of a robust and reliable infrared fiber, such as the germanium oxide fiber, has played an important role in the establishment of the market for Er:YAG medical lasers and has stimulated study on new medical procedures and laser types. For example, Dr. Detlef Russ at the Institut für Lasertechnologien in der Medizin und Medtechnik (University of Ulm), in conjunction with Dornier MedTech, is investigating the use of an Er:YAG laser for the surgical treatment of carpal-tunnel syndrome [1]. They have developed a new surgical procedure to decrease the recurrence rate using the laser as a dissection tool for the carpal ligament by ablating a small amount of the carpal ligament and denaturing its ends. The laser energy was transmitted via a germanium oxide glass fiber. With this system they performed 11 carpal ligament dissections (Figure 3) without any complications in the follow-up period, and all patients were free of pain and recurrence.
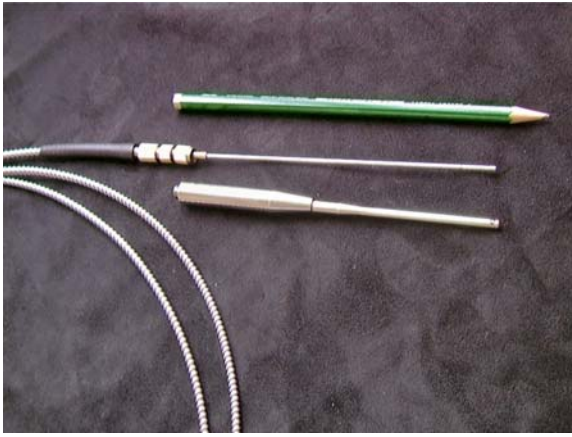
Figure 3. Left - the shielded fiber and sterilizable handpiece. Right – carpal surgery being performed.

Also at the University of Ulm, Dr. R. Hibst has used the Er:YAG laser for ENT surgery. Beginning in 1989, the benefit of different lasers for tympasnoplasty and stapedotomy (middle ear surgery) was investigated. It was demonstrated that the Er:YAG laser was optimum for operating on the ear drum, along the ossicles as far as the footplate without carbonization, and with sharp-edged canals "drilled" through the bone with a diameter of 0.2 mm [2]. Using this technique, children with mucotympanon could potentially have their eardrum reopened in the office without the need for draintubes.

Initial experimental studies conducted in collaboration with the Johns Hopkins Medical School also show that "hybrid" optical fibers consisting of a germanium trunk fiber and a low-OH silica tip are capable of transmitting up to 180 mJ of Er:YAG laser for potential medical applications requiring contact tissue ablation through a flexible endoscope [3]. This pulse energy is more than sufficient for ablation of a variety of both hard and soft tissues.

In urology, the germanium fibers are being tested for use with flexible endoscopes for precise Er:YAG laser incision of urethral, bladder neck, and ureteral strictures, and fragmentation of kidney stones [3,4]. The Er:YAG laser is approximately 10-20 times more precise for soft tissue ablation than the Holmium:YAG laser (λ = 2.12 µm), which is currently the laser of choice in urology. Figure 4 shows the wound healing results at Day 0 and Day 15, after precise incision of the bladder neck performed in a pig with the Er:YAG laser. Bladder neck strictures are defined as a narrowing or stenosis of the bladder neck which may result in recalcitrant scarring and urinary incontinence. A significant number (5-20 %) of patients undergoing surgery for benign or malignant prostate cancer suffer from bladder neck strictures, and there is currently not a simple and effective minimally invasive method of treatment.
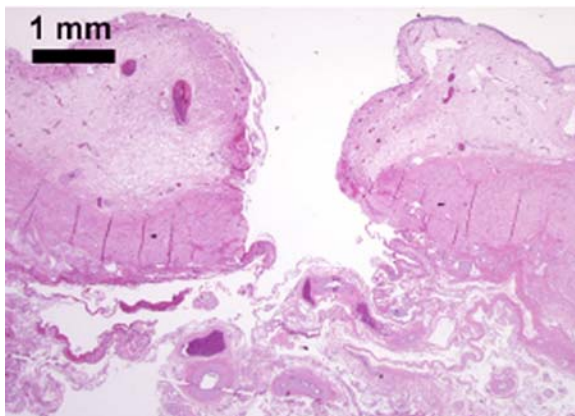
(a) 0 Days
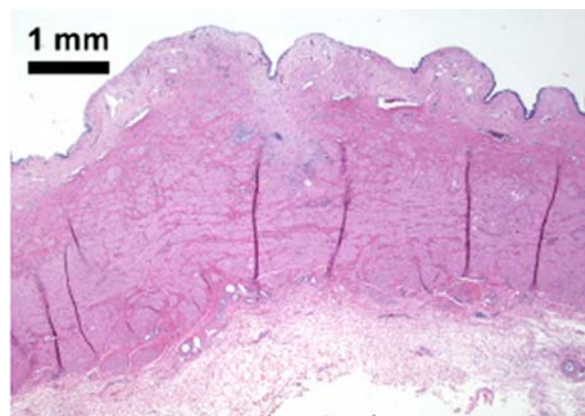
(b) 14 Days

Figure 4. H&E stained histological cross-section of the pig bladder neck after incision with the free-running Er:YAG laser. (a) At Day 0, a clean incision is made with the Er:YAG laser with no significant thermal damage present. (b) At Day 15, the incision has almost completely healed, with only a narrow zone of scar tissue present.

Another promising application is the short-pulse, Q-switched Er:YAG laser for procedures requiring high precision, e.g. in dentistry and ophthalmology. Preliminary results obtained with Johns Hopkins demonstrate that over 40 mJ of 500 nsec pulses are capable of being transmitted through the germanium oxide fiber [5]. Although fiber transmission losses are greater in Q-switched mode (Figure 5), this laser energy should also be sufficient for ablation of both hard and soft tissues. Delivery of Erbium laser radiation in a short-pulse, Q-switched mode may be important because it results in greater precision compared to the free-running Er:YAG. For example, the free-running Er:YAG laser with a pulse length of approximately 300 µs typically produces 10-50 µm of thermal damage in tissue, while short-pulse, Q-switched laser pulses of 500 ns duration reduces the thermal damage zone to only 5-10 µm resulting in improved precision during tissue ablation. Currently, the germanium fiber is being optimized for transmission of higher power in both short-pulse mode and for use with the hybrid fibers in the free-running mode.

Conclusions

The availability of a reliable, low loss, chemically durable and high damage threshold fiber for delivery of mid-infrared laser radiation has made possible the widespread use of these lasers in a variety of medical and dental areas. These applications are expected to increase in the future as new procedures are investigated by the medical community. Improvements in fiber strength have allowed the use of the Er:YAG laser in procedures, such as invasive surgery, where tight fiber bending is required. Further improvements in fiber power handling will allow for even higher-power applications especially for Q-switched Er:YAG and Er:YSGG lasers.

References

1. Russ D., Ebinger T., Illich W., Steiner R.   Er:Yag Laser for the Surgical Treatment of the Carpal Tunnel Syndrome. Therapeutic Laser Applications and Laser-Tissue Interactions. Proc. SPIE Vol. 5142, p. 76-81, 2003.

2. Pfalz R., Hibst R., Bald N.   Suitability of different lasers for operations ranging from the tympanic membrane to the base of the stapes- Adv Otorhinolaryngol (Basel) 49: 87-94, 1995.

3. Chaney CA, Yang Y, Fried NM. Hybrid germanium / silica optical fibers for endoscopic delivery of Erbium:YAG laser radiation. Lasers in Surgery and Medicine 34:5-11, 2004.

4. Fried NM, Tesfaye Z, Ong AM, Rha KH, Hejazi P. Optimization of the Erbium:YAG laser for precise incision of ureteral and urethral tissues: in vitro and in vivo results. Lasers in Surgery and Medicine 33:108-114, 2003.

5. Fried NM, Yang Y, Chaney CA, Fried D. Transmission of free-running and Q-switched Erbium:YAG laser radiation through sapphire and germanium fibers. Proc. SPIE. In Press.

Figure 5.   Percent transmission (T) of free-running (300 µs) and Q-switched (500 ns) Erbium:YSGG laser pulses through 450-µm-core germanium oxide optical fibers of 1 meter length.   Data points represent the mean $\pm$ S.D. (n = 7).
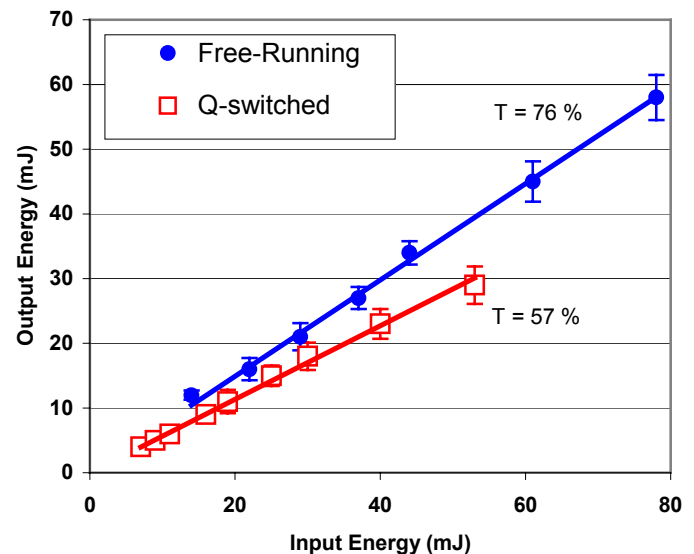
Transmission of Free-Running and Q-switched Er:YAG and Er:YSGG Laser Energy Through Germanium Oxide / Silica Fibers

Nathaniel M. Fried[a*], Yubing Yang[a], Kyunhee Lee[b], Hussain A. Tafti[a]

[a] Dept. of Urology, Johns Hopkins Medical Institutions, Baltimore, MD
[b] Dept. of Biomedical Engineering, Johns Hopkins University, Baltimore, MD

ABSTRACT

Endoscopic Erbium laser applications have been limited by the lack of a suitable optical fiber. This study describes a hybrid germanium oxide / silica fiber for transmission of Q-switched and free-running Er:YAG and Er:YSGG laser radiation. Hybrid fibers consisted of a 1-meter-long germanium trunk fiber connected to a 1-cm-long silica fiber tip using PTFE, PET, or PTFE/FEP heat-shrink tubing. Maximum transmission of Er:YAG energy through fiber trunk/tip diameters of 250/365, 350/365, and 450/550 μm were recorded. The transmission rates through 450/550 μm fibers using Q-switched (500 ns) and free-running (300 μs) Er:YAG and Er:YSGG laser pulses were also measured. Maximum free-running Er:YAG pulse energies (fluences) measured up to 103 mJ ($98 \ J/cm^2$), 112 mJ ($107 \ J/cm^2$), and 233 mJ ($98 \ J/cm^2$), respectively, through 250/365, 350/365, and 450/550 hybrid fibers. Free-running Er:YAG and Er:YSGG transmission averaged 56% and 65%, with an attenuation of 1.1 ± 0.1 dB/m and 0.6 ± 0.1 dB/m, respectively, after correction for Fresnel losses (n = 7). Q-switched Er:YAG and Er:YSGG laser transmission averaged 55% and 62%, with an attenuation of 1.1 ± 0.2 dB/m and 0.9 ± 0.3 dB/m, respectively. Both Q-switched lasers transmitted a maximum pulse energy of 13 mJ (n = 7). The germanium / silica fiber is promising for use with the Erbium laser in applications requiring contact laser tissue ablation through a flexible endoscope.

Keywords: erbium, Q-switched, germanium, hybrid, mid-IR, fiber, oxide glass

1. INTRODUCTION

The Er:YAG ($\lambda = 2.94$ μm) and Er:YSGG ($\lambda = 2.79$ μm) lasers are used in dermatology and dentistry for precise tissue ablation. Recent urology studies have also shown that the Er:YAG laser is more precise for incision of soft urological tissues and more efficient for ablation of urinary stones than the Ho:YAG laser ($\lambda = 2.12$ μm), due to the increased water absorption near 3 μm [1-3]. However, Er:YAG laser applications in endoscopy are limited due to the lack of a suitable optical fiber. Several mid-infrared fibers are available, including chalcogenide, zirconium fluoride, sapphire, germanium oxide, and hollow silica waveguides. All of these optical waveguides have major limitations, including limited power delivery, chemical degradation in fluid environments, limited flexibility, low melting temperatures, tissue toxicity, and high cost [4,5]. The ideal mid-infrared fiber for use in endoscopic tissue ablation would combine high-power delivery, chemical and mechanical durability, flexibility and biocompatibility.

Previous preliminary studies in our laboratory have demonstrated that a hybrid fiber consisting of a germanium oxide trunk fiber and a silica fiber tip may be promising for use in endoscopic Erbium laser tissue ablation in contact mode [6-8]. The germanium trunk fiber is capable of delivering high Erbium laser pulse energies, and it is also sufficiently flexible to be inserted into most flexible endoscopes. The main limitation of the germanium fiber is its low melting temperature (~ 680 °C), which prevents its use for tissue ablation in contact mode. However, attachment of a robust and biocompatible low-OH silica tip with a higher melting temperature (~ 1175 °C) to the germanium fiber may allow for contact tissue ablation during endoscopic applications without fiber tip damage. During preliminary studies, the germanium fiber tip damage threshold during contact tissue ablation was increased significantly from 9 mJ without silica tip to 180 ± 30 mJ with the silica tip [6].
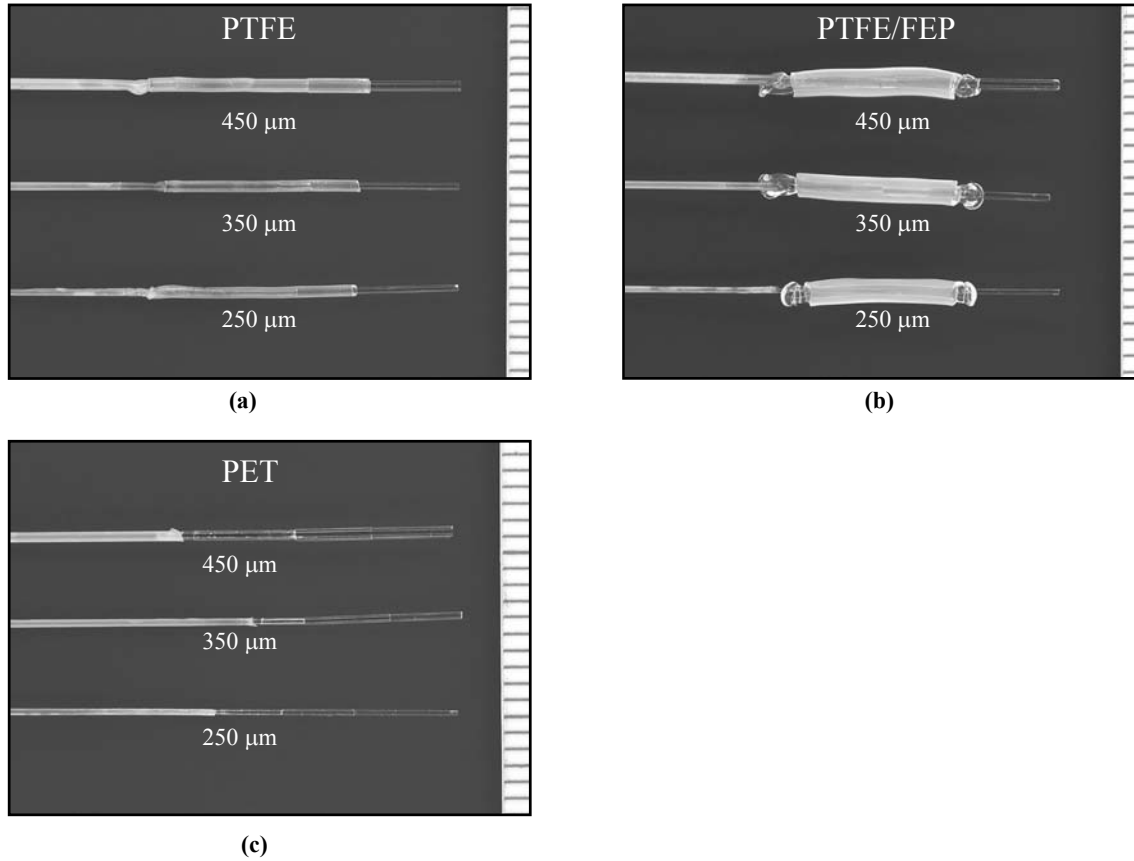
This study describes the high-power transmission properties of a hybrid germanium / silica optical fiber for potential use in endoscopic surgery. The hybrid fiber design was optimized, energy transmission was maximized, and transmission rates for Q-switched and free-running Er:YAG and Er:YSGG laser pulses were measured.

2. MATERIALS AND METHODS

A Schwartz Electro-Optics SEO 1-2-3 laser, operated with either an Er:YSGG ($\lambda = 2.79$ μm) or an Er:YAG ($\lambda = 2.94$ μm) laser rod, was used for the experiments. The laser was operated in free-running mode with a 300 μs pulse length and in short-pulse mode with a 500 ns pulse length produced by a rotating mirror Q-switch. The Q-switched Er:YAG and Er:YSGG laser pulse energy measured 25 mJ at 3 Hz. The laser pulse energy was measured using a Molectron EPM 1000 pyroelectric detector and the temporal pulse length was measured using a Boston Electronics PD-10.6 photovoltaic infrared detector. The laser radiation was focused with a 20-mm-focal-length calcium fluoride lens into hybrid germanium / silica optical fibers consisting of a 1-meter-length germanium oxide trunk fiber (Infrared Fiber Systems, Silver Spring, MD) with a 1-cm-length low-OH silica fiber tip. The trunk/tip fiber-core diameters measured 250/365, 350/365, and 450/550 μm and were attached with three different types of heat-shrink tubing: (a) PTFE, (b) PET, and (c) PTFE / FEP combination (Table 1, Figure 1). A linear fit to the data points provided the average percent transmission of the fibers, which was then corrected by subtracting the Fresnel losses, and the attenuation calculated in dB/m. The data points for each graph represent the average of 7 independent measurements from 7 different fibers, and the error bars represent the minimum and maximum values recorded.

Table 1. Heat-shrink tubing materials used to connect hybrid fibers.

Material	Pre-/Post-Shrink ID (μm)	Wall Thickness (μm)	Shrink Temp. (^{o}C)
PTFE	850 / 375	150	343
PTFE / FEP	900 / 0	575	343 / 17
PET	350 / 280	12.5	85-190
	450 / 360	12.5	
	725 / 580	25	

(a)

(b)

(c)

Figure 1. Hybrid germanium/silica fibers assembled using: (a) PTFE; (b) PTFE / FEP; (c) PET. A 1-cm-long, silica tip was attached to a 1-m-long germanium fiber. Germanium fiber diameters are 450, 350, and 250 μm. Ruler bar = 1 mm increments.

3. RESULTS

3.1 Hybrid Fiber Assembly

PTFE was found to be the most reliable material producing the highest Er:YAG pulse energy transmission, although the high shrink temperature resulted in melting of the Hytrel coating on the germanium fiber (Figure 1a). The PTFE / FEP shrink-melt combination produced the worst results. The shrink pressure and melted FEP tended to push the silica tip away from the germanium trunk fiber, causing sub-optimal alignment at the fiber interface and resulting in poor laser transmission and low damage thresholds (Figure 1b). The major limitation of the PET tubing was its wall thickness (12.5 – 25 μm), which results in weak bending strength (Figure 1c). PET is also limited to only approximately 20% shrinkage, so the trunk and tip fiber outer diameters need to match more precisely than with PTFE. However, PET has some advantages: its low shrink temperature eliminates melting of the germanium Hytrel jacket, its transparency provides better alignment of the fiber interface, and it shrinks more uniformly than PTFE.

3.2 Peak Output Energies

Maximum hybrid fiber transmission of free-running Erbium:YAG laser radiation was measured with the silica tips placed in contact with human urinary stones ex vivo, in a saline bath (Table 2). The peak hybrid fiber transmission of Erbium:YAG laser energy was approximately 100 J/cm^2 for all of the fiber diameters (250/365, 350/365, 450/550) tested, with pulse energies reaching as high as 233 mJ at 10 Hz. Average fiber transmission measured approximately 70 J/cm^2 for these fiber diameters. Transmission of Q-switched Er:YAG laser energy was also measured through 450/550 hybrid fibers, with peak pulse energies of 13 mJ.

Table 2. Peak and average Er:YAG pulse energies transmitted through hybrid germanium / silica fibers.

Fiber Core (μm) (Trunk / Tip)	Maximum		Average	
	Energy (mJ)	Fluence (J/cm^2)	Energy (mJ)	Fluence (J/cm^2)
250 / 365	103	98	74 $\pm$ 29	71
350 / 365	112	107	79 $\pm$ 24	75
450 / 550	233	98	157 $\pm$ 46	66

3.3 Transmission and Attenuation Measurements

The percent transmission of free-running and Q-switched Er:YAG and Er:YSGG laser radiation through 1-meter-length germanium oxide trunk fibers with a 1-cm-length low-OH silica tip was measured (Figure 2). Transmission rates for the free-running Er:YAG and Er:YSGG lasers measured 56% and 65%, respectively (n = 7 fibers). After correction for the Fresnel reflection losses at the fiber interfaces, the fiber attenuation measured 1.1 $\pm$ 0.1 dB/m and 0.6 $\pm$ 0.1 dB/m, respectively. The transmission rate for the Q-switched Er:YAG and Er:YSGG lasers was 55% and 65%, with an attenuation of 1.1 $\pm$ 0.2 dB/m and 0.9 $\pm$ 0.3 dB/m, respectively. Both Q-switched lasers transmitted a maximum pulse energy of 13 mJ (n = 7 fibers).
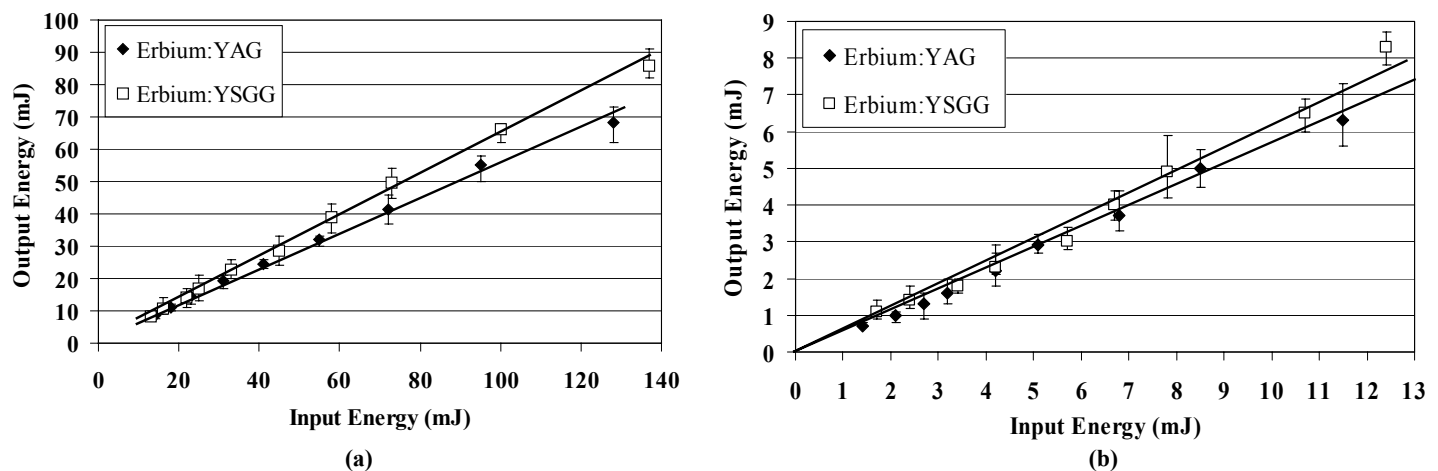

Figure 2. Hybrid fiber transmission rates for Er:YAG and Er:YSGG laser radiation during (a) free-running (300 μs) and (b) Q-switched (500 ns) operation. All fibers tested were 450 / 550 μm hybrid fibers.

4. DISCUSSION

In this study, we demonstrated a simple, biocompatible, and inexpensive method of assembling hybrid germanium / silica optical fibers using PTFE heat-shrink tubing. Peak hybrid fiber energies of up to 233 mJ at 10 Hz were transmitted through the fibers with the fluence reaching approximately 100 J/cm^2 for all the fiber diameters (250/365, 350/365, 450/550) tested. Although average pulse energies were lower and bending losses have previously been recorded [6], transmitted energies are still well above what is necessary for Er:YAG laser ablation of most soft and hard tissues. For example, for soft tissues a low laser fluence of only 1-5 J/cm^2 is sufficient [9], while for hard tissues a higher laser fluence of 20-40 J/cm^2 may be necessary for efficient tissue ablation [10,11].

This study also demonstrated for the first time Q-switched transmission of Er:YAG and Er:YSGG laser radiation through the hybrid germanium / silica fibers. Q-switched delivery of Erbium laser energy provides an ultra-precise method of tissue ablation. For example, peripheral thermal damage caused in tissue during Er:YAG laser ablation may be reduced from 10-50 μm in the free-running mode to only 5-10 μm in Q-switched mode [9]. Previous studies have shown that Q-switched Er:YAG laser energy could be transmitted through germanium oxide fibers [12,13]. However, the Q-switched pulse energies of up to 13 mJ measured in this study are sufficient for ablation of soft tissues and demonstrate that delivery of Q-switched Er:YAG laser energy through a flexible, germanium oxide fiber in contact mode with tissue is feasible.

Not surprisingly, fiber attenuation was lower at the 2.79-μm Er:YSGG wavelength, due to lower OH$^-$ absorption in the germanium and sapphire fibers than at the longer, 2.94-μm Er:YAG wavelength. Tables 3 and 4 provide a comparison of free-running and Q-switched Er:YAG and Er:YSGG laser fiber transmission and attenuation between the hybrid fibers and previous studies characterizing the bare germanium and sapphire fibers [13]. The attenuation through the hybrid fiber is significantly higher than that through the germanium and sapphire fibers. This is most likely due to coupling losses at the germanium / silica interface as well as the high attenuation through the silica tip. However, considering the relatively low pulse energies necessary to ablate tissue (a few mJ), the availability of high-power Erbium lasers (Joules/pulse), and the need for only a few meters of fiber length for most medical applications, a fiber attenuation of 0.6 – 1.1 dB/m is more than adequate.

Table 3. Percent transmission of Er:YAG and Er:YSGG laser radiation through mid-IR fibers.

Fiber Type	Er:YSGG ($\lambda = 2.79\ \mu m$)		Er:YAG ($\lambda = 2.94\ \mu m$)	
	Free-running	Q-switched	Free-running	Q-switched
Sapphire	88 ± 6	65 ± 3	77 ± 5	74 ± 4
Germanium	76 ± 2	57 ± 1	68 ± 2	64 ± 6
Hybrid	65 ± 2	62 ± 5	56 ± 3	55 ± 4

Table 4. Attenuation (dB/m) of Er:YAG and Er:YSGG laser radiation through mid-IR fibers.

Fiber Type	Er:YSGG ($\lambda = 2.79\ \mu m$)		Er:YAG ($\lambda = 2.94\ \mu m$)	
	Free-running	Q-switched	Free-running	Q-switched
Sapphire	0.2 ± 0.1	1.0 ± 0.2	0.4 ± 0.2	0.6 ± 0.2
Germanium	0.3 ± 0.1	1.3 ± 0.1	0.7 ± 0.1	0.9 ± 0.3
Hybrid	0.6 ± 0.1	0.9 ± 0.3	1.1 ± 0.1	1.1 ± 0.2

5. CONCLUSIONS

A novel, hybrid germanium oxide / silica optical fiber was optimized for the delivery of free-running and Q-switched Er:YAG and Er:YSGG laser radiation. Peak fiber transmission and attenuation was measured. Sufficient Erbium laser energy was transmitted for potential use in both hard and soft tissue ablation. This optical fiber may be useful in endoscopic medical applications requiring a flexible fiber for contact tissue ablation.

REFERENCES

1. J. M. H. Teichman, K. F. Chan, P. P. Cecconi, N. S. Corbin, A. D. Kamerer, R. D. Glickman, A. J. Welch, "Er:YAG versus Ho:YAG lithotripsy," J. Urol., vol. 165, pp. 876-879, 2001.
2. N. M. Fried, "Potential applications of the Er:YAG laser in endourology," J. Endourol., vol. 15, 889-894, 2001.
3. N. M. Fried, Z. Tesfaye, A.M. Ong, K.H. Rha, P. Hejazi, "Optimization of the Erbium:YAG laser for precise incision of ureteral and urethral tissues: in vitro and in vivo results," Lasers Surg. Med., vol. 33, 108-114, 2003.
4. G. N. Merberg, "Current status of infrared fiber optics for medical laser power delivery," Lasers Surg. Med., vol. 13, 572-576, 1993.
5. J. A. Harrington. Infrared fibers and their applications. SPIE Press: Bellingham, WA, 2004.
6. C. A. Chaney, Y. Yang, N. M. Fried, "Hybrid germanium / silica optical fibers for endoscopic delivery of Erbium:YAG laser radiation," Lasers Surg. Med., vol. 34, pp. 5-11, 2004.
7. K. Levin, D. Tran, A. Tchapijnikov, N. M. Fried, "Specialty fiber expands infrared laser applications," Biophoton. Internat., vol. 11, 41-43, 2004.
8. Y. Yang, C. A. Chaney, N. M. Fried, "Erbium:YAG laser lithotripsy using hybrid germanium / silica optical fibers," J. Endourol., vol. 18, 830-835, 2004.
9. J. T. Walsh Jr, T. J. Flotte, T. F. Deutsch, "Er:YAG laser ablation of tissue: effect of pulse duration and tissue type on thermal damage," Lasers Surg. Med., vol. 9, pp. 314-326, 1989.
10. D. Fried, N. Ashouri, T. Breunig, R. Shori, "Mechanism of water augmentation during IR laser ablation of dental enamel." Lasers Surg. Med., vol. 31, pp. 186-193, 2002.
11. N. M. Fried, D. Fried, "Comparison of Er:YAG and 9.6-µm TE CO2 lasers for ablation of skull tissue," Lasers Surg. Med., vol. 28, pp. 335-343, 2001.
12. E. Papagiakoumou, D. N. Papadopoulos, N. Anastasopoulou, A. A. Serafetinides, "Comparative evaluation of HP oxide glass fibers for Q-switched and free-running Er:YAG laser beam propagation," Opt. Commun., vol. 220, pp. 151-160, 2003.
13. N. M. Fried, Y. Yang, C. A. Chaney, D. Fried, "Transmission of q-switched Erbium:YSGG ($\lambda = 2.79$ mm) and Erbium:YAG ($\lambda = 2.94$ mm) laser radiation through germanium oxide and sapphire fibers at high pulse energies," Lasers Med. Sci. In press.

Erbium vs. Holmium Laser Incision of the Urethra and Bladder Neck

Ioannis M. Varkarakis[a], Takeshi Inagaki[a], Mohamad E. Allaf[a], Theresa Y. Chan[a,b], Craig G. Rogers[a],
E. James Wright[a], Nathaniel M. Fried[a*]
Depts. of Urology[a] and Pathology[b], Johns Hopkins Medical Institutions, Baltimore, MD

ABSTRACT

The objective of this study is to evaluate in an animal model differences in wound healing and scar formation in healthy urethra and bladder neck incised with the Erbium:YAG and Holmium:YAG lasers. In each of 18 domestic pigs, three 1-cm-long incisions were made, two at the bladder neck and one in the mid-urethra using either the Er:YAG laser (9 pigs) or the Ho:YAG laser (9 pigs). In each laser group, three animals were sacrificed on postoperative (POD) days 0, 6, and 14. Width of collateral damage, as evidenced by coagulation necrosis and granulation tissue at the wound base, and incision depth were evaluated during tissue analysis. Collateral damage with the Er:YAG laser at POD 0, 6 and 14 was 20 ± 5 μm, 900 ± 100 μm, and 430 ± 100 μm, respectively. Damage with the Ho:YAG laser was 660 ± 110 μm, 2280 ± 700 μm, and 1580 ± 250 μm, respectively. The granulation tissue was significantly less ($p < 0.05$) at all time points with the Er:YAG laser. Similarly, incision depths for the two laser groups at days 6 (1100 ± 200 μm vs 1500 ± 300 μm) and 14 (670 ± 140 μm vs 1240 ± 140 μm) were also significantly less ($p < 0.05$) for the Er:YAG laser group, indicating faster healing of the wound created. In this in vivo animal study, incisions in the urethra and bladder neck made with the Er:YAG laser healed faster and with less scar formation than incisions made with the Ho:YAG laser.

Key Words: urethra, bladder neck, laser, erbium, holmium, incision, stricture

1. INTRODUCTION

The management of urethral strictures is challenging because of their tendency to recur. Minimally invasive techniques (e.g. balloon dilatation and cold knife incision) have been used as an alternative to surgical reconstruction, but and have widely variable success rates ranging from 20-80% [1-3]. During internal urethrotomy, the scarred epithelium is separated and healing occurs by secondary intention. Epithelialization progresses from the wound edges, while at the same time wound contracture ensues. If wound contraction significantly narrows the urethral lumen before completion of epithelialization, stricture recurrence occurs. The race between these two phenomena is difficult to modify [4]. A vicious cycle between incision of the stricture and new scar formation from injury caused during therapy is a potential mechanism responsible for these failures.

A variety of lasers, including CO_2 [5] argon [6], Nd:YAG [7,8] KTP [9] and Ho:YAG [10-12] have been used to vaporize rather than incise the scar tissue, but they have had mixed results. These lasers produce significant thermal damage and necrosis, and they have proven to be no better than simple cold knife internal urethrotomy [5-13]. The ideal laser to use for urethral strictures and bladder neck contractures would be one that totally vaporizes the scar tissue, without causing collateral thermal damage. This should minimize postoperative scarring and result in higher success rates. In an acute animal model, the Er:YAG laser has been shown to be very precise, with a peripheral thermal damage zone of only 10-20 μm, compared to 300-400 μm seen with the Ho:YAG laser [14,15]. This large difference in collateral damage is due to the specific wavelength of the Er:YAG laser, which matches a major water absorption peak in tissue allowing it to be more strongly absorbed than the Ho:YAG laser.

The objective of this study is to evaluate in an animal model differences in wound healing and scar formation in healthy urethra and bladder neck incised with the Er:YAG and Ho:YAG lasers. The hypothesis evaluated is that decreased peripheral thermal damage caused by the Er:YAG laser will translate into more rapid wound healing and less scar formation compared to the Ho:YAG laser. This will potentially find an application in treating urethral strictures and bladder neck contractures, where minimal new scar formation is required to decrease recurrence rates.

2. MATERIALS AND METHODS

2.1 Laser Parameters

An Er:YAG laser (SEO 1-2-3, Schwartz Electro-optics, Orlando, FL) operating at a wavelength of 2.94 μm, a pulse duration of 70 μs, fiber output pulse energy of 20 mJ, and repetition rate of 10 Hz was used. The laser radiation was focused into a 250-μm-core sapphire optical fiber (Photran, Amherst, NH). A Ho:YAG laser (SEO 1-2-3) operating at a wavelength of 2.12 μm, pulse duration of 300 μs, fiber output energy of 500 mJ, and repetition rate of 3 Hz, was also used. The laser radiation was focused into a 300-μm-core silica optical fiber (Table 1).

Table 1. Summary of laser parameters used in this study.

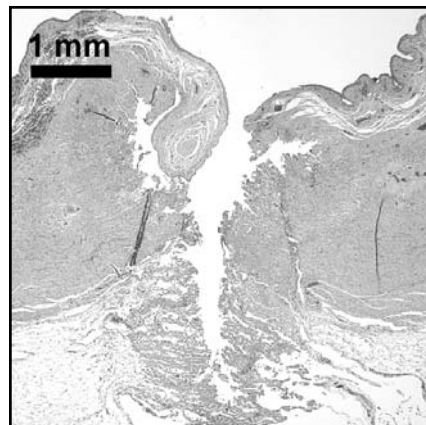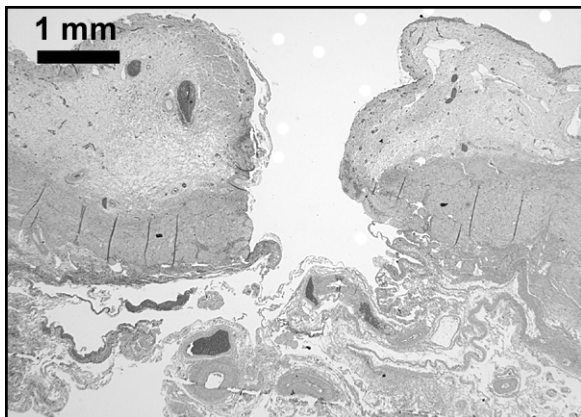| Laser Parameters	Holmium	Erbium
Wavelength (μm):	2.12	2.94
Energy / pulse (mJ):	500	20
Pulse Length (μs):	300	70
Pulse Repetition Rate (Hz):	3	10
Fiber Core Diameter (μm):	300	250
Fiber Type:	silica	sapphire

2.2 Animal Studies

All procedures were approved by the JHU Animal Review Committee (ACR# SW01M293). A total of 18 female pigs (30-45 kg) were divided into two arms, with 9 pigs in each laser arm. Three animals in each arm were sacrificed on postoperative days 0, 6, and 14. During the procedure, access to the urethra and bladder neck was obtained using a 17F rigid cystoscope with 30-degree lens. Three 1-cm-long incisions were made in each pig, two at the bladder neck and one in the mid-urethra. After the procedure a 14F urethral catheter was left in the bladder then removed after 3-4 hours. The pigs were euthanized, and the bladder and urethra samples were removed for histopathological processing. Quantitative measurements of collateral injury and incision depth were made. Collateral damage on day 0 was recorded as coagulative necrosis from the incision outward, while on days 6 and 14 as the extent of granulation width at the wound base. These parameters were analyzed using a Student's t-test.
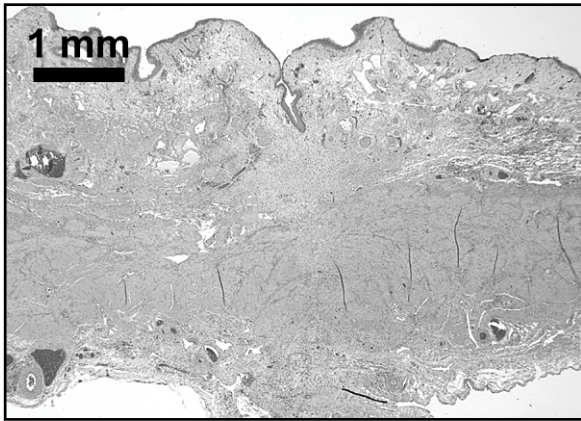
3. RESULTS

On day 0, Er:YAG and Ho:YAG laser incisions in the mid-urethra and bladder neck were of comparable depth, averaging 2540 ± 390 μm and 2530 ± 780 μm, respectively ($p = 0.49$) (Table 2). The zone of coagulative necrosis (Figure 1a-b) was significantly higher for the Ho:YAG laser than for the Er:YAG laser (660 ± 110 μm vs 20 ± 5 μm, respectively, $p = 0.01$). On day 6 (Figure 1c-d), the granulation tissue width at the incision base was 900 ± 100 μm and 2280 ± 700 μm, for the Er:YAG and Ho:YAG lasers, respectively ($p = 0.04$). After 14 days the granulation tissue created by the Er:YAG laser was less than the Ho:YAG laser (430 ± 100 μm vs 1580 ± 250 μm, respectively, $p = 0.03$) (Figure 1e-f). As wound healing progressed, granulation tissue filled the wound bed and decreased the incision depth. At day 6, the Er:YAG and Ho:YAG laser incisions were 45% and 60% of initial depth (1100 ± 200 μm vs 1500 ± 300 μm, respectively, $p = 0.04$). On day 14, the Er:YAG and Ho:YAG incisions were 25% and 50% of initial depth (670 ± 140 μm vs 1240 ± 140 μm), respectively ($p = 0.02$). Images of the tissue surface at 14 days also demonstrate accelerated wound healing after Er:YAG incision compared with Ho:YAG incision (Figure 2a-b).

Table 2. Injury parameters after incisions made with Ho:YAG and Er:YAG lasers at postoperative day 0, 6, and 14.
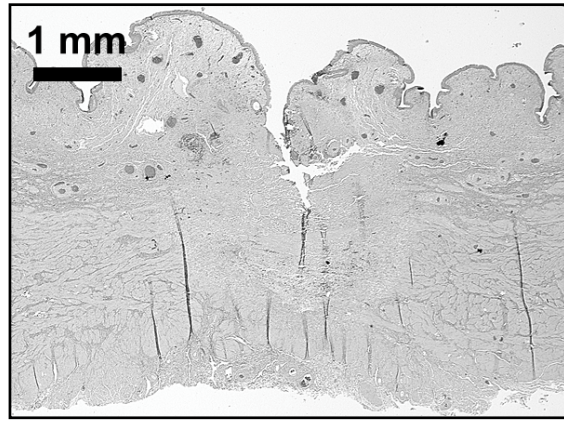
Laser	n	Day 0		n	Day 6		n	Day 14	
		Incision Depth (μm)	Thermal Damage (μm)		**Incision Depth** (μm)	**Granulation Width** (μm)		Incision Depth (μm)	Granulation Width (μm)
Holmium	3	2530 ± 780	660 ± 110	3	1500 ± 300	2280 ± 700	3	1240 ± 140	1580 ± 250
Erbium	3	2540 ± 390	20 ± 5	3	1100 ± 200	900 ± 100	3	670 ± 140	430 ± 100
P value		0.49	0.01		0.04	0.04		0.02	0.03

(a) Er:YAG, Day 0   **(b)** Ho:YAG, Day 0

(c) Er:YAG, Day 6   **(d)** Ho:YAG, Day 6

(e) Er:YAG, Day 14   **(f)** Ho:YAG, Day 14

Figure 1. H&E stained histologic cross-sections of incisions made with the Er:YAG and Ho:YAG laser on post-operative days 0, 6, and 14. Arrows demarcate the border between native tissue and thermally coagulated tissue.

(a) Er:YAG, Day 14   **(b)** Ho:YAG, Day 14

Figure 2. Images of the incisions made with the Er:YAG and Ho:YAG lasers at day 14. (a) Er:YAG; (b) Ho:YAG.

4. DISCUSSION

This study confirms the minimal collateral thermal damage caused acutely by the Er:YAG laser by gross and histologic examination. Histologic examination demonstrated that the Er:YAG laser produced approximately four times less scar tissue than the Ho:YAG laser. The granulation zone and incision depth were also less in the Er:YAG laser arm than in the Ho:YAG laser for a given POD. Incisions made with the Er:YAG laser healed twice as rapidly as those with the Ho:YAG laser. This difference was also observed with tissue examination prior to formalin fixation. Er:YAG laser incisions at day 14 were difficult to identify because of almost complete healing.

Although the Er:YAG laser is a promising new technology for potential clinical use in endourologic applications, the laser has several limitations. First, due to the precise cutting of the Er:YAG laser and the limited coagulation it produces, the Er:YAG laser is not recommended for applications requiring hemostasis. Bleeding was more pronounced during incisions with this laser, although this did not translate into any postoperative problems.

Second, low-OH silica optical fibers do not transmit in the mid-infrared spectrum and therefore cannot be used at the 2.94-μm Er:YAG wavelength. Therefore, mid-infrared optical fibers are necessary for use with the Er:YAG laser. Unfortunately, mid-IR fibers (e.g. sapphire, germanium oxide, zirconium fluoride, and hollow silica waveguides) have major limitations, including inferior mechanical and chemical durability, or they are inflexible, toxic in tissue, and expensive. Although the sapphire fibers used in this study are adequate for use with rigid endoscopes in the lower urinary tract, these fibers are not sufficiently flexible for use with flexible scopes in the upper urinary tract.

Finally, the results presented in this short-term animal wound healing study refer to the incision of healthy, and not scarred, urethral and bladder neck tissue. It is predicted that the reduced water content in scar tissue compared to healthy tissue would result in greater thermal damage and scar formation after both Er:YAG and Ho:YAG incision. However, since both lasers rely predominantly on water absorption for tissue ablation, the large differential in thermal damage and scar formation between the Er:YAG and Ho:YAG lasers reported in this study should remain.

5. CONCLUSIONS

Incisions created in the urethra and bladder neck of an animal model with the Er:YAG laser heal more rapidly and with less scar formation than incisions made with the Ho:YAG laser. Clinical studies are currently in development to evaluate use of the Er:YAG laser in the treatment of urethral strictures and bladder neck contractures.

REFERENCES

1. R. A. Santucci, J. W. McAninch, "Urethral reconstruction of strictures resulting from treatment of benign prostatic hypertrophy and prostate cancer," Urol. Clin. North Am., vol. 29, pp. 417-427, 2002.
2. C. F. Heyns, J. W. Steenkamp, M. L. De Kock, P. Whitaker, "Treatment of male urethral strictures: is repeated dilation or internal urethrotomy useful?," J. Urol., vol. 160, pp. 356-358, 1998.
3. P. Albers, J. Fichtner, P. Bruhl, S. C. Muller, "Long-term results of internal urethrotomy," J.Urol., vol.156, pp.1611-1614, 1996.
4. G. H. Jordan, S. M. Schlossberg, C. J. Devine, "Surgery of the penis and urethra," In P. C. Walsh, A. B. Retik, E. D. Vaughan, A. J. Wein (Eds): Campbell's Urology. 7th ed, Philadelphia, W. B. Saunders, vol 3, pp 3341-3347, 1998.
5. T. A. McNicholas, J. Colles, S. G. Bown, J. E. A. Wickham et al, "Treatment of urethral strictures with a prototype CO_2 laser endoscope," Lasers Med. Sci., vol. 3, p. 427, 1988.
6. H. C. Becker, J. Miller, H. D. Noske, J. P. Klask, W. Weidner, "Transurethral laser urethrotomy with argon laser: experience with 900 urethrotomies in 450 patients from 1978 to 1993," Urol. Int., vol. 55, pp. 150-153, 1995.
7. J. A. Smith, "Treatment of benign urethral strictures using sapphire tipped Nd:YAG laser," J.Urol., vol.142, pp.1221-1222, 1989.
8. P. N. Dogra, G. Nabi, "Core-through urethrotomy using the neodymium: YAG laser for obliterative urethral strictures after traumatic urethral disruption and/or distraction defects: long-term outcome," J. Urol., vol. 167, pp. 543-546, 2002.
9. P. J. Turek, T. R. Malloy, M. Cendron, V. L. Carpiniello, A. J. Wein AJ, "KTP-532 laser ablation of urethral strictures," Urology, vol. 40, pp. 330-334, 1992.
10. A. R. Kural, E. R. Coskuner, I. Cevik, "Holmium laser ablation of recurrent strictures of urethra and bladder neck: preliminary results," J. Endourol., vol. 14, pp. 301-304, 2000.
11. B. A. Laven, R. C. O'Connor, G. D. Steinberg, G. S. Gerber, "Long-term results of antegrade endoureterotomy using the holmium laser in patients with ureterointestinal strictures," Urology, vol. 58, pp. 924-929, 2001.
12. K. Matsuoka, M. Inoue, S. Lida, K. Tomiyasu, S. Noda, "Endoscopic antegrade laser incision in the treatment of urethral stricture," Urology, vol. 60, pp. 968-972, 2002.
13. T. Niesel, R. G. Moore, H. J. Alfert, L. R. Kavoussi, "Alternative endoscopic management in the treatment of urethral strictures," J. Endourol., vol. 9, pp. 31-39, 1995.
14. N. M. Fried, "Potential applications of the Erbium:YAG laser in endourology," J. Endourol., vol. 15, pp. 889-894, 2001.
15. N. M. Fried, Z. Tesfaye, A. M. Ong, Koon H. Rha, Pooya Hejazi, "Optimization of the Erbium:YAG laser for precise incision of ureteral and urethral tissues: in vitro and in vivo results," Lasers Surg. Med., vol. 33, pp. 108-114, 2003.

Delivery of Erbium:YAG Laser Radiation Through
Side-Firing Germanium Oxide Fibers

Anthony K. Ngo[a], Nathaniel M. Fried*[b]

Depts. of [a]Electrical & Computer Engineering, [b]Urology, Johns Hopkins University, Baltimore, MD 21224

ABSTRACT

The Erbium:YAG laser is currently being tested experimentally for endoscopic applications in urology, including more efficient laser lithotripsy and more precise incision of urethral strictures than the Holmium:YAG laser. While side-firing silica fibers are available for use with the Ho:YAG laser in urology, no such fibers exist for use with the Er:YAG laser. These applications may benefit from the availability of a side-firing, mid-infrared optical fiber capable of delivering the laser radiation at a 90-degree angle to the tissue. The objective of this study is to describe the simple construction and characterization of a side-firing germanium oxide fiber for potential use in endoscopic laser surgery. Side-firing fibers were constructed from 450-μm-core germanium oxide fibers of 1.45-m-length by polishing the distal tip at a 45-degree angle and placing a 1-cm-long protective quartz cap over the fiber tip. Er:YAG laser radiation with a wavelength of 2.94 μm, pulse duration of 300 μs, pulse repetition rate of 3 Hz, and pulse energies of from 5 to 550 mJ was coupled into the fibers. The fiber transmission rate and damage threshold measured 48 ± 4 % and 149 ± 37 mJ, respectively (n = 6 fibers). By comparison, fiber transmission through normal germanium oxide trunk fibers measured 66 ± 3 %, with no observed damage (n = 5 fibers). Sufficient pulse energies were transmitted through the side-firing fibers for contact tissue ablation. Although these initial tests are promising, further studies will need to be conducted, focusing on assembly of more flexible, smaller diameter fibers, fiber bending transmission tests, long-term fiber reliability tests, and improvement of the fiber output spatial beam profile.

Keywords: ablation, endoscopic, erbium, fiber, germanium, mid-infrared, sculpted, side-firing, urology

1. INTRODUCTION

Recent studies in urology have shown that the Erbium:YAG laser (λ = 2.94 μm) is more precise for incision of soft urological tissues [1-4] and more efficient for ablation of urinary stones than the Holmium:YAG laser (λ = 2.12 μm) [5,6], due to the increased water absorption near 3 μm. However, the main limitation to use of the Er:YAG laser in endoscopic applications is the lack of a suitable optical fiber. Several mid-infrared fibers are available, including zirconium fluoride, sapphire, germanium oxide, and hollow silica waveguides. All of these fibers have significant limitations, including limited power delivery, chemical degradation in fluid environments, limited flexibility, low melting temperatures, tissue toxicity, and high cost [1,7]. The ideal mid-IR fiber for use in endoscopic tissue ablation would combine high-power delivery, chemical and mechanical durability, flexibility and biocompatibility.

Several approaches are currently being considered to circumvent the limitations of mid-IR fibers for use in endoscopic Er:YAG laser surgery. These include the use of hollow waveguides sealed with either quartz caps [8-10] or sapphire rods [11] and hybrid optical fibers consisting of germanium oxide fibers with silica tips [12-14]. Our laboratory has focused on the use of germanium oxide trunk fibers due to their high flexibility, high power transmission, and relative biocompatibility [15-17]. However, the main limitation of the germanium fiber is its relatively low melting temperature ($\sim$ 680 $^{\circ}$C), which prevents its use for tissue ablation in contact mode. The attachment of a robust and biocompatible low-OH silica tip with a higher melting temperature ($\sim$ 1175 $^{\circ}$C) to the germanium fiber may allow contact tissue ablation during endoscopic applications without fiber tip damage. During preliminary studies, the germanium fiber tip damage threshold during contact tissue ablation was increased significantly from 9 mJ without silica tip to 180 ± 30 mJ with the silica tip [12].

Side-firing optical fibers are currently used in urology with the Neodymium:YAG, Holmium:YAG, and KTP lasers during laser lithotripsy, ablative treatment of benign prostatic hyperplasia (BPH), incision of strictures, and other soft-tissue applications [18-21]. This study describes the assembly and preliminary testing of a side-firing germanium oxide fiber for delivery of Er:YAG laser radiation and potential use in endoscopic surgery.

2. MATERIALS AND METHODS

An Erbium:YAG laser (SEO 1-2-3, Schwartz Electro-Optics, Orlando, FL) was operated in free-running mode with a pulse duration of 300 μs, a pulse repetition rate of 3 Hz, and output pulse energies from 5-550 mJ, with single-mode, Gaussian spatial beam quality. The laser pulse energy was measured using a pyroelectric detector (ED-200, Gentec, Quebec). The temporal pulse length was measured using a photovoltaic infrared detector (PD-10.6, Boston Electronics, Brookline, MA). The laser radiation was

focused with a 50-mm-FL CaFl lens into the 1.45-m-length germanium oxide fiber with a 450-μm-core diameter (Infrared Fiber Systems, Silver Spring, MD).

The side-firing germanium fiber was assembled by polishing the distal tip at a 45 degree angle using a fiber optic polisher (Fibrmet, Buehler, Lake Bluff, IL), and then placing a 1-cm-long quartz cap (CV7087Q, Vitrocom, Mountain Lakes, NJ) over the tip and fiber jacket (Figure 1). The quartz cap had an inner diameter, outer diameter, and wall thickness of 700 μm, 870 μm, and 85 μm, respectively. The entire fiber assembly had an outer diameter of less than 1 mm, for potential insertion through the working port of an endoscope. Fiber damage tests were performed to determine the maximum output pulse energies that the side-firing germanium fibers could handle. Preliminary tissue ablation studies were also performed using the 450-μm side-firing fiber for Er:YAG laser incision of porcine ureteral tissue, ex vivo. The side-firing fiber was moved across the tissue surface in contact mode, creating 1-cm-long full-thickness incisions.
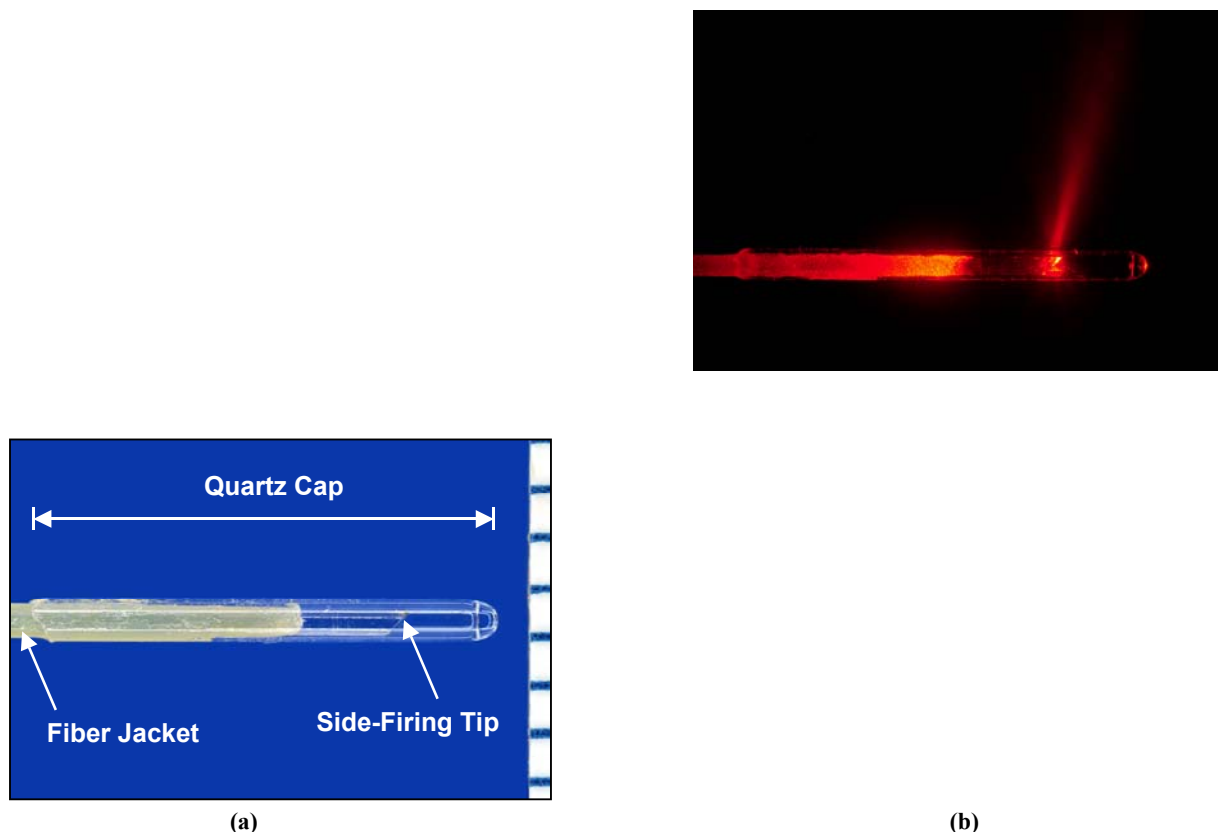

(a)   **(b)**

Figure 1. (a) Image of side-firing germanium oxide fiber tip with quartz cap. Scale bars on the right = 1 mm; (b) Image of HeNe aiming beam delivered through side-firing fiber.

3. RESULTS

Fiber transmission and damage threshold studies were conducted with the side-firing germanium oxide fibers. Fiber transmission averaged 48 ± 4 % for the 1.45-m-long fibers, and the damage threshold was 149 ± 37 mJ at 3 Hz (n = 6 fibers). The maximum damage threshold measured for an individual fiber was 210 mJ. These measurements are lower than the normal germanium oxide and hybrid germanium / silica fibers previously tested but still sufficient for contact tissue ablation [12,14] (Table 1). For comparison, the transmission rate of the normal germanium trunk fibers measured 66 ± 3 %. Figure 2a shows a plot of the transmission for a typical side-firing fiber. At the damage threshold, the transmission drops sharply, and the forward transmission increases sharply, as the angle-polished tip experiences damage. Figure 2b shows an H&E-stained histologic cross-section of porcine ureteral tissue precisely incised using the Er:YAG laser and a side-firing germanium fiber with an output pulse energy of 80 mJ. Note that the thermal damage zone at the edges of the incision measures only approximately 30 μm, as compared to a 300- m thermal damage zone typically produced using the conventional Holmium:YAG laser [1].

Table 1. Comparison of germanium fiber delivery systems for delivery of Er:YAG laser radiation at $\lambda = 2.94$ μm.

Fiber Type	Assembly Method	Damage Threshold (mJ)	Transmission (%)	N
Normal Germanium fiber	None	2000*	66 ± 3	5
Hybrid germanium/silica tip	Heat-shrink tubing / silica tip	180 ± 30	56 ± 3	7
Side-firing germanium	45° angle polish / quartz cap	149 ± 37	48 ± 4	6

* Commercial germanium oxide fibers are rated for use at up to 2 J / pulse at 10 Hz or 20 W by Infrared Fiber Systems.

(a)   (b)
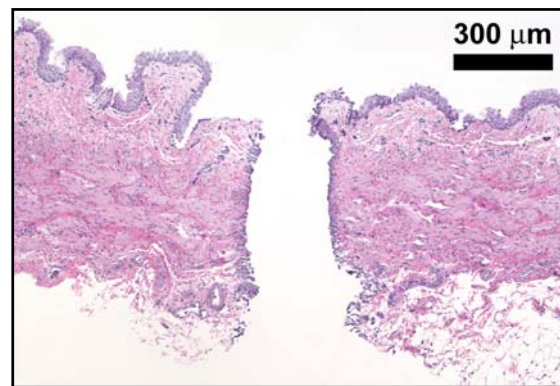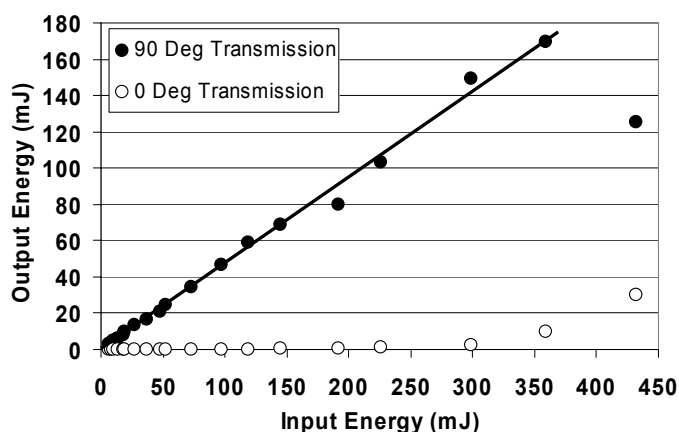
Figure 2. (a) Plot of transmission rate through side-firing fiber in both the 90 degree side and 0 degree forward directions. Damage to the fiber tip is clearly observed by a sharp drop in the side transmission and a corresponding sharp increase in the forward transmission, occurring at an output pulse energy of greater than 170 mJ for this fiber; (b) H&E-stained histologic cross-section of porcine ureteral tissue incised with the Er:YAG laser and a 450-μm side-firing germanium fiber at a pulse energy of 80 mJ. Note that the thermal damage zone at the edges of the incision measures only approximately 30 μm, as compared to a minimum thermal damage zone of 300 μm typically produced with the conventional Holmium:YAG laser in urology [1].

4. DISCUSSION

In this study, we described a simple design for a side-firing mid-infrared fiber consisting of a germanium oxide fiber with a 45-degree angle-polished tip, protected by a quartz cap. The fiber damage threshold averaged 149 $\pm$ 37 mJ, corresponding to a fluence of 94 J/cm^2 for a 450-μm-core fiber. For soft tissues, a laser fluence of only 1-5 J/cm^2 is probably sufficient, while for hard tissues, fluences of 20-40 J/cm^2 may be necessary for efficient tissue ablation.

Our experimental values for fiber transmission compare well with theory. For example, the normal germanium oxide fibers have an attenuation of 0.7 dB/m at a wavelength of 2.94 μm [14,15]. If this is multiplied by the length of the fibers (1.45 m), this gives an attenuation of 1.02 dB or 21%. The index of refraction is n = 1.84 [7], which leads to Fresnel reflection losses of 8.7% at each end of the fiber, or a total loss of 17.4%. Subtracting these losses due to fiber attenuation and reflection, gives a theoretical transmission rate of 61.6%, which compares well with the experimentally measured value of 66 $\pm$ 3 %.

For the side-firing fiber, there are additional losses due to the quartz cap. The quartz cap wall thickness is 85 μm. However, the attenuation for quartz is approximately 800 dB/m at 2.94 μm [7]. Multiplying the quartz cap thickness by this attenuation gives 0.07 dB or 1.5%. The index of refraction for quartz is n = 1.46, which leads to Fresnel losses of 3.5 % at each interface, or a total loss of 7%. Furthermore, there was a small loss attributable to forward transmission through the fiber tip. This loss was negligible at small output pulse energies, but was measured to be approximately 1.2 % at the higher pulse energies. At the highest pulse energies, forward transmission increased rapidly as the side-firing output energy decayed, indicating damage to the fiber tip. Subtracting these losses due to quartz cap attenuation and reflection and forward transmission, gives a theoretical transmission rate of 51.9 %, which compares well with the experimentally measured value of 48 $\pm$ 4 % (Table 2).

Table 2. Sources of transmission losses in germanium oxide fiber, side-firing tip, and quartz cap at λ = 2.94 μm.

Type of Losses			100%
Fiber attenuation:	(0.7 dB/m) x 1.45 m = 1.02 dB;	=	- 21%
Fresnel losses:	n = 1.84; [(1.84 − 1)/ (1.84 + 1)]^2 = 8.7 % losses at each interface x 2	=	- 17.4 %
Transmission of bare fiber:	**Experimental = 66 $\pm$ 3 %** vs. **Theoretical**	=	**61.6 %**
Side-firing fiber losses:			
Quartz cap:			
Attenuation:	quartz cap thickness = 85 m, (800 dB/m) x (8.5 x 10^{-5} m) = 0.07 dB;	=	- 1.5%
Fresnel Losses:	n = 1.46; [(1.46 − 1)/(1.46 + 1)]^2 = 3.5% losses at each interface x 2	=	- 7%
Forward transmission losses:	losses due to imperfections in angle-polished fiber tip	=	- 1.2%
Transmission of side-firing fiber:	**Experimental = 48 $\pm$ 4 %** vs. **Theoretical**	=	**51.9%**

There were several limitations to this study. First, fiber bending tests were not performed. The 450 μm-core fiber used in the experiments has a minimum bend radius of 25 mm, and therefore would not be used in most flexible endoscopes in urology.

However, the fiber bend radius decreases with a corresponding decrease in fiber core diameter. Since, germanium oxide optical fibers can be manufactured with core diameters ranging from 100-700 μm, it should not be a problem to miniaturize the side-firing fiber assembly method in future studies to provide more flexible bending for use in flexible endoscopes. Second, it is expected that smaller diameter fibers will have lower damage thresholds for the fiber tips. This fiber damage threshold should scale as a function of the fiber tip surface area, or r^2. Finally, the quality of the laser spatial beam profile both at the input end of the fiber and at the fiber tip interface is critical to achieving consistent results and a robust side-firing fiber. During our initial fiber tests, the beam profile was rectangular, resulting in high beam divergence, lower fiber tip damage thresholds (81 ± 3 mJ), and lower transmission (40 ± 4 %). Through the use of improved fiber polishing methods, the beam divergence was reduced, the beam shape was made approximately circular, and both the fiber damage threshold (149 ± 37 mJ) and the fiber transmission rate increased (48 ± 4 %).

5. CONCLUSIONS

Side-firing germanium oxide optical fibers were assembled using a simple method of polishing the distal tip at a 45 degree angle and then placing a protective cap over the fiber tip, for use in contact tissue ablation. The 450-μm-core-diameter and 1.5-m-long fiber delivered an average of 149 ± 37 mJ of Erbium:YAG laser radiation at a 90 degree angle, with a transmission rate of 48 ± 4 %, before the fiber damaged. This pulse energy is sufficient for precise Erbium:YAG laser ablation of soft tissues. This mid-infrared side-firing optical fiber may be useful for applications in which the surgical field is confined and the fiber tip cannot be easily manipulated, such as ophthalmology and endoscopic applications in urology. Future studies will focus on assembly of smaller diameter fibers, other delivery angles, fiber bending transmission tests, and further improvement of the spatial beam profile.

ACKNOWLEDGMENTS

REFERENCES

1. N. M. Fried, "Potential applications of the Er:YAG laser in endourology," J. Endourol., vol. 15, 889-894, 2001.
2. N. M. Fried, Z. Tesfaye, A.M. Ong, K.H. Rha, P. Hejazi, "Optimization of the Erbium:YAG laser for precise incision of ureteral and urethral tissues: in vitro and in vivo results," Lasers Surg. Med., vol. 33, 108-114, 2003.
3. H. Jelinkova, O. Kohler, M. Nemec, P. Koranda, J. Sulc, V. Kubecek, P. Drlik, M. Miyagi, Y. W. Shi, Y. Matsuura, M. R. Kokta, P. Hrabal, M. Jelinek, "Comparison of mid infrared lasers effect on ureter tissue," Laser Phys. Lett., vol. 1(3), pp. 143-146, 2004.
4. I. M. Varkarakis, T. Inagaki, M. E. Allaf, T. Y. Chan, C. G. Rogers, E. J. Wright, N. M. Fried, "Comparison of Erbium:YAG and Holmium:YAG lasers for incision of the urethra and bladder neck in a chronic porcine model," Urology, vol. 65, pp. 191-195, 2005.
5. J. M. H. Teichman, K. F. Chan, P. P. Cecconi, N. S. Corbin, A. D. Kamerer, R. D. Glickman, A. J. Welch, "Er:YAG versus Ho:YAG lithotripsy," J. Urol., vol. 165, pp. 876-879, 2001.
6. H. Lee, H. W. Kang, J. M. H. Teichman, J. Oh, A. J. Welch, "Urinary calculus fragmentation during Ho:YAG and Er:YAG lithotripsy," Lasers Surg. Med. In press.
7. J. A. Harrington. Infrared fibers and their applications. SPIE Press: Bellingham, WA, 2004.
8. K. Iwai, Y.-W. Shi, K. Nito, Y. Matsuura, T. Kasai, M. Miyagi, S. Saito, Y. Arai, N. Ioritani, Y. Okagami, M. Nemec, J. Sulc, H. Jelinkova, M. Zavoral, O. Kohler, P. Drlik, "Erbium:YAG laser lithotripsy by use of a flexible hollow waveguide with an end-scaling cap," Appl. Opt., vol. 42, pp. 2431-2435, 2003.
9. K. Iwai, T.-W. Shi, M. Endo, Y. Matsuura, M. Miyagi, H. Jelinkova, "Penetration of high-intensity Er:YAG laser light emitted by IR hollow optical fibers with sealing caps in water," Appl. Opt., vol. 43, pp. 2568-2571, 2004.
10. K. Iwai, Y.-W. Shi, Y. Matsuura, M. Miyagi, S. Saito, Y. Arai, "Characteristics of calculus fragmentation with Er:YAG laser light emitted by an infrared hollow optical fiber with various sealing caps," Appl. Opt., vol. 44, pp. 3266-3270, 2005.
11. M. Vardi, "Salivary gland stones and the use of Er:YAG laser for lithotripsy," M.S. Thesis, Biomedical Engineering Department, Tel-Aviv University, Israel, 2005.
12. C. A. Chaney, Y. Yang, N. M. Fried, "Hybrid germanium / silica optical fibers for endoscopic delivery of Erbium:YAG laser radiation," Lasers Surg. Med., vol. 34, pp. 5-11, 2004.
13. Y. Yang, C. A. Chaney, N. M. Fried, "Erbium:YAG laser lithotripsy using hybrid germanium / silica optical fibers," J. Endourol., vol. 18, 830-835, 2004.
14. N. M. Fried, Y. Yang, K. Lee, H. A. Tafti, "Transmission of free-running and Q-switched Er:YAG and Er:YSGG laser energy through germanium oxide / silica fibers," Proc. SPIE, vol. 5691, pp. 115-119, 2005.
15. E. Papagiakoumou, D. N. Papadopoulos, N. Anastasopoulou, A. A. Serafetinides, "Comparative evaluation of HP oxide glass fibers for Q-switched and free-running Er:YAG laser beam propagation," Opt. Commun., vol. 220, pp. 151-160, 2003.
16. N. M. Fried, Y. Yang, C. A. Chaney, D. Fried, "Transmission of q-switched Erbium:YSGG (λ = 2.79 mm) and Erbium:YAG (λ = 2.94 mm) laser radiation through germanium oxide and sapphire fibers at high pulse energies," Lasers Med. Sci., vol. 19, pp. 155-160, 2004.

17. K. Levin, D. Tran, A. Tchapijnikov, N. M. Fried, "Specialty fiber expands infrared laser applications," Biophoton. Internat., vol. 11, 41-43, 2004.
18. K. Anson, G. Buonaccorsi, M. Eddowes, A. MacRobert, T. Mills, G. Watson, "A comparative optical analysis of laser side-firing devices: a guide to treatment," Br. J. Urol., vol. 75, pp. 328-334, 1995.
19. C. F. van Swol, R. M. Verdaasdonk, R. J. van Vliet, D. G. Molenaar, T. A. Boon, "Side-firing devices for laser prostatectomy. An overview," World J. Urol., vol. 13, pp. 88-93, 1995.
20. J. M. Teichman, R. D. Rao, R. D. Glickman, J. M. Harris, "Holmium:YAG percutaneous nephrolithotomy: the laser incident angle matters," J. Urol., vol. 159, pp. 690-694, 1998.
21. M. Gurdal, A. Tekin, E. Yucebas, S. Kirecci, F. Sengor, "Contact neodymium: YAG laser ablation of recurrent urethral strictures using a side-firing fiber," J. Endourol., vol. 17, pp. 791-794, 2003.